Master's Thesis

Techno-economic evaluation of solar powered High temperature Direct Air Capture technology (sHT-DAC)

Institute of Future Fuels, German Aerospace Center (DLR)

University of Applied Sciences, Bremerhaven

By:	**Nipun Jagtap**
Matriculation Number:	**38757**
External Guide:	**Ms. Nathalie Monnerie**
Internal Guide:	**Prof. Msc. Hubert Stell**
Supervised by:	**Mr. Enric Prats Salvadó**
Submission date:	**05.12.2022**

Declaration of Originality

I hereby declare that I have composed this thesis by myself and without any assistance other than the sources jotted in my reference list. This document has not been submitted in the past or present for examination elsewhere. All direct quotes, as well as indirect quotes, which in phrasing or original idea have been taken from a different text (written or otherwise), have been marked as such clearly and in every single instance under a precise specification of the source. I am aware that any false claim made here results in failing the examination.

Nipun Jaikrishna Jagtap

Bonn, 05.12.2022

Acknowledgement

Abstract

Today's world is drastically undergoing the global energy transition to meet the sustainability goals signed at the Paris Conference in 2015. Moreover, many organizations have also acknowledged the inevitable carbon emissions in the development process of circular economy, which may cause rise in global temperature beyond 1.5 °C. For the same, many of them have considered reducing these emissions by investing hefty sum of money in the development of negative emission technologies (NETs). It should not only be an economical solution but also scalable up to giga scale capacity in order to match capture annual emissions. From all NETs, Direct Air Capture technology (DAC) has found to be more engineered and scalable solution. From the descriptive comparisons of various direct air capture solutions by Fasihi, Prof. Keith's CNG based High Temperature Direct Air Capture (HT-DAC) process seemed to have a real potential of meeting the emission control demands. In order to enhance the net carbon removal capture beyond 66% of a conventional HT-DAC process, the employment of solar technologies in it has been vividly studied from technical and economical point of view. Considering various factors like climate effect, 16 different scenarios of solarized HT-DAC process (sHT-DAC) have been evaluated. From the analysis, Jordan based location is more suitable for sHT-DAC. The results indicated that a CSP system having around 800 MW of thermal capacity is required to capture carbon at a million tonnes per year scale. And the levelized cost of sHT-DAC process is estimated to around 187 €/tCO$_2$ when compared to 181 €/tCO$_2$ capture cost of Keith's process. This research also investigated the influence of possible impactful factors and drawn few inferences to make the sHT-DAC business economically more attractive. Lastly, it concludes with the possible benefits of framing an effective policy on reducing the levelized cost and making the HT-DAC business more lucrative.

Table of contents

Table of Figures

Table of Tables

Table of Equations

List of Abbreviations

[OH-]	Hydroxide Ion
ΔC	Difference in the purchase and sell cost of power
AC	Air Contactor
ACHE	Air Cooled Heat Exchanger
APEA	ASPEN process economic analyzer
Area	Mirror area (m^2)
BD	Beam down
BECCS	Bioenergy with carbon capture and storage
$Ca(OH)_2$	Calcium Hydroxide
Ca^{2+}	Calcium Ion
$CaCO_3$	Calcium Carbonate
CaO	Calcium Oxide
Capex	Capital investment (€)
Carbon captured_n	Carbon captured throughout lifetime of plant
CCS	Carbon capture and sequestration
CCU	Carbon capture and utilisation
CE	Carbon Engineering
CO_2	Carbon dioxide
CO_3^{2-}	Carbonate ion
Cost_CPC	Cost of compund parabolic concentrator used in CPS system
Cost_Heliostat	Cost of heliostats used in CSP system
Cost_Reflector	Cost of reflector used in CSP system

Cost_Tower	Cost of solar tower used in CSP system
CPC	Compound parabolic concentrator
CSP	Concentrated Solar Power
CUF	Capacity utilization factor
DAC	Direct air capture
DBT	Dry bulb Tenmperature
DLR	Deutsches Zentrum für Luft- und Raumfahrt
DNI	Direct Normal Irradiation
EAI	Estimated annual installment
EBIT	Earnings before Interest and Tax
EBITDA	Earnings before Interest, Tax, Depreciation and Amortization
EOR	Enhanced Oil Recovery
EPCM	Engineering, procurement, construction and maintenance
ETS	Emission trading system
HFLCAL	Heliostat Field Layout calculator
HT	High Temperature
HT-DAC	High temperature direct air capture
IEA	International Energy Agency
IRENA	International Renewable Energy Agency
IRR	Internal rate of return
kW_p	Kilo-watt peak
$LCOC_{BS}$	Levelized cost of carbon capture (using balance sheet method)
$LCOC_{WACC}$	Levelized cost of carbon capture (using WACC)

LFR	Linear Fresnel reflector
LT	Low temperature
LT-DAC	Low temperature direct air capture
M€	Million euros
Misc	Collection of low power consuming equipments like filter, pump, etc
$MtCO_2$	Million tonnes of CO_2
n	Lifetime of plant
NET	Negative Emission Technology
NGR	Natural Gas Recovery
NIST	National Institute of Standards and Technology
NPV	Net Present Value
Opex	Annual manufacturing cost
Opex_n	Manufacturing cost throughout lifetime of plant (€)
PAT	Profit after tax
PBT	Profit before tax
PLF	Plant load factor
PV	Photovoltaics
r	Loan interest rate %
RH%	Relative humidity
ROI	Return over investment
tH_2O/tCO_2	Tonnes of water loss per tonne of CO2 captured
Tow	Height of Tower (m)

TT	Tower top
Turbine -1	Turbine installed in the continuous process
Turbine -2	Turbine installed in the intermittent process
UN	United Nations
WACC	Weighted average cost of capital
Y	Solar specific yield (kWh/kWp)

1   Introduction

Every year almost 40 Gt of CO_2 are released in the atmosphere through various means in order to meet the demands of the modern arena (*2*). In the context of rising climate issues all over the world, many governments, organizations and corporates are researching the ideal way to avoid the repercussion of the enhanced carbon dioxide (CO_2) emission in the atmosphere, also known as climate change. The most recent IPCC report states that the warming is expected to stabilize once the global net zero emission is attained. According to the Emission gap report by UN, the CO_2 concentration is around 420 ppm and is rising drastically. Hence, it is high time to actively progress in reducing the CO_2 emissions in the environment (*2*). Even though many institutions are working on increasing the share of renewable energy to make the economy greener and more sustainable, the usage of fossil fuels is inevitable in the development of circular economy. The transition of energy sources from fossil to renewable energy may reduce the emission of greenhouse gases (GHG), but the target of the Paris climate agreement will not be achieved without the involvement of negative emission technologies (NET).

Currently, there are various NETs available to be employed. However, it is impossible to capture carbon with 100% capture rate, for example: the installation of point source carbon capture (PSCC) technology captures carbon at 50-94% efficacy and it cannot be installed in old retrofitted power plants (*3*). In addition to this, there are multiple sources of small emitters like long distance aviation and marine transport, which accounts for 50% of the total GHG emissions and is also impossible to capture. Thus, it is mandatory to exercise direct air capture to attain the carbon neutrality (*1*).

At the moment, there are two major methodologies considered for the removal of CO_2 from atmosphere. One of them is Bioenergy combined with carbon capture and storage (BECCS). It has found to be very slow and land intensive but natural and cost effective process (*4*). Whereas, the other methodology of extracting CO_2 from atmospheric air is by using Direct air carbon capture and storage (DACCS) as a promising technology in terms of attaining climate neutrality.

According to the report by National academy of sciences, there has been lot of NETs which cost less than 100 $/tCO$_2$ (*4*). Out of these NETs, direct air capture-based technology has been widely discussed because of its scalability, effectivity, and the maturity of technologies involved. In addition to this, the direct air capture technologies are more flexible in terms of location of installation and further sequestration. Direct air capture (DAC) technologies can be categorized as (1) High Temperature (HT) direct air capture, which are chemical liquid-solvent based technologies, and (2) Low Temperature (LT) direct air capture, which are majorly solid-sorbent-based carbon capture technologies. Currently, there are numerous high temperature (HT) and low temperature (LT) process-based solutions costing from 100-1000 $/tCO$_2$.

Around 3 decades ago, Lackner had developed a process to capture CO$_2$ from air, which inspired many to investigate and find a robust, sustainable and economical solution to capture carbon from air (*5*). Moreover, many organizations like Carbon Engineering (CE) have been developing a carbon capture process since 2009. The founder of this organization, Keith has developed a very promising process in HT category and assessed its scalability using the ASPEN simulation software (*6*). Even though their process is very energy intensive, it is easily scalable to higher capacity and has currently low capture cost compared to LT technologies.

According to Fasihi (*1*), CE's carbon capture process is an unsustainable solution because of the usage of fossil-based natural gas as an energy sources in their process. The combusted natural gas contributes around 34% of total captured carbon, which will end up in atmosphere if the CO$_2$ would be utilized instead of stored. This has broadly increased the cost of net captured carbon (*1*). It was also inferred that the overall cost of the carbon capture may get reduced when energy technologies with less carbon footprint are used in the process.

Therefore, with the inspiration from the Keith's study and with a keen interest in investigating the application of solar technologies in the carbon capture process, this research has been conducted. It is majorly focused on the process modification and techno-economic evaluation of Keith's process in order to fully power it by solar energy. The overall thermal and electrical energy demand of the process is fulfilled by

employing an integrated hybrid system of Concentrated Solar Power (CSP) plants and Photovoltaics (PV) plant.

2   Aim

The aim of the study is to evaluate the feasibility of solar powered High temperature direct air capture (sHT-DAC) process from technical and economical point of view.

- The conventional carbon capture process is modified according to the solar energy technology system requirements and further simulated in ASPEN.
- After optimizing the novel process, heat integration and energy optimization were conducted.
- Further, sensitivity analysis of 6 major influential factors and 4 potential locations were studied.
- Based on the results obtained from simulation, detailed cost of captured carbon was estimated and economic viability assessed.

3   Literature review

In the light of rising global warming issues and the immense desire of the world towards carbon neutrality, negative emission technologies have gained a peak attention from research perspective. Moreover, the world has also recognized the importance of the carbon capture and utilization or sequestration (CCU or CCS) to save the planet from catastrophic time.

Out of all the NETs, direct air capture technologies are burgeoning exponentially. At present, many researchers and scientists have developed and evaluated various DAC processes to meet the climate goals. Lackner started the mission to capture CO_2 from Air around 3 decades ago, and later many researchers continued the advancements in this technology as shown in Table 1 below.

Table 1: History of development of carbon capture process.

Year	Author	Process Description	Solvent	Reference
1999	Lackner	Commercial flue gas absorber	$Ca(OH)_2$	(*7*)
2003	Zeman	Commercial flue gas absorber	NaOH	(*8*)
2006	Baciocchi	Commercial flue gas absorber (two variations of the process)	NaOH	(*9*)
2006	Keith	Air contactor	NaOH	(*10*)
2008	Stolaroff	Aqueous spray tower	NaOH	(*11*)
2011	APS	Contactor (Absorbers in parallel)	NaOH	(*12*)
2012	Kulkarni	Amine functionalized monolith contactor	Amine	(*13*)
2012	Holmes	Slab geometry air contactor	NaOH	(*14*)
2013	Mazotti	Contactor (modelled as absorber, alternate packings)	NaOH	(*15*)
2018	Keith	First prototype complete plant design	KOH	(*6*)

In the Figure 1 below, the cost of technologies developed in the recent years having major and promising advances are illustrated. As aforementioned, these can be categorized into two main categories (i) High temperature DAC (HT-DAC); (ii) Low temperature DAC (LT-DAC). High temperature DAC involves the capture of carbon dioxide using the conventional method of employing the liquid-based sorbent like alkaline solutions, where the temperature requirement of the process may reach up to 900 °C. Whereas, in LT-DAC processes, solid sorbents are used to adsorb carbon dioxide physically, and then sorbents are regenerated by varying temperature or moisture. The variation of the temperature ranges from 70–100. Although these technologies operate to remove CO_2 from ambient air (~400 ppm), they differ broadly in perspective of energy and capital investment requirement as well as with respect to scalability*(1).*

HT-DAC is comparatively more energy intensive and capital intensive than LT-DAC. Whereas, LT-DAC can be operated on the available waste heat in the process industry and has a large potential because of its modularity. However, it has not matured enough to scale up to higher capacity as compared to HT-DAC. As unlike LT-DAC, the quality of heat required in the HT-DAC process cannot be fulfilled by the industrial waste heat streams and large investments in the energy technology are required

separately. Nevertheless, the maturity of technologies involved in HT-DAC and recent advancements and its scalability provide a hope to attain the giga scale targets.
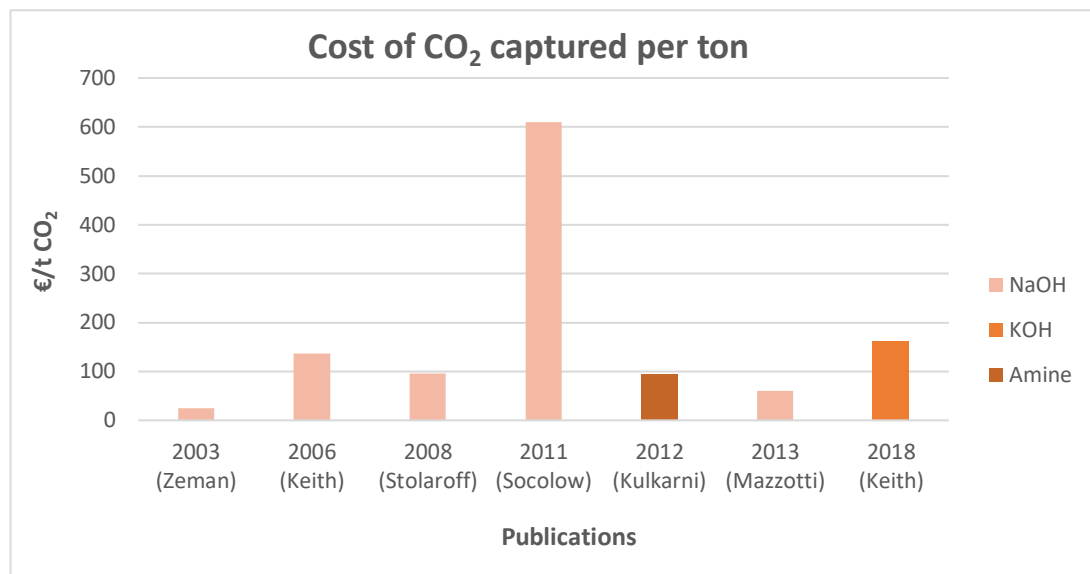
Figure 1: Cost comparison of various carbon capture processes (1).

Although the LT-DAC process seems an economically viable solution because of low energy requirement and the low operation cost, there are numerous issues with solid sorbents used in it. One of the major challenges is the requirement of large structures with regeneration facility disengaged from atmospheric air at low pressure. Secondly, conflicting demands for the low cost high sorbent performance and having a long economic life of sorbents in impure ambient air makes it an unviable option to meet the target capacity at the current state of the art (*16, 6*). Whereas, an alkaline based aqueous sorbent is employed in HT-DAC process, which helps in continuous operation of the plant as well as in building a plant of matured technologies with high operational lifetimes (*6*). The major drawbacks of using aqueous systems are significant water losses and complex regeneration system.

By recognizing the potential of the HT-DAC, Keith has developed an innovative and unique carbon capture process over a decade ago. His company named Carbon Engineering is very actively engaged company in the field of HT-DAC technology, which is also partly funded by Bill Gates foundation. They have launched a small plant of 1 tCO_2/d back in October 2015 and aims to establish a commercialized process for the

production of synthetic fuels. Keith has not only simulated the CNG fueled carbon capture process in ASPEN, but also performed a detailed cost estimation for a 1 MtCO$_2$/a capture capacity. In addition to this, they have provided their simulation results from ASPEN for 1 MtCO$_2$/a capture capacity. Also, they have provided detailed cost analysis of it.

In the exhaustive report by Fasihi, the cost of carbon capture for various technologies were compared (*1*). The LT based carbon capture process developed by Global Thermostat (USA) works on the waste heat at temperature of 85-95 °C for CO$_2$ regeneration. They have built up a model of 40 ktCO$_2$ and have estimated the capture cost around 113 €/tCO$_2$. In comparison to this, Keith's HT based carbon capture costs around 151-209 €/tCO$_2$, which is powered by natural gas (*1*).

HT based Keith's process is explicitly shown in Figure 2: Carbon Engineering's HT-DAC process. In his process, there are basically 4 major reactions carried out in 2 loops. Firstly, atmospheric CO$_2$ interacts with dissolved KOH at Air contactor in potassium loop and K$_2$CO$_3$ as a product flows through its outlet stream. Later, K$_2$CO$_3$ reacts with concentrated Ca(OH)$_2$ slurry in a pellet reactor, regenerating KOH and causing the formation of CaCO$_3$ salt. At the end, CaCO$_3$ solids undergo a high temperature calcination process and CO$_2$ is captured in pure form. Out of all the reactions involved in this process, calcination step is the most energy intensive step, where the temperature of around 900 °C is required. This heat is being supplied using the oxy-fuel based CNG combustion system. Equation 1 is the representation of CNG combustion. The CO$_2$ emitted from this combustion chamber further contributes more than 30% in the overall CO$_2$ captured.

$$CH_4 \ + \ 2\,O_2 \ \rightarrow \ CO_2 \ + \ 2\,H_2O \hspace{4cm} \textit{Equation 1}$$
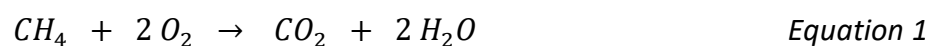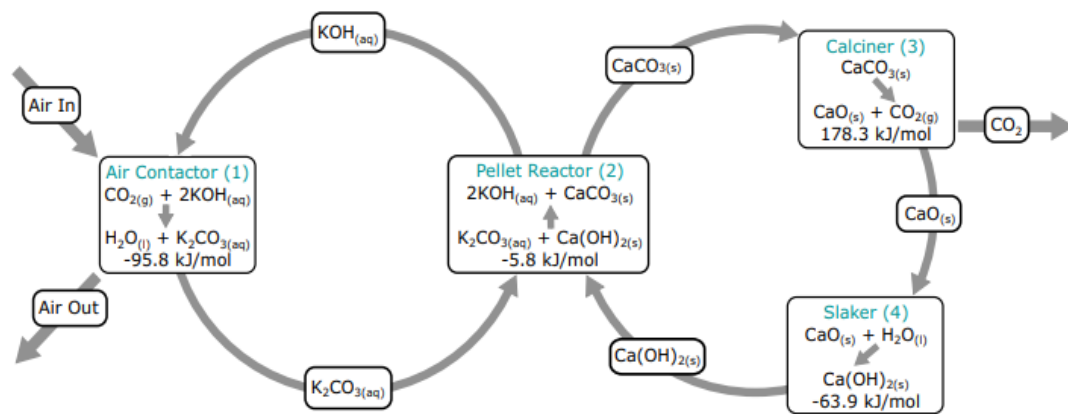
Figure 2: Carbon Engineering's HT-DAC process (6).

According to Fasihi, the cost of carbon capture is effectively high in the case of the Keith's process because the net carbon capture capacity is comparatively low. Almost 1/3 of the total carbon captured comes from the on-site combustion of natural gas to supply thermal and electrical energy to the process. Hence, the overall cost of net carbon capture is approximately 50% higher. In addition to that, more carbon from beneath the earth is being thrown out in the atmosphere, in case of utilization of the captured CO_2 (*1*). To overcome this conundrum, it becomes mandatory to employ fossil free based energy systems to attain high net carbon capture rate and low carbon capture cost.

In the vast literature research by Fasihi and Casaban (*17, 1*), many current state-of-the-art DAC technologies having enhanced net carbon removal capability have been discussed. However, they are found to be not only energy intensive but also cumbersome to operate and scale up at the moment. After considering the energy quality and quantity required by HT-DAC at giga scale, exhaustive research over various sustainable energy technologies has been performed. From this research, solar energy based Concentrated Solar Power (CSP) technology is found to be quite promising to meet the high clean energy demands of CE's process. There have been lot of advancements in the field of CSP technology in not only enhancing its scalability and operational reliability but also making it cost effective and one of the cleanest renewable energy technologies (*18*). It could attain high temperatures up to 1000 °C as well as can be scaled up to hundreds of MW capacity.

3.1 Solar Technology

Every year we receive around 885 million terawatt hours (TWh) of solar irradiation across the globe, making it the most abundant source of energy on earth. Realizing the potential of it, many scientists have developed innovative technologies to harvest this energy. As per the report by IRENA (*19*), the power generated from the CSP based system has comparatively lower levelized cost of electricity than photovoltaic based system. The combination of CSP with energy storage system has proven to be valuable in California in maintaining the demand and supply of power smoothly (*19*). In addition to this, thermal energy produced by CSP has been widely utilized as a clean energy source in many industries (*20*).

As shown in Figure 3, there are 4 major types of CSP technologies widely used in industry: Linear Fresnel Reflector (LFR); Parabolic dish; Parabolic trough and Central receiver. These technologies are basically characterized based on the optical design, shape of receiver, nature of heat transfer and capability to store heat. Considering the high temperature thermal energy requirement of a process operating at a MW scale, central receiver model with a solar tower is chosen for this study.

Table 2: Comparison between line focus and point focus based CSP technologies.

Focus Type	Line focus	Point focus
Fixed System	Linear Fresnel reflector	Solar tower
Mobile system	Parabolic troughs	Parabolic dishes
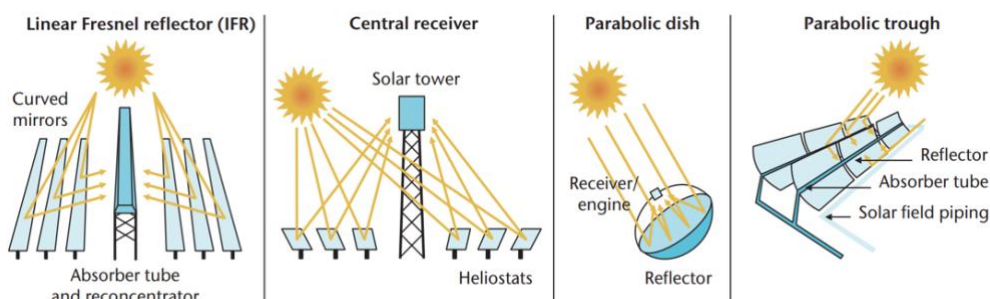
Figure 3: Types of concentrated solar power technologies (20).

Concentrated solar tower

In contrast to other linear systems, solar tower is more efficient at high temperature and less sensitive to seasonal variations. However, it demands for high concentration factor to reduce the heat losses in receiver (*20*). The heliostats in the solar field redirect the solar rays towards the receiver installed on tower. The temperature attained at receiver could go beyond 1000 °C, depending on the material employed in the receiver. Usually, CSP projects calls for heavy capital investment, but the return on investment could be improved with optimal design.

Towers could be designed in multiple ways depending on the number of receivers, field sizes and field orientation. In addition to this, heliostats are also designed in numerous shapes and sizes having surface areas ranging from 1 to 160 m^2. The number of heliostats is optimally calculated based on the overall area required. Moreover, they must be installed with an adequate space to avoid the shading and blocking issues (*20*).

As per the report by Solar paces, there are around 142 operating and developing CSP plants across the world. Out of which, there are more than 30 projects having solar tower based technology (*21*). At present, NOOR III is the largest concentrated solar tower project in the world. It is a Moroccan project having an investment of 877 million USD of investment and a total power capacity of 500 MW. In this solar project, a 247 m high solar tower surrounded by a solar field with around 1.3 million m^2 of heliostats has been installed. (*22*)

Photovoltaics (PV)

Out of all the renewable technologies, photovoltaics (PV) system has found to be comparatively clean, sustainable and promising power generating technology (*23*). Solar PV system is a photoelectric technology which converts the incoming abundant solar energy directly into electricity. Figure 4 shown below is the pictorial representation of the solar PV set up and solar cell. At present, PV are available with different solar cell types having different materials and configurations, cell arrangements, etc. (*24*)

Earlier, PV was not an economically viable technology that could be commercialized to increase its share in the total power production. But with advancement in the technological innovation and reduction of manufacturing cost by approximately 100 times, the global installation of PV has been constantly rising up. It is expected a record breaking mark of more than 300 GW installations across the globe in a coming year, and unmatched acceleration in the upcoming years, according to Branker and *reports* by IEA (*25*), (*23*).
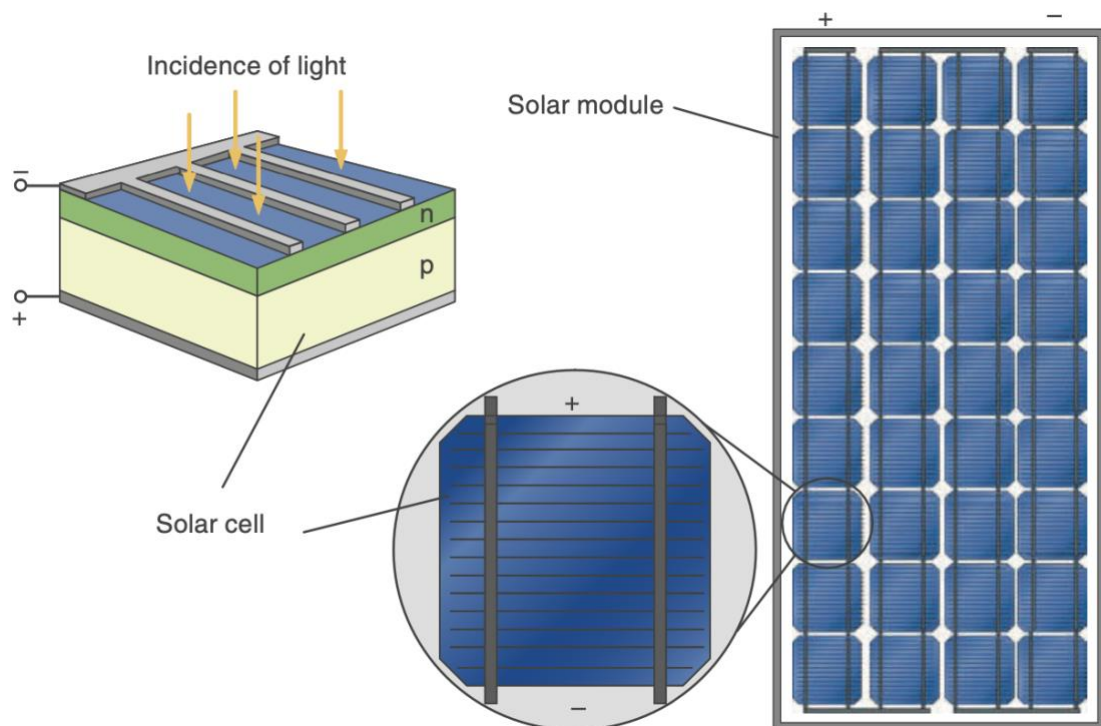
Figure 4: Pictorial representation of solar cell and solar module (24).

3.2 Overview
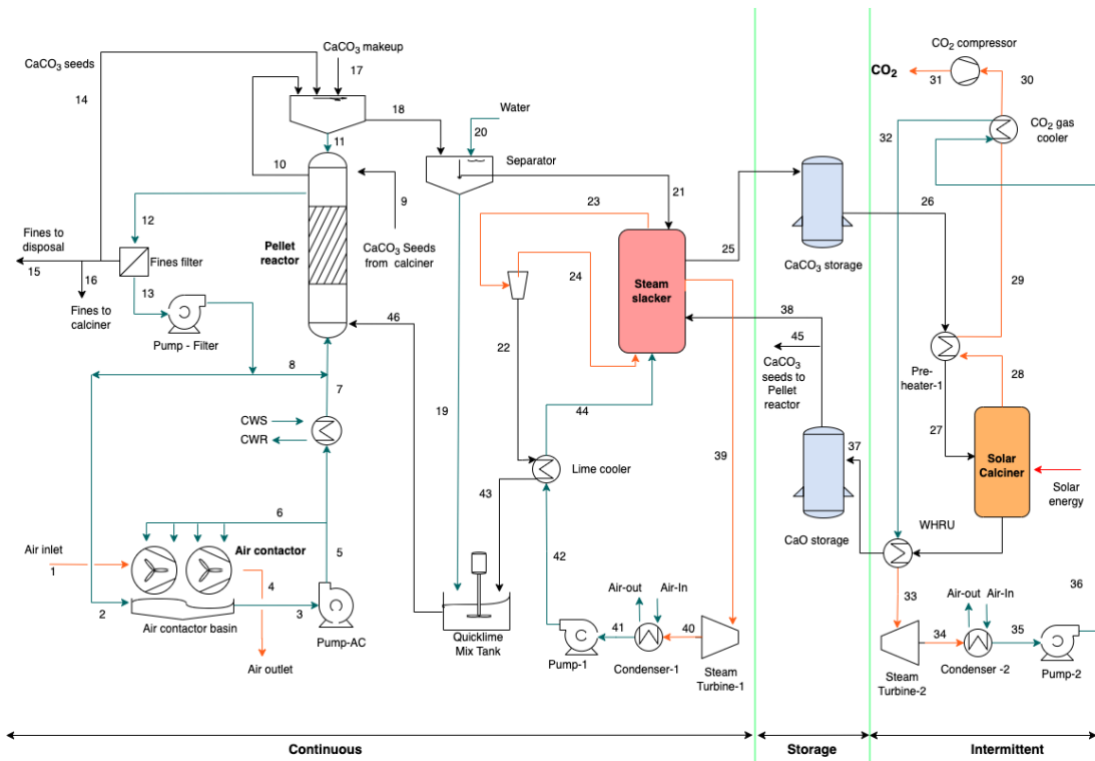
Figure 5: Process flow diagram of the modified HT-DAC process.

Figure 5 is the conceptualized modifications in the well-studied and commercialized direct air capture process of CE. In this process, the conventional oxy-fueled calciner has been altered to a solar calciner, which is used to regenerate CaO through a calcination process. Solar calciners are operated with the input solar thermal energy from CSP. As CSP receives intermittent solar irradiation across the year, the solar calciner, the associated heat recovery equipment and the CO_2 gas compressor are operated only during the effective solar irradiation. Whereas, the rest of the process is operated continuously with the defined operation capacity. The operation capacity is calculated based on multiple influential variables. It is descriptively explained in the chapter 4.8. Moreover, the storage section of CaO and $CaCO_3$ is a bridging zone of continuous and intermittent process. The dimensioning of optimal chemical storage is broadly discussed in the dedicated storage calculation section further.

Basically, there are four major unit operations being carried out in four pieces of equipment: Air Contactor, Causticizer, Slaker and Calciner. The reactions occurring in this equipment are as follows:

$$CO_2 \ + \ 2\,KOH \rightarrow \ K_2CO_3 \ + \ H_2O \qquad\qquad \textit{Equation 2}$$

$$K_2CO_3 \ + \ Ca(OH)_2 \rightarrow \ CaCO_3 \ + \ 2\,KOH \qquad \textit{Equation 3}$$

$$CaCO_3 \rightarrow \ CaO \ + \ CO_2 \qquad\qquad\qquad \textit{Equation 4}$$

$$CaO \ + \ H_2O \rightarrow \ Ca(OH)_2 \qquad\qquad \textit{Equation 5}$$
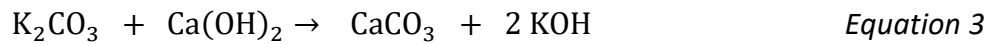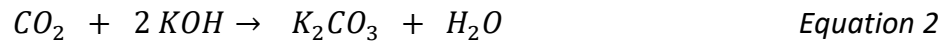
3.3 Air Contactor

The contactor is the heart of the carbon capture process, where it directly absorbs the CO_2 from the ambient air into the aqueous alkaline solution. CE's contactor is based on the cooling tower technology. It consists of a large setup of numerous draft fans responsible to build a turbulence for an effective mass transfer and overcome the pressure drop across the contactor. It works on the similar principle of the industrially wide used cooling tower. CO_2 is captured from the air passing through the structured plastic packing horizontally, where the alkaline solution is flowing downwards, having a film thickness of around 50 μm in a cross-flow manner. Based on CE's study, the contactor designs based on the traditional vertical packed towers are found to be more expensive. In comparison to common cooling towers, the height of packing used in this novel AC is more than double.

As per the study of CE, the mass transfer coefficient for CO_2 on the liquid side varies majorly with [OH]$^-$ ion concentration and temperature. In order to understand the influence of these parameters on the carbon capture rate, the detailed sensitivity analysis has been carried out and the obtained results are discussed explicitly in section 6.1. In addition to this, the profound research by Keju has broadly helped in understanding the influence of temperature and relative humidity on the carbon capture rate and the water losses from AC (*16*). Based on the empirical formula and the dimensions of the contactor provided by CE, CO_2 capture rate has been calculated by maintaining the optimum air flow velocity of around 1.44 m/s. The pressure drop

across the packing bed is assumed to be constant for the given air velocity, liquid flow and packing dimensions.

3.4 Pellet reactor

The pellet reactor is a fluidized bed reactor used for the removal of carbonate ions (CO_3^{2-}) from the carbonated alkaline solution by causticization. Along with the carbonated alkaline solution, solid coarse $CaCO_3$ particles are added from the top of reactor and 30% concentrated $Ca(OH)_2$ slurry is injected into the reactor bed. The $CaCO_3$ pellets ranging from 0.1-0.9 μm diameter acts as nuclei by providing surface to Ca^{2+}, which reacts further with CO_3^{2-} ions, as per Equation 3. The product $CaCO_3$ precipitates on the surface of solid pellets. This phenomenon leads to increment in the pellet size, which is then controlled by the continuous circulation of slurry in the reactor. The circulation in the reactor avoids the localized growth of the particles. As the pellets grow, they settle in the bed until the finished pellets are discharged at the bottom. The finished pellets size around 0.1-0.6 mm. Around 10% of $CaCO_3$ leaves the vessel as fines, which are captured and separated out in the filtration process.

3.5 Slaker

The slaker is also fluidized bed reactor, where the hydrolysis of CaO (commonly referred as lime slaking) is occurring simultaneously with the drying and pre-heating of grown $CaCO_3$ pellets. It receives $CaCO_3$ pellets at room temperature from the washing unit and hot CaO at 674 °C from the calciner's outlet or CaO storage. The pellets are dried and pre-heated using the waste heat generated in the slaking reaction, which is also responsible to sustain the slaking reaction. As the reaction enthalpy is released at higher temperatures in a steam based slaking process, it has a thermodynamic advantage over traditional water slaking process. Even though the maximum temperature could be around 520 °C, the operation has been optimized by Keith at around 300 °C to achieve faster kinetics (*6*).

The fluidization in the reactor using the compressed steam flow in circulation plays a crucial role in the slaking process. With a fluidization velocity of 1 m/s, quicklime (CaO) particles are transported and slaked to form $Ca(OH)_2$. A primary cyclone and loop seal elute and circulate small quicklime particles, while much smaller slaked particles largely avoid the cyclone and are collected in a dust collector. Heat from the slaking reaction is combined with the sensible heat recovered from the 300 °C hydrated lime in the outgoing stream to dry and heat the pellets.

3.6 Solar Calciner

The calciner is the most critical equipment carrying the calcination process in it. The dried and pre-heated $CaCO_3$ solid particles at the outlet of slaker are further heated in the CO_2 gas cooling exchangers. As the temperature required for the calcination process is quite high (~900 °C), it shares the maximum part of the energy required in the entire carbon capture process. Solar calciners are basically designed and developed to decarbonize the calcination process in cement industry, which shares 13% of global greenhouse gas emissions from industrial sector (26). Its cleanliness leads to pure lime production without any contamination of combustion by-products (27).

To decarbonize the calcination process, there are majorly two types of solar receiver-based techno-economically well studied calcination system: Rotary kiln and Centrifugal receiver. From the internal research, former receiver type not only gives freedom to construct the kiln system independently but also offers to operate separately. From the techno-economic analysis of optimized versions of both reactor types in the same research, levelized cost of heat was estimated to around 42.4 €/MWh and 39.6 €/MWh respectively (28). For the desired application of CO_2 capture, a matured rotary kiln concept is a more suitable choice in this project. Figure 6 shown below is the pictorial description of the working model of rotary kiln.
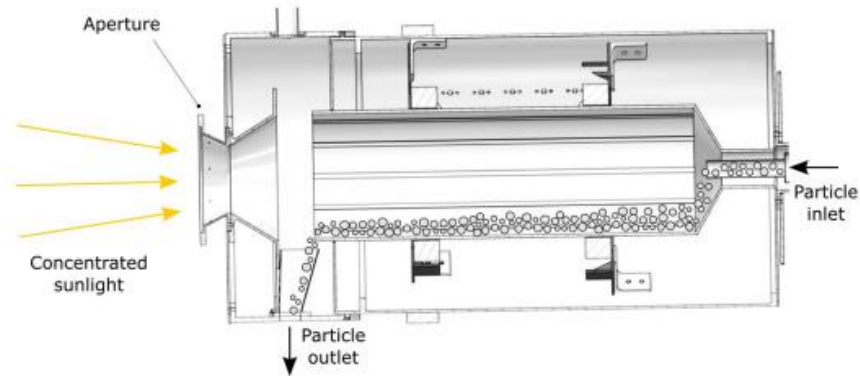
Figure 6: Working model of rotary kiln (29).

As per the literature by Meier (*30*), there are basically two different possible arrangements for solar tower receiver to operate the solar kiln efficiently: Tower top (TT) system and beam down (BD) system. The representation of both configurations is shown in the Figure 7 below*.*
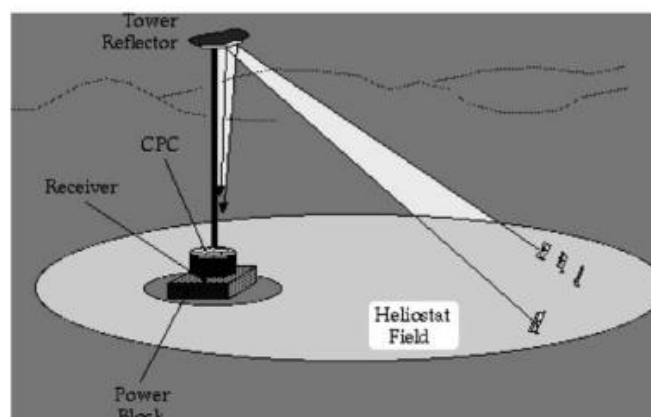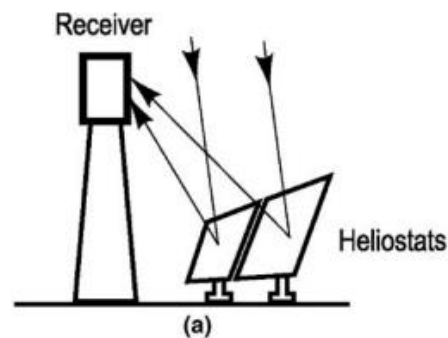
Figure 7: Pictorial representation of (a) Top tower, (b) Beam down (30).

In the tower top system, the rotary kiln is mounted on top of tower. Whereas in the case of the beam down solar system, the hyperbolic reflector re-directs the sun rays downwards in the rotary kiln, which is installed on the ground level. BD systems are reinforced by the non-imaging compound parabolic concentrator (CPC), which helps in augmenting the solar irradiation entering the kiln. BD is favored CSP arrangement system in case of use of more than two calciners because of technical and operational issues. In the case of peak concentrated solar flux around 1200 suns (1 sun = 1 kW/m^2), CPC might also be required in TT system if the temperature attained in calciner is not adequate (*30*).

3.7 Storage

The storage section is one of the most important sections of process, as it bridges the continuous section and the intermittent calcination section. It mediates the smooth operation of intermittent side of the process by controlling the flow of $CaCO_3$ to the calciner. Simultaneously, it maintains the flow rate of CaO to the slacker for the continuous operation of the CO_2 absorption process. According to Wang (*31*), the storage of $CaCO_3$ is not very arduous. In the case of CaO storage, it has high affinity towards water or moisture. This chemical reaction of CaO and water molecule leads to high heat liberation. It could be dangerous for other inflammable chemicals, if anything in vicinity. Therefore, the storage needs to be dry, cool and properly ventilated. In this study, the storage of CO_2 has not been considered, as the captured CO_2 is compressed further for direct utilization or transportation. Also, the heat liberation from the storage is negligible, as per the report over thermal energy loss by Falter (*32*). Therefore, this heat liberation is not considered in the calculation of the heat balance.

4　Modelling of solar DAC plant

Based on the exhaustive literature survey, the strategy deployment of potential solar energy technologies in the direct air carbon capture process has been conceptualized. In this section, the development and simulation approach of novel process in ASPEN V10 simulation software is explained. In addition to this, HFLCAL and Greenius software have been used in this project for the designing, optimization and cost estimation of the solar energy technologies like CSP and PV respectively. It also discusses about the approach for the heat optimization and energy estimation in section 4.2, Heliostat field layout designing in section 4.3, meteorological data analysis in section 4.4, energy analysis in section 4.5, utility estimation in section 4.6, PV plant dimensioning in section 4.7, and estimation of storage facility in section 4.8. To understand the dynamics of the weather conditions and develop a robust carbon capture system, meteorological data for four different locations has been analyzed and used for the accurate calculation of energy demand, storage, and the other required utilities.

4.1　ASPEN Simulation

In order to simulate the chemical process of carbon capture, ASPEN is one of the best simulation software with various property methods and unit operation models. It also allows to customize the simulation model for the non-conventional equipment. With regards to performing unit operation-based calculations or modelling, simulating, optimizing, or performing regression analysis, sensitivity analysis, energy estimation and energy savings, ASPEN is very powerful and reliable tool. In addition to this, ASPEN plus economic analyzer (APEA) module helps in estimating the project cost and in performing an economic analysis. Many researchers like Keith has performed techno-commercial analysis of various process, technologies in ASPEN (*33, 6, 34*).

For the case of the ionic chemical reactions, ELECNRTL property method was used as a suitable method and relevant properties were retrieved from NIST data bank. This data was further validated with Henry's constant. Using the Electro wizard option, ionic

species of the components also referred as true components in the process were determined and amended in the component list.

In the simulation environment, the process was developed on the flowsheet using the existing models for conventional unit chemical process and operations. Whereas, for the non-conventional chemical process equipment like the Air contactor, USER2 model has been considered and connected with an Excel sheet having an air contactor's process model. After simulating the developed flow sheet, preliminary results were obtained.

In order to optimize the process, the impact of the key influential parameters was observed using the sensitivity analysis tool. Further, the design specification tool has also been employed to get the optimal design of the process. Nevertheless, the entire final design could not be operated continuously using the non-continuous energy supply from intermittently operating solar technologies. Therefore, the entire process is bifurcated into two sub process: (a) Continuous process, (b) Intermittent process. This division has been carried out based on optimum energy consumption in the process with closed heat integration network. The detailed description of the process flow sheet is available in 0*.*

(a) Continuous Process

In this section, all the unit operations working without solar thermal energy and its associated equipment, employed in attaining the optimum energy consumption, has been considered. All the operations in this section will run continuously for 24 hours. From the above Figure 5, the continuous side of the process consists of AC, pellet reactor, slaker, filter, Turbine-1 and pumps. The operation of these equipment is independent of the incoming solar energy during solar hours.

(b) Intermittent process

In contrast to the continuous section, it consists of unit operations totally dependent on effective solar irradiation like the Solar calciner and other connected equipment like the CO_2 compressor, waste heat recovery exchangers, etc. Assuming the daily average of 10 hours of total sunlight irradiation, the

intermittent process has been developed and simulated accordingly. Therefore, the equipment sizes are designed to operate at comparatively higher flowrates, in order to conduct the operation in limited sunlight hours compared to normal continuous operation. After converting the CNG based conventional HT-DAC process into the novel solar based carbon capture process, a sensitivity analysis of various process variables like the ambient air temperature, relative humidity, temperature of pellet reactor, etc has been performed. The sensitivity analysis feature of ASPEN gives an excellent opportunity to meticulously monitor the influence of multiple variables. At the same time, it is also possible to monitor influence of single variable over multiple defined dependent variables. This variation of these parameters was extensively studied to complete the optimization from process capacity and energy consumption perspective.

APSEN Energy Analyzer and ASPEN Process Economics Analyzer (APEA) have been utilized to broadly understand the energy saving potential and get an estimation of project cost respectively. After simulating the materially optimized process, the energy analysis facility of ASPEN smartly performed the heat balance and estimated the saving potential of up to 86% of energy in the unoptimized process. The result obtained from energy analysis motivated further to investigate the potential parameters and to consider appropriate modifications in the process.

With a careful observation of entire process, the intermittent process found to have excess of energy on product line after the completion of calcination process. In an unoptimized process, the products line having mostly CaO and some $CaCO_3$ solids are cooled down using cooling medium in heat exchangers, like cooling water available at 30 °C. However, the high enthalpy of stream demands for massive cooling water flow. In the view of sustainability, this option does not sound as a viable process because an effective solar field are mostly located in water scarce regions. Therefore, it is always desirable to operate the novel process with a minimum possible water consumption. In order to recover the excess energy from the CaO stream side, a separate steam loop cycle has been designed. It collects the energy until the desired temperature of the CaO flow stream is attained. Super-heated steam generates power in Turbine-2 and gets converted into low pressure saturated steam. This steam is condensed through

an air-cooled heat exchanger (ACHE-2), pumped and re-vaporized through a network of heat exchangers (like the CO_2 gas cooler), that act as the boiler in the Rankine cycle.

Similarly, abundant amount of heat is also liberated in the exothermic slaking reaction of continuous process. The heat is collected from the slaker through an integrated steam loop, which runs the turbine later for power generation. The steam available at 300 °C in the slaker is formed by the interaction of hot CaO coming out of calciner at 674 °C and the $CaCO_3$ solids flowing with an associated liquid from washer. At the washer, the associated alkali solution is replaced by clear water. This water will then support the steam formation for slacking reaction. If excess water is added in comparison to the enthalpy associated with the CaO particles, part of the liberated heat is then utilized in evaporating the excess water. This leads to less heat available for collection and more volume of vapor flow in circulation across the reactor. Otherwise, the yield of slaking process will be compromised causing an ineffective operation and low heat collection. Also, the quick lime mixer will be overburdened.

In order to effectively optimize the energy recovery as well as water consumption, an exhaustive task of sensitivity analysis has been performed. Through sensitivity analysis of various influential parameters like the pump pressure, temperature & flow rates of water and steam, the impact of these variation on the chemical reaction yield and the power generation in turbines was carefully studied. In addition to this, the heat exchanger network was also analyzed using pinch analysis method.

At the end, these parameters were tuned to obtain the optimized version of this process having lowest utility consumption. This optimized version of process has been considered to gather results for energy savings, energy generated and energy required in process. These results obtained from simulation of mega scale carbon capture capacity were further used in CSP plant designing.

4.2 Energy estimation

Even though most of the energy utilized in the HT-DAC process is in the form of thermal energy, significant portion of it is shared by the electrical energy utilized in various equipment and instruments. The CO_2 compressor is one of the major consumers of electric power followed by the fans employed in the Air contactor and ACHE, filter, pumps for circulation, and agitator in mixing tank. In contrast to all these energy consumers, there are two turbines installed for electric power generation from available waste heat. From the ASPEN simulation, the power generated from turbines does not compensate the power demand of plant in normal operation. However, the bifurcated novel process calls for a more dynamic model for the estimation of annual energy demand in different cases.

With the division of the process, the equipment employed in each process has been listed separately in the Table 3 below. Continuous process operates every hour of the year. Whereas, the intermittent process operates only during the effective sunlight hours. Since the solar irradiation vary throughout the year, the overall energy consumption or production is calculated separately for every hour of the year. During these solar hours, the mean CO_2 capture capacity is determined through the method discussed in section 4.5.

Table 3: Power consumers and producers in two sub-processes of HT-DAC.

Process types	Continuous	Intermittent
Power sources	Turbine-1	Turbine-2
Power Consumers	Pump-1	CO_2 compressor
	Pump-ACHE	Pump-2
	Pump-Filter	ACHE-2
	ACHE-1	
	Mixer	
	Filter	

There are basically two cases considered for an energy estimation, as follows-

a) **Solar hour**

During this period, the calcination process is operated productively using the incoming adequate solar thermal power. These hours mostly range from 8 to 11 hours a day. The number of these solar hours per day varies largely with the season and location. The intermittent process leads to CaO production and collection of pure CO_2. Depending upon the CO_2 production capacity, the operation capacity for the dedicated turbine is determined and the energy consumption as well as generation in the intermittent process is estimated.

The total captured carbon on intermittent side is spread across the year. This average carbon capture rate is considered as a basis for the calculation of energy utilized for various equipment except AC in the process. Contactor tends to have different carbon capture rate based on the atmospheric temperature and the relative humidity. Using the correlation of dry bulb temperature (DBT) and relative humidity (RH%) value, overall energy demand in AC and other equipment is calculated together as mentioned in section 4.6.

b) **Non-solar hour**

During this period, which is mostly observed in the evening, night and early morning, the non-existent incoming solar irradiation is inadequate to energize calciners up to 900 °C and perform the calcination. Hence, the intermittent process is kept on stand-by mode. However, the continuous process captures carbon regularly and store it in the form of $CaCO_3$. Therefore, only the surplus energy available in the continuous process is considered in this case.

Grid connection supports the continuous operation of the process, in case of additional power required in certain hours. Whereas, the surplus energy is provided back to grid, which is generated during non-solar hours. After performing the detailed estimation of energy in both solar and non- solar hours, the annual energy demand is calculated. In order to fulfil the annual energy demand, PV based system is accordingly designed and scaled up.

4.3   Heliostat field layout

In this novel HT-DAC process, CSP is the only source of thermal energy. In order to harvest massive solar thermal energy, a large CSP plant consisting of solar tower, heliostats, receiver, reflectors, etc. are required. Out of all these equipment, heliostats share the biggest portion in total capital required for the CSP project. Therefore, it is quite important to design the CSP project with an optimal dimension. For the same, DLR based very convenient and helpful tool referred as HFLCAL (Heliostat Field Layout calculator) software has been used.

HFLCAL tool is majorly employed for designing and optimizing heliostat fields for solar towers projects having certain energy production capacity. In HFLCAL software, the design aspects of heliostats like size, shape, spacing between them needs to be initially provided. It also provides few already existing standardized models of the heliostats. Further, other design parameters like location details, tower height, solar DNI, aperture shape and size, design time point is set for a specific plant. In addition to this, the field layout details like orientation of field, field angle around the tower are also provided. Based on this data, the software estimates the optimized CSP field characteristics. An optimization based on a genetic algorithm identifies the most cost-effective field layout with total field size, mirror area and the optical efficiency chart. Figure 8 is an example of the heliostat field layout generated in HFLCAL for the case of Jordan-800MW. More details related to the HFLCAL can be found in the literature (*35, 36*).

From the literature (*30*), the correlation between the CSP heliostat field and the land required for installation of plant is determined. From the simulation in HFLCAL, the total heliostat mirror area and the tower height of an optimized heliostat field are obtained. Using the previous correlation, the total land required for that specific field is calculated. In the result section of HFLCAL simulation, the total field efficiency chart can also be obtained, which helps in systematically analyzing the meteorological data, explained in the next section.
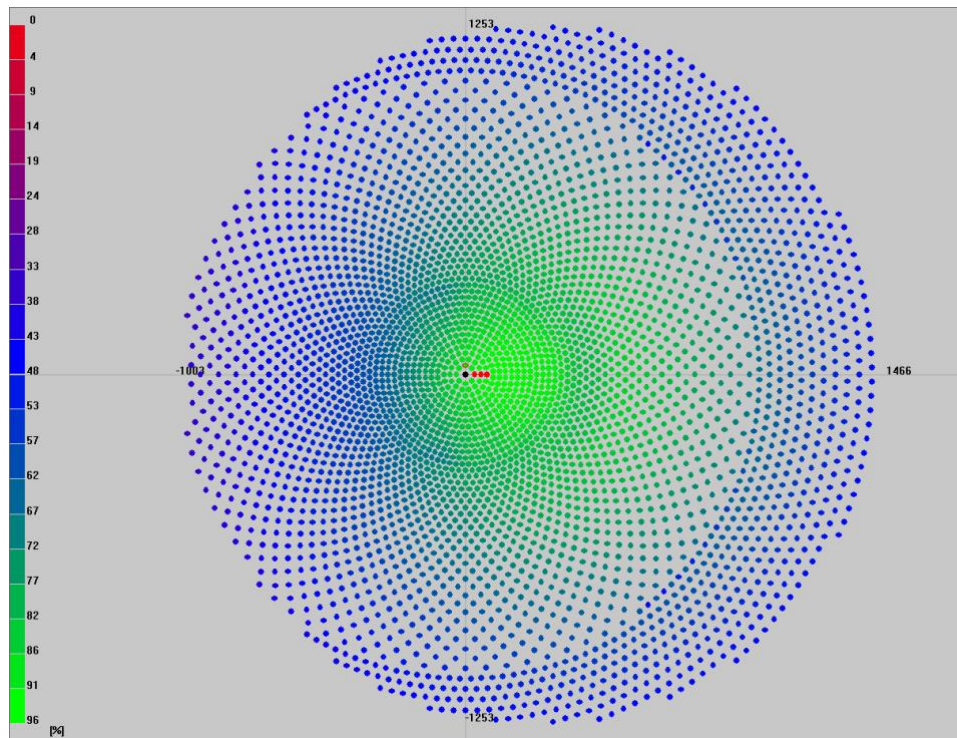
Figure 8: CSP field plot with efficiency of each heliostat installed.

4.4 Meteorological data

In order to observe the influence of location on the carbon capture cost, four most promising locations are shortlisted out of more than 25 suitable locations for CSP installation. Following are the six criteria used to shortlist those suitable locations:

   i.   High Temperature

  ii.   High relative humidity

 iii.   Good DNI

 iv.   Less deviation of solar hours

  v.   Good water availability

 vi.   Good transport facilities

According to the research, the relative humidity and temperature helps in better carbon capture rate and low water losses in AC (*16*). However, CSP plants demand a good DNI for an effective energy production. Along with this, it is better to have less deviation in daily solar hours, in order to have minimum storage capacity and simple process control system. CSP systems are majorly installed in the DNI rich regions, which also found to have less availability of water resource. But, the HT-DAC is quite water intensive process. Hence, it is one of the most important criteria in shortlisting the locations. Hence, the good accessibility of sea water for desalination and further utilization in process has been considered. Lastly, the good network of transport facilities is considered for the logistics of the captured carbon to the desired place of storage and utilization.

Based on these criteria, preliminary analysis for all locations was conducted and 4 major potential locations were shortlisted. Out of these 4 locations, two of them are CSP favored locations (Morocco and Chile), and the rest are chosen as suitable locations for DAC and CSP installations (Spain and Jordan). For these shortlisted countries, the meteorological dataset is collected for the four selected locations: Calama in Chile, Amman in Jordan, Granada in Spain, and Ouarzazate in Morocco.

Using Meteonorm software, the hourly based meteorological dataset for the aforementioned locations is collected from the nearest weather station (*37*). Raw meteorological dataset with sample calculation has been provided in 9.2. Based on this data, the average of the DNI available at 3 hours (11 AM to 1 PM) of five specific days (19th to 23rd of March) is calculated. As the climate is changing, it is quite difficult to predict the shading caused by clouds. Therefore, this mean DNI value is calculated and used further for the CSP plant layout design in HFLCAL for the 12 PM on 21st of March. Moreover, the dataset is analyzed to get hourly averaged DNI incident in each month. This average DNI table is used in the estimation of CO_2 capture capacity of plant. Also, the average temperature in each month is also extracted from the raw dataset. This average temperature values are used for the calculation of convectional heat losses in energy analysis (section 4.5). The hourly temperature and RH% values are used in the estimation of water losses from AC.

4.5 Energy Analysis

This section explains the approach of estimating the annual CO_2 capture capacity on the basis of hourly solar irradiation available in every month of the year. Using the same raw meteorological dataset, the CO_2 capture capacity of plant is calculated by following 6 steps of method shown in Figure 9.
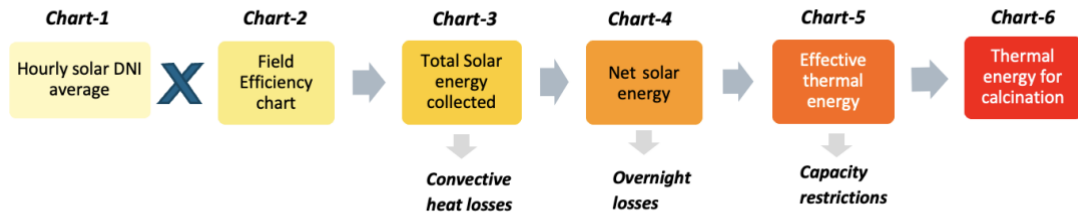
Figure 9: Flow chart of energy analysis method.

Initially, the DNI values are analyzed to get the chart having 24 rows (one for every hour of the day) against the 12 months of year. The chart contains the average DNI incident at the specific hour and month of year. It considers the issues related to seasonal variation in atmospheric conditions like particulate matter, fogginess, cloudiness at the desired location. This chart is then clubbed together with the heliostat surface area and field efficiency chart (Chart-2), which is obtained from HFLCAL, as per the Equation 6. Chart-3 gives the average hourly solar energy harvested in the form of thermal energy in each month.

$$\text{Power} = \text{Area}_{\text{mirror}} \times \text{DNI} \times \eta_{\text{field}}$$ *Equation 6*

Even though the solar energy is harvested efficiently from an optimized field layout, the convective heat loss caused due to the lower atmospheric temperature is considered. In addition to this, the dataset is analyzed to get the monthly average ambient temperature and then plotted as shown in Figure 10 below. Based on the variation of temperature across the year, convective heat losses are assumed varying from 5% to 10%. The result of the overall thermal energy collected is represented by Chart-4.

Temperature variation in Jordan
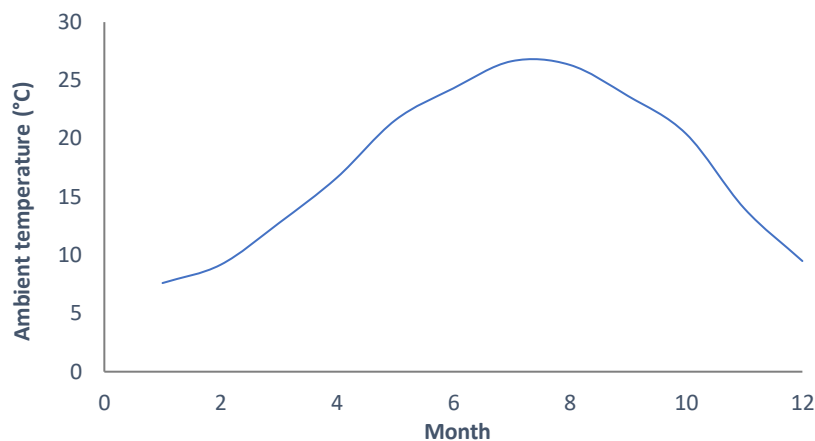
Figure 10: Annual variation of ambient temperature in Jordan.

In addition to the convective heat lost to the atmosphere at the receiver throughout the operation period, the energy lost from calciners during non-solar hours is also assumed. Although the solar calciners are assumed to be well insulated, temperature is expected to decrease below the operating temperature during the non-operational hours. In order to roughly estimate this loss of energy overnight, half of the design heat capacity of reactors is assumed to be dispersed during the non-solar hours. Therefore, it is mandatory to recover this energy and attain the temperature around 900 °C every morning before the calcination process begins. For this study, at least 27.5 MW of solar thermal power is required to initiate process in calciner reactors having a maximum capacity of 55 MW. Some part of thermal energy in morning hours is subtracted from Chart-4 to obtain the effective solar thermal energy for operation, which is represented in Chart-5.

Since only a fraction of incoming energy can be utilized by calciners up to their design capacity, the effective solar thermal energy is further screened to get Chart-6. It signifies the range of thermal energy available for the set of calciner, which can potentially operate minimum of one calciner and maximum of all calciners. Beyond the total heat required to operate all calciners, all the excess energy is diverted from the system. Putting this capacity restriction, gives out Chart-6, which represents the actual thermal energy utilized in the calcination system.

Based on the simulation results, the thermal energy requirement of around 350 MW for the operation of 256 tCO_2/h was obtained. This boils down to an energy demand for calcination of around 11821.6 MWh/tCO_2 including a kiln efficiency of 45% of kiln efficiency. Using this value in Chart-6, the average hourly CO_2 production in different months is calculated and arranged in final product chart. This product chart also gives the total carbon captured throughout the year and the average rate of carbon capture. Moreover, the CaO production rate for every hour of month is also calculated using the simple reaction stoichiometry and molar mass ratios.

The hourly average carbon capture rate obtained from the product chart helps in accurately estimating the overall energy required for all calcination and non-calcination hours. Along with this, the annual average carbon capture rate value is broadly used in the calculation of utility.

4.6 Utility calculation

HT-DAC process has huge water loss and significant usage of power in various process equipment like pumps, fans used in air contactors, CO_2 compressor, etc. Needless to say, it is one of the crucial parameters in understanding the sustainability of the process and determine the environmental viability of it. In this section, the detailed approach for the calculation of water and power usage is explained, and finally the results for various scenarios are discussed vividly in the result section further.

4.6.1 Power estimation

Basically, there are two approaches to estimate the annual power consumption in plant. Either, the annual CO_2 capture is calculated with the constant power supply, or the total power consumed by various process equipment is estimated with a targeted constant CO_2 capture per annum. In order to focus the research on estimating the energy demand of million tons capacity plant, latter approach has been employed in this study.

Based on the defined CSP thermal capacity, the CO_2 production capacity of calciners is obtained. Power consumption in most of the equipment from continuous process is assumed to vary linearly with the average CO_2 production rate. However, the power consumed by fans in contactor is considered to vary with given hourly temperature and relative humidity data. Using Equation 6, the power consumption in AC is estimated. The detailed calculation with an example is provided in the 9.2. The carbon capture rate (CR%) of AC is calculated using Equation 7. This correlation based on relative humidity (RH%) and the ambient dry bulb temperature (T) in degree Celsius is determined using the simulation data provided in the literature (*16*). Using this correlation and the hourly based meteorological data, the power consumed is estimated for every hour.

$$P \propto \frac{\dot{n}_{CO2_{abs}} \cdot T}{CR\%} \qquad \textit{Equation 7}$$

$$CR\% = 47.66 + 0.89 \cdot T + 0.137 \cdot RH\% \qquad \textit{Equation 8}$$

Whereas, the amount of power generated in Turbine-2, and power consumed in CO_2 compressor is highly dependent on the CO_2 production rate of the intermittent process. Based on the product chart obtained in the energy analysis, the average monthly CO_2 capture rate in every hour of the day has been estimated. Using this calculated rate and the simulation results as reference, the hourly consumption and production of power in compressor and Turbine-1 have been scaled respectively. Power consumption in air-cooled heat exchanger (ACHE-2) is assumed to vary linearly with the average CO_2 capture rate.

Similarly, significant power consumed by various equipment employed in continuous process (like ACHE-1, Filter and contactor pumps, mixer and other contingency pumps) needs to be estimated. Also, the power generated in Turbine-1 using the waste heat from the slaker needs to be addressed. This power generation varies linearly with the supply of CaO to the slaker, corresponding to the CO_2 absorption capacity of the contactor.

As the calculations for power consumption in continuous process majorly depend on the average CO_2 capture capacity, a constant has been finally obtained separately for solar and non-solar hours. In the non-solar hours based constant, only ACHE-2 is not included. It represents a summation of power consumed and power generated in overall process. These constants are further used directly.

At the end, the overall power consumed or produced in each hour is calculated by adding the determined power constant, power consumed in intermittent process equipment and in the AC. The sum of hourly calculation leads to the annual power demand of process in different scenarios. In order to meet this power demand, there are basically three solutions

i)   Autonomous off-grid

In case the carbon capture plant needs to be completely operated using green and sustainable source of energy, this type of energy system could be installed. In this type of energy system, the total required power would be supplied by solar energy-based system. In non-solar hours, the excess power generated from the process is stored in a battery-based system. This energy can be further utilized in the energy intensive solar hours. For the additional energy demand during solar hours, PV based system is installed to provide the adequate amount of power throughout the year.

After carefully analyzing this type of power system, it has comparatively found to be more expensive option, leading to a rise in overall carbon capture cost. In addition to this, it is not a robust and well-integrated energy solution.

ii)   Grid powered

In comparison to previous energy solution, this system borrows all the required energy from the robust grid connection. Since grid power is mostly shared by the non-renewable based sources at many locations, the carbon footprint of the entire process is increased significantly leading to increased net cost of carbon removal from atmosphere.

iii) **Grid connected PV system**

From all the solutions, this type of energy system is the most reliable, robust and cleaner than second option. In this system, the additional energy required during solar hours is supplied by the energy produced from the PV farms. As the power generation in the PV system is majorly dependent on the atmospheric condition, the offset power demand is covered by borrowing the power from grid. Whereas, the excess energy generated during the non-solar hours is sold back to the grid.

Post detailed analysis of all the above cases, the grid connected PV system found to be more robust, economical and reliable. Based on this system, the excess annual energy required in process is generated in the PV system. Using this energy capacity value, the adequate sizing of the PV plant is designed.

4.6.2 Water loss estimation

According to the reports of UN water (*38*), almost two thirds of the world population is affected by the water scarcity for at least a month in a year. As not every drop of water can meet the basic demands of largely populated humans, it is absolutely unfair to consider the freshly available water.

In order to make this novel carbon capture process sustainable, a long lasting and reliable water source needs to be considered. Moreover, water is usually scarcely available in high DNI based regions, which is effective for solar technologies. Hence, desalinated water as a matured technological solution for the continuous and dependable operation is considered in this study. Even though the production cost is higher at the moment, high learning curve and scale up possibility across the world makes it more promising solution.

In an exhaustive research by Keju (*16*), the water loss and the absorption rate of CO_2 in AC has been discussed in detail. From the data provided in this source, a strong correlation with 97% accuracy was determined to predict the water losses at various temperature and relative humidity values ranging from 0 to 40 °C and 10-97% respectively. Using this correlation and the atmospheric conditions of each hour, H_2O

loss to CO_2 captured ratio (Y) is separately calculated. Equation 11 depicts the correlation used for the calculation of the water loss. This calculation further gives an hourly water loss for the AC, when clubbed with the hourly CO_2 capture rate.

$$m = -0.006 \cdot T - 0.07 \qquad \textit{Equation 9}$$

$$c = 0.159 \cdot T + 11.299 \qquad \textit{Equation 10}$$

$$Y = m \cdot RH\% + c \qquad \textit{Equation 11}$$

In addition to this, the water consumed in the CSP systems, like the water used for the cleaning of heliostats, has also been considered. According to the report by Falter (*32*), the annual water consumption in the cleaning and other maintenance of the heliostat fields has been estimated to around 58 liters/m². Using this value, the annual water consumption in each scenario has been determined and added to the water losses in AC to get the total water demand of the process.

4.7 PV plant dimensioning

Photovoltaic systems are majorly employed to support the additional power demand of process. Ideally, the combined power generated by both the turbines is not adequate to fulfil the power demands in certain hours of operation for ex: during solar hours. During these period, the robust and stable support of grid connection is considered. However, additionally borrowed energy from the grid is expected to be compensated from an integrated PV system, to minimize the carbon footprint of system.

Currently, there are numerous performance metrics for solar PV systems of all sizes and technologies like capital utilization factor (CUF), plant load factor (PLF), Specific yield (Y) (*39, 40*). These factors are quite similar and found to be majorly useful for the comparison of different locations for PV installations, PV design analysis as well as to assess the health of PV system. In order to accurately design the PV plant, the specific yield (Y) factor has been used. It represents the amount of power generated per unit of the installed PV peak capacity over the long-term, and is measured in kilowatt hours

per installed kilowatt-peak capacity of the system (kWh/kW$_p$). The specific yield factor considers the seasonality, shading and soiling, topography and air temperature of a region affecting the system performance (*41*). For most European countries, it has been normalized to the value of 2.93 kWh/kW$_p$ (*42*). However, the specific yield for the potential locations has been considered, based on the large dataset provided by Global Solar Atlas (*41*). Table 4 indicates the specific yield values for potential locations.

$$Y = \frac{\text{PV panel energy demand (kWh)}}{\text{Peak power load (kW}_p)}$$

Equation 12

Using the above Equation 12 specified in the report by Leonics for PV plant sizing (*42*), the peak power capacity is evaluated from the previously estimated mean of daily energy demand and the panel generation factor (also known as specific yield) for all potential locations. By providing the peak power capacity to the Greenius software, the PV plant has been effectively designed having a specified solar cell type and module system.

Table 4: Specific yield values for potential locations (43).

Country	Specific yield (kWh/kW$_p$)
Chile	5.365
Jordan	5.315
Spain	4.413
Morocco	5.007

Greenius software is a powerful simulator, which is developed by the German Aerospace Center (DLR) Institute of Solar Research. It is widely used to analyze or design the renewable energy projects like solar thermal plants, solar PV, Fuel cells, wind parks etc. It provides results of both technical and economical calculations for planning and installation of renewable energy projects (*44*). It allows user provide the meteorological data consisting of RH%, ambient temperature, DNI as well as the elevation of desired location of study. Further, it also gives room to select the type of

module having a uniform set of single cell type. For this project, poly-silicon based solar cell has been preferred as an economical option.

For the same PV module, the annual operational cost of 10 €/kW$_p$ has been assumed. In addition to this, the software allows to change the inverter settings if required. For this research the default settings having a nominal efficiency of 95% have been considered. In the PV system section, it allows to scale up the PV system by varying the number of modules and inverters with multiple orientation and tracking facility like single axis or 2-axis tracking. Considering the installation of PV systems to harvest maximum possible energy, 2-axis tracking has been chosen for the PV plant.

Along with this, the software provides an opportunity to consider the energy storage facility in the PV plant design. As the PV power is directly supplied to grid, energy storage is not considered in the PV plant design. For the final PV plant design, detailed economic analysis is obtained with detailed costing distribution. At the end, the net investment required for the installation of this plant is obtained and used further in the cost analysis.

4.8   Storage estimation

As previously discussed, the storage section is the most crucial part of the process because it bridges the intermittent and continuous part of the process. In this unique carbon capture process, the intermittent solar energy supply leads to the non-continuous operation of calciners. During the solar hours, calcination process occurs in comparatively higher scaled calciners to compensate the calcination demand in non-solar hours. Similarly, the CaCO$_3$ produced during the non-solar hours also needs to be stored before its utilization in calciners. This chemical storage capacity needs to be optimally designed for smooth and regulated operation of continuous side of process.

In order to optimally design the storage section, two different approaches were considered for the calculation: i) Monthly analysis; ii) Cut-1-month analysis. In the monthly analysis approach, the consumption and the production of CaO and CaCO$_3$ is accounted for every month of the year. Whereas in the latter approach, mass flow through the storage is considered for only 11 months, assuming one month of

complete shutdown in process. From the analysis of 4 major scenarios, the cost of capture was found to be relatively higher when calculated through a second approach. In addition to that, the maintenance period is assumed as a period less than a month and can be adjusted non-continuously throughout the year. Taking all these into account, the former method was considered as a suitable option for the storage field sizing and optimization.
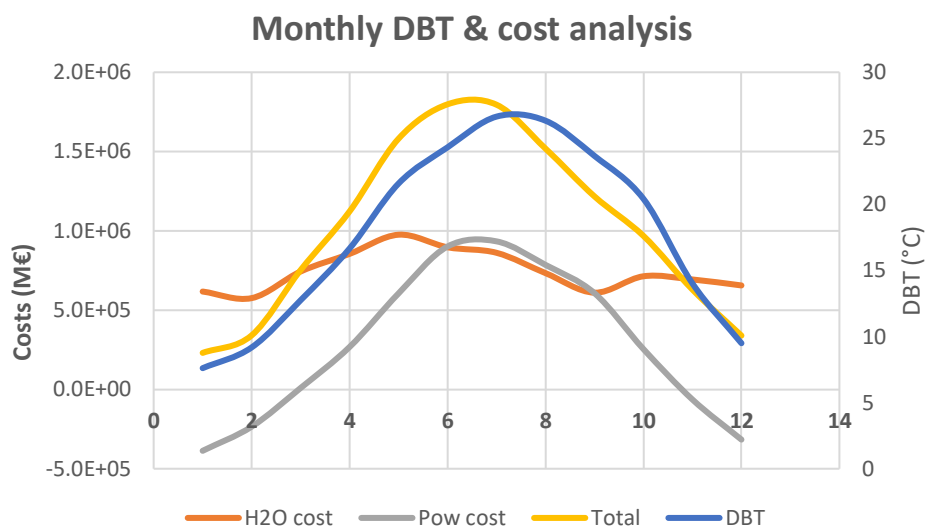
Figure 11: Variation of DBT, and cost of utilities and operation.

Referring to CaO product chart obtained in the energy analysis section, monthly production of CaO is determined from the product Chart-2. Plus, the raw meteorological dataset is preprocessed and then pivoted to get the water consumption, power consumption and the total operation cost, as shown in Figure 11 above. Various factors such as the average ambient temperature, relative humidity of each month, etc. are incorporated into this power and water consumption to keep the carbon capture rate constant. Based on this monthly variation in the cost of operation, the plant operational capacity is also varied ranging from 70-90%. Using this plant operational capacity values, the monthly consumption of CaO in the continuous process has been determined.

Balancing the overall consumption and production of CaO in entire process throughout the year gives out the optimal capacity of the CaO storage section. Figure 12 represents

the variation of production and consumption of CaO and CaCO₃ in a year for the case of Jordan-800MW. Based on this variation, the storage capacity was optimally estimated. Similarly, the storage capacity of the $CaCO_3$ was also estimated. However, in this case, the consumption of the CaO is considered as the basis for the production of $CaCO_3$, referring to the slaking process. And the consumption of $CaCO_3$ is calculated using the calcination reaction stoichiometry, molar masses and the monthly CaO production rate. This method was repeated to calculate the minimum storage capacity required for the two chemicals for all scenarios.

(a) Monthly consumption and production CaO

(b) Monthly consumption and production CaCO₃
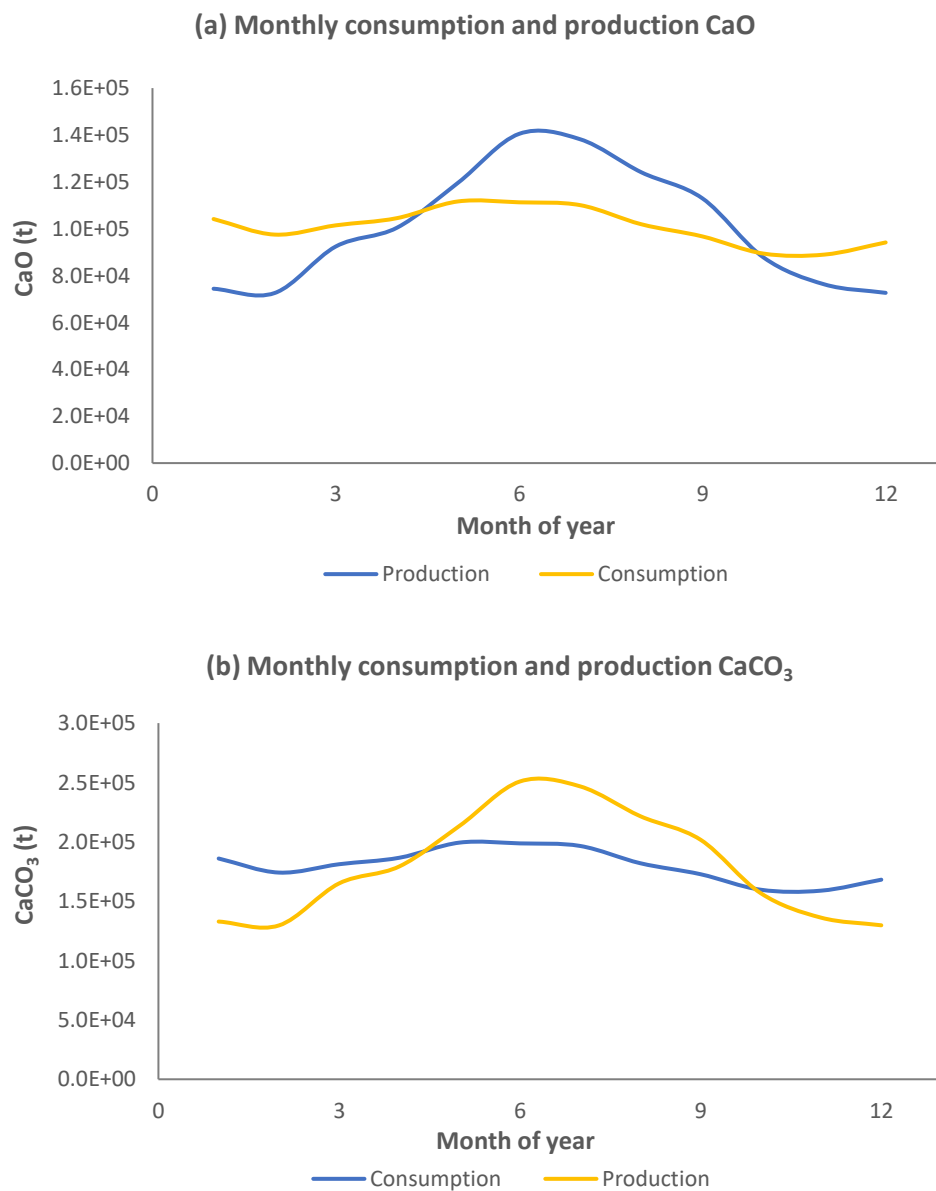
Figure 12: Monthly variation in production and consumption of CaO (a) and CaCO₃ (b) for Jordan-800MW.

5   Economic Analysis

From the last three decades, many scientists and researchers are working meticulously with an aim to make the carbon capture process efficient and economical. In order to understand the economic feasibility of technically most optimized process, a detailed study over various impacting factors needs to be conducted. In this section, the exhaustive cost analysis will be explained in detail. In addition to that, vast economic analysis using the cash flow analysis method will be discussed. The detailed economic analysis includes creating balance sheet, estimation of economic indicators, etc.

5.1   Cost Analysis

In order to correctly estimate the required investment, the precise cost of all the equipment has been evaluated using APEA, correlations from research articles and the widely used methods mentioned in project economics-based literature. To further accurately estimate the cost of the entire project, the overall cost is distributed into capital cost and operating cost.

The capital cost majorly comprises of the investment required in the equipment procurement & installation, project engineering, construction, legal expenses, contractor's fee and contingency. The overall fixed investment is estimated using the widely used method of 'Percentage of equipment cost' and 'Economy of Scale' method, which are explicitly explained in (*45*). As shown in Table 5 below, the following percentages have been used for the calculation of total process equipment installation cost. Whereas in operational expenses, the cost of utilities, the cost of raw material required in the process, the annual maintenance and the labor cost have been considered. For the calculation of the same, the results obtained from the simulation of 1 $MtCO_2$ capture capacity have been considered for the further cost estimation of equipment having different sizes and capacity.

Table 5: Additional costs as percentage of purchased equipment cost.

Categories	% of purchased equipment cost
Engineering	12%
Construction expenses	25%
Legal expenses	3%
Contractor´s fee	10%
Contingency	20%
Total process equipment installation cost	**170%**

In order to accurately estimate the total investment required in each scenario, all the equipment and energy system are segregated into 4 major categories: 1) Process equipment, 2) Storage, 3) CSP system and 4) PV system. Based on the different geographical locations having diverse weather conditions, the capacity of various required equipment has found to vary. Hence, the following method of cost estimation has been employed to determine the capital investment more precisely.

5.1.1 Process Equipment Cost

Since the overall costing is comprehensively dependent on the total equipment cost, the cost of each equipment was estimated with an acceptable level of accuracy. Collectively, the broad list of equipment has been segregated into two main segments as shown in Table 13.

i.   Continuous process

In continuous process, most of the equipment employed is conventional and the cost for most of this conventional equipment was evaluated using APEA. Some of this conventional equipment like the filter, slaker, separator, turbine, etc. were oversized to design, procure and install. APEA could not estimate the cost of oversized equipment because of the restriction on the data provided to it. Therefore, their cost was manually evaluated based on available literature data for their maximum designed capacity. Then, this maximum sized equipment was deployed in multiples to meet the actual required capacity of

equipment. In case of non-conventional equipment like the AC, the figures provided in Keith's study are used for the 800 MW CSP capacity model, considering the case of 1 $MtCO_2$ capture capacity. Whereas, for other equipment like pumps, washer, separators, splitters, solid separators and mixers, the additional cost has been approximated to around 102.9 M€ for the Jordan-800 MW scenario, similar to the value specified in the Keith's report.

ii.   Intermittent process

The intermittent process has also conventional equipment like compressor, cyclone, turbine and pumps. However, their costs are estimated manually using the aforementioned method because of the same capacity restrictions from the APEA side. Whereas, intermittent process also consists of many non-conventional equipment like the solar calciner and solid-solid heat exchangers. For the cost evaluation of solid-solid heat exchangers, the proposed cost for the innovative heat exchangers provided by external experts like Solex Technologies has been used. In this research, the required solar calciner capacity was estimated in the range of 275-1200 MW. Maximum capacity of solar calciner has been designed upto 55 MW thermal, which costs around 5 M€ (*29*).

As aforementioned, installation of more than two solar calciners in TT arrangement is technically very cumbersome process. Hence, BD solar calciner arrangement has been considered in this study. For the solar calcination system cost estimation, Meier's study was referred to obtain the correlation for the cost of associated equipment in beam down arrangement like CPC respectively (*29, 30*). Using these values, the overall cost of calciners is estimated by considering the employment of multiple 55 MW solar calciners to fulfill the net CO_2 capture capacity. For example: If the process needs total calcination process capacity of around 1100 MW, then the total of 20 small 55 MW capacity based calciners will be systematically arranged around the solar tower. The overall investment in calciners is calculated simply for 20 calciners.

At the end, all the conventional process equipment were clubbed together to get the total equipment cost for 800 MW capacity. Using this clubbed value, and the process capacity and year factor, the process equipment cost has been estimated for different scenarios through 'Economy of Scale' method. Based on this total cost of equipment involved in intermittent and continuous process, the final installation cost of process equipment is evaluated. As mentioned in Table 5, it involves the cost of installation, engineering, construction, legal expenses, contractor's fee and contingency.

5.1.2 Storage

In this section of the process, two major storage facilities for CaO and $CaCO_3$ have been considered. In order to evaluate the cost of the storage section, the maximum design capacity of the closed storage vessel for solid has been assumed to be 1000 m^3. These storage vessels are considered in multiples to fulfil the total storage capacity demand of the process. As per the correlation (Equation 13) between the cost ($€_{2021}/m^3$) and the designed capacity(m^3) of this storage vessel obtained from literature (*46*), the storage vessel having 1000 m^3 costs precisely 8520.3 $€_{2021}/m^3$. Considering this value as a basis, the overall investment required in the entire storage section has been estimated.

$$\boldsymbol{Cost_{Storage}} = 3156 \cdot CSP^{0.0003 \cdot capacity} \cdot CEPCI \qquad \textit{Equation 13}$$

5.1.3 CSP system

The investment required in procurement and installation of CSP based thermal energy system is distributed into 6 subsections: 1) Heliostat cost, 2) Land, 3) Tower cost, 4) Reflector cost, 5) CPC cost and 6) Kiln additional cost. Each of these investments are evaluated on the basis of separate correlation obtained from Meier (*30*).

i.   Heliostat cost

Heliostats represent the major share of the overall investment required in the CSP system. From the simulation results obtained from HFLCAL for the desired thermal energy output, the required mirror area in the project is obtained. Hence, the lowest marginal cost of the heliostat of 93.32 €/m^2 has been considered (*47*). In general, the share of heliostat in the total CSP equipment investment is found to lie around 71%. Therefore, the cost of the heliostats plays a crucial role in estimating the required investment for CSP system.

ii.   Land cost

For the installation of CSP plant, the suitable land has been chosen for every potential location. Flat, barren, non-industrial and non-green land has been assumed for the installation of CSP plant. Therefore, the cost of land is not expected to be very expensive. The cost of land varies from region to region. However, it has been assumed to be around 2 €/m^2, referring to Meier's report (*30*). Using the HFLCAL simulation software, the optimized area of land required in each scenario is determined. From this correlation and the simulation result, total investment required in the required land is calculated. On an average the land cost is found to share 6% of overall CSP equipment cost.

iii.   Tower cost

Tower is one of the most critical parts of CSP system. Similar to the previously mentioned method, the cost of the CSP tower has been evaluated. The simulation results obtained from the HFLCAL for the tower height of the optimized CSP plant and the correlation between the tower height and the investment obtained from Meier, the cost of tower is approximated (*30*). As stated in Equation 14, the cost of tower (Cost$_{Tower}$) is correlated with height of tower (Tow). It has been observed that the cost of tower shares approximately 6% of total CSP equipment cost.

$$Cost_{Tower} = 27.09 \cdot Tow + 186.75 \qquad \textit{Equation 14}$$

iv. Reflector cost

For the beam down based solar based calcination system, reflectors are additionally used in the CSP plants. In order to calculate the approximate investment required in this section, the correlation between reflector cost ($Cost_{Reflector}$) and the CSP thermal capacity (MW) has been used. This correlation is obtained from the Meier (*30*) and shown in the Equation 20 below. In general, it shares around 6% of the total CS equipment cost.

$$Cost_{Reflector} = 47.6 * CSP^{0.8286} \qquad \textit{Equation 15}$$

v. CPC cost

In the beam down based CSP plants, the additional equipment known as compound parabolic concentrator (CPC) are employed to concentrate the solar irradiation. The cost of this component has been evaluated on the basis of correlation obtained against the CSP capacity (CSP) in MW, as per report by Meier (*30*). Equation 16 below is the exact correlation used for the CPC cost estimation. CPC cost shares around 10% of the total CSP equipment cost.

$$Cost_{CPC} = 27.09 * CSP + 186.75 \qquad \textit{Equation 16}$$

vi. Kiln additional cost

In addition to normal calciner cost estimated in the intermittent process, some extra cost for the arrangements of the system has been considered to integrate the calciners setup and the CSP base tower, and optimize the operation of calcination system. It contributes to 1% of the total CSP equipment cost.

After estimating the investment required for each of these CSP components, the total project investment is evaluated by considering EPCM constant (Engineering, procurement, construction and maintenance) and contingency constant of around 11% and 15% of total equipment cost respectively, as per Meier (*30*).

5.1.4 PV system

For the cost estimation of the PV system, the Greenius simulation software has been used in this study (*44*). This software considers the location based meteorological data and other details of the PV system to approximate the size and cost of the PV system. It provides the facility to specify the cost of operation, cleaning and maintenance. From the simulation results, two types of costs are obtained: i) Capital cost and ii) Project cost. The capital cost includes the cost of equipment involved in the project. Whereas, the latter one includes the additional costs like operating cost, land rent, etc. Referring to Table 6, the project cost of PV system shares only 1% of the total project investment. The annual operating cost of PV is assumed to be negligible in comparison to others.

After performing a detailed cost analysis of each section, the total capital investment of the project is calculated, as shown in the Table 6 below.

Table 6: Distribution of the total capital investment for Jordan-800MW.

Category	Investment (M€)	% sharing
Process equipment	894	53%
CSP system	289	17%
PV system	8.0	0.5%
Storage	0.9	0.1%
EPCM	326	19%
Contingency	161	10%
Total	**1678**	

Annual manufacturing cost consists of 3 major types of non-variating operational costs: 1) Raw materials cost, 2) Utility cost, 3) Maintenance cost and 4) Labor cost. The calculation of these costs is descriptively explained in the following sections.

i.   Raw material cost

In this novel carbon capture process, there is only one additional raw material continuously feed in the process: $CaCO_3$. Coarse particles of $CaCO_3$ are fed to the process and the waste fine particles are filtered out and sent for the

disposal. In order to operate the process continuously, the flow of $CaCO_3$ is maintained constantly. The cost of $CaCO_3$ coarse particles lies around 3.4 €/tCO_2.

ii. Utility cost

The continuous operation of the carbon capture process, demands for two major utilities i.e. water and electricity. As solar based plant, it is situated mostly in the water scarce region and a desalination plant is assumed for continuous water supply. For the same, the levelized cost of the desalinated water of around 1.65 €/t has been considered. In addition to this, the power generated from the PV is equivalent to the power borrowed from the grid connection. As the green power generated from PV system can be comparatively expensive than the grid power, the difference in the rates could build up an additional revenue. However, the real time pricing of the power is location and technology centric. To estimate the utility cost simply, the selling value of PV power has been considered equivalent to the purchasing power cost of the grid. Hence, the annual power cost is considered as negligible.

iii. Maintenance:

As aforementioned, the annual maintenance cost of the entire installation has been assumed to be around 1% of net capital investment in each scenario. Adding this value to the above stated other operational costs, it results into the annual manufacturing cost of the process.

Table 7: Distribution of operating cost for Jordan-800MW.

Category	Annual cost (M€)	% sharing
Maintenance	16.8	55%
Raw material	4.52	15%
Utility	9.22	30%

iv.   Labor cost:

Labor cost has been considered to vary every year. For the initial year, the cost of labor has been assumed to be around 5 M€. The cost involved in the employment of the labor is assumed to compound every year by 8%, which is considered to be a minimum inflation rate. Although it has been considered as a part of manufacturing cost, it is not clubbed with other constant costs and is deducted from the gross profit in the balance sheet.

Summation of all the equipment costs and the manufacturing cost (excluding labor cost) for an entire life time of equipment gives the overall investment required in the carbon capture process.

5.2   Revenue generation

In order to understand the economics of carbon capture process, the revenue generated from the carbon capture business is separated into two fragments: i) Carbon Tax; ii) Sales of CO_2. These are the two main possibilities of revenue generation considered in this research.

5.2.1   Carbon Tax

Under section 45Q of the Energy Improvement and Extension Act of 2008, the carbon credits could be issued for the sequestration of CO_2 (*48, 49*). It acts as a performance based incentivizing carbon capture and sequestration or utilization. The major intention of Internal Revenue Service (IRS) department for the environmental protection in designing this section was to support the deployment of CO_2 enhanced oil recovery. This has resulted into subsequent reduction in the energy prices.

For the carbon capture technology installed after 2018, the carbon credit is separately valued under many subsections for permanent sequestration and utilization in the Enhanced Oil Recovery (EOR) or Natural Gas Recovery (NGR) purposes. The carbon capture capacity above 500,000 metric tons qualify for the value of 50 €/tCO_2, if it is

further utilized. However, if the annual capture capacity does not cross the 500,000 scale, then the credit value of 35 €/tCO$_2$ for the EOR application, which is also considered in this study.

European emission trading system (ETS) is world's biggest carbon trading system, sharing around 45% of the world capacity. According to the report by the internal revenue services, the carbon credits issued for the carbon capture and further utilization variates from 22.6 to 50 €/tCO$_2$ for year 2016 to 2025 (*48*). However, these values are estimated to rise in the near future because of a number of events happening across the world like rising awareness of the climate change, surging global economy, etc. As per the report by Reuters, the credit value for the carbon capture and utilization has been forecasted to rise higher than an average value of 55 €/tCO$_2$ (*50*). Using this value, the annual revenue generated by selling carbon credits is calculated for each scenario.

5.2.2   Sales of CO$_2$

In addition to the credits obtained from industry partners in exchange of capturing carbon, the selling price of the captured CO$_2$ is also considered in the economic analysis of process. Initially, the current selling price of CO$_2$ of around 75 €/tCO$_2$ in industries like beverage industry was considered as an initial guess value for economic analysis.

5.3   Balance sheet

Based on the annual revenue generated and the annual manufacturing cost, the balance sheet of the carbon capture unit has been developed with the help of assumptions and considerations, as shown in Table 8.

Table 8: Assumptions and considerations in economic analysis.

Parameters	Values
Lifetime of plant (n)	25 years
Loan interest rate (r)	1.43 (*51*)
Weighted average cost of capital (WACC)	7.5%
Taxation rate (%)	30%
Increment of carbon tax	€5 every 5 years
Increment in labor cost	8% every year
Amortization value	50 M€
Procurement and installation period	2 years

As per the research published by Keith and Meier, the lifetime of equipment is considered to be 25 years. Plus, the loan interest rate is referred from the statistics provided in the report by European central bank. Based on these assumptions, the annual depreciation is calculated using the amortization value, lifetime of assets and initial capital investment (Capex). As per the Equation 17, the depreciation constant value for all years is calculated using the straight-line method. Further, the Estimated Annual Installment (EAI) is also figured out using the Equation 18 stated below.

$$Annual\ depreciation = \frac{(Capex - Amortization)}{Life\ time\ of\ years} \qquad Equation\ 17$$

$$EAI = \frac{Capex \times r \times (1 + r)^n}{(1 + r)^n - 1} \qquad Equation\ 18$$

As shown in the Table 9 and Table 12, the manufacturing cost is subtracted from the annual revenue generated to get the Gross Profit (GP). From this GP, the annual labor cost is deducted to get the Earnings before Interest, Tax, Depreciation and Amortization (EBITDA) of process. Further, the aforementioned annual depreciation amount is deducted to get the Earnings before Interest and Tax (EBIT) value.

For every year the interest value is calculated separately based on the net principal loan amount, except for the installation years. This interest is deducted from the EBIT to get the Profit before tax (PBT). Tax is levied further over this PBT value to get the Profit after tax (PAT) value. Depreciation is added back to the PAT value to get the cash flow of the year. From the above calculated EAI, the interest over the loan amount is subtracted to calculate that small part of loan included in EAI, which is also referred as principal. This principal value is further subtracted from the cash flow to get the net annual profit of the carbon capture business.

In the following year, the loan amount is slightly reduced because of the principal paid in the previous year. Hence, the interest amount in the following year is comparatively low and the principal paid for constant EAI is higher. These steps are further repeated for every year to calculate the annual cash flows and the net profit. Ideally, the constant rise of cash flows and the net profit is expected with increasing revenue and decreasing interest amount.

Procurement and installation period is an anomaly for the above-mentioned steps of developing annual balance sheet. In these years, the total capital investment of the project is distributed equally as a manufacturing cost. As no revenue generation is assumed in these years, all the later steps are skipped. Therefore, the net cash flows for this period are nothing but the mean project capital investment. The detailed balance sheet for 25 years of duration is represented by Table 12 as shown in 9.3.2**.**

5.4   Economic parameters

From the estimated capital investment and the annual operational cost of the project, it is difficult to judge the potential of the business as well as predict the returns. Hence, the economic indicators like payback period, turnover period, Net Present Value (NPV), Return Over Investment (ROI), etc. are extremely helpful for many investor, bankers or financial professionals in summarizing the economics of any business case. Some of these major indicators have also been precisely evaluated in this research.

Payback period denotes the number of years required to equalize the cumulative cash flow with the capital investment. Depending on industry, the payback period is

acceptable up to a certain number of years. As shown in Table 9 of 9.3.2, the payback period is calculated from the annual cash flow.

Turnover ratio is the ratio of annual revenue generated to the total capital invested initially. Net present value (NPV) is the value explaining if the project worth more than it costs. This helps in evaluating the actual return that the investors can claim if they invest the same amount in the capital markets. By calculating the NPV value, the net value of annual cash flows is estimated to the present day. Therefore, the NPV is nothing but the summation of the discounted future cash flows at a defined discounting rate. If NPV is positive, then the business is profitable and vice versa. For zero NPV, the discounting rate is referred to as the internal rate of return (IRR) (*52*).

These economic parameters were repeatedly determined for all 16 techno-economically optimized scenarios. The results are vividly discussed in the results and discussion section.

5.5 Levelized cost of carbon capture

In order to compare various methods of carbon capture having different technologies, the levelized cost is found to be a very helpful parameter. The levelized cost of carbon capture ($LCOC_{BS}$) presents the net present value of the total investment in the carbon capturing plant and cost per ton of CO_2 throughout its lifetime. It depicts a clear picture of the profitability of business. It is nothing but the minimum selling price of CO_2 when the zero NPV value is attained. Generally, if the levelized cost of the product is estimated to be more than the selling price of the product, then the investment does not result into good returns.

One of the easiest methods to calculate the levelized cost is the consideration of only WACC and the lifetime of assets, which is denoted as $LCOC_{WACC}$. In this study, the WACC and the lifetime of the equipment is assumed to be around 7.5% and 25 years respectively. Using these parameters in Equation 19 and Equation 20 for all the 16 scenarios, the levelized cost has been calculated. As Keith has also evaluated the levelized cost through this simplified method, the $LCOC_{WACC}$ values are compared with the Keith's values.

$$CRF = r \times \frac{(1+r)^n}{((1+r)^n - 1)}$$

$$LCOC_{WACC} = \frac{Capex \times CRF \times n + Opex_n}{Carbon\ captured_n}$$

The levelized cost estimated through the previous method majorly focuses on only two parameters. However, there are numerous other factors, which plays a crucial role in the more realistic business case. In this research, there are three additional parameters considered in the second calculation method of levelized cost: Loan interest rate, Carbon tax and Taxation over the profits. The aforementioned values for all these parameters are considered in the balance sheet based levelized cost calculation method. $LCOC_{BS}$ is nothing but the value of selling price in the balance sheet, which nullifies the NPV. Hence, at the given set of values for those parameters, the $LCOC_{BS}$ is capture cost obtained at zero NPV by variating the selling price in the balance sheet for 16 scenarios.

Further, the $LCOC_{BS}$ results obtained for all the 16 scenarios are categorized on the basis of CSP capacity and different potential locations. In addition to this, the influence of various economic parameters has been broadly studied through a detailed sensitivity analysis, which is discussed in the following section.

6 Results and Discussion

With the aim of avoiding ~34% of fossil-based carbon releasing from the outlet of process, the novel HT-DAC process was designed for solar application. After simulating the process in the ASPEN software, the results obtained were quite undesirable. Because the energy analysis indicated the energy saving potential in unoptimized process. In order to enhance the process efficiency as well as to make it scalable, the sensitivity analysis of various influential parameters was performed to understand the extent of impact on process.

6.1 Sensitivity Analysis

Commonly used sensitivity analysis tool available in the ASPEN software was employed to study the influence of parameters like temperature in pellet reactor, water flow in the heat recovery systems, calciner conversion efficiency, outlet pressures in the turbines and pressures in condenser pump outlets. As shown in the Figure 13 below**,** the effect of variation in the turbine outlet pressure on the power output was determined. The results of sensitivity analysis of other parameters are added further in the section 1.1. Through this analysis, the dynamics in variation of these parameters were carefully studied, and later tuned appropriately to get the most optimized version of HT-DAC process. For example: Considering the impact of sensitivity analysis on Turbine-1 power output, pump and turbine outlet pressure has been optimally set to 3300 and 100 kPa. This result in 21.22 MW of electrical energy generation in Turbine.
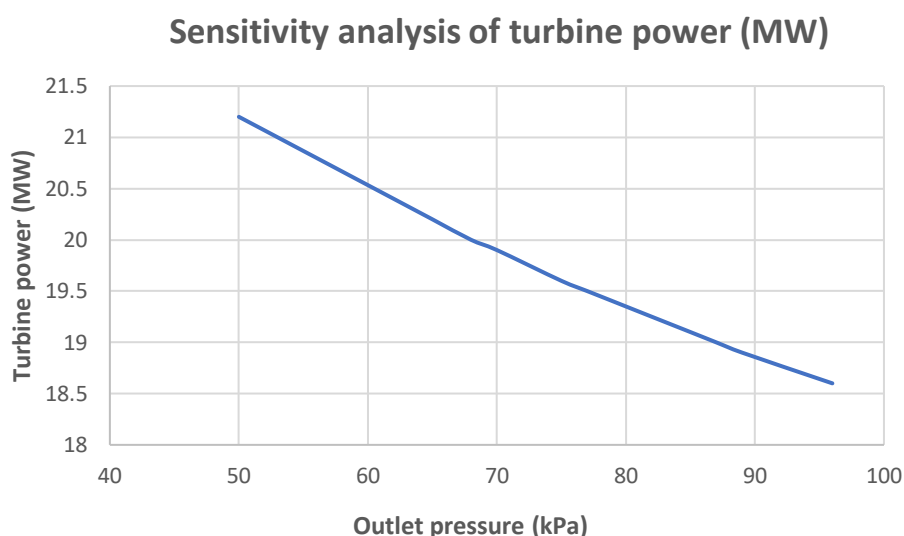
Figure 13: Sensitivity analysis of turbine power for 1 MtCO$_2$ capacity.

Keju's has considered multiple factors like relative humidity and mass transfer coefficient of the AC unlike ASPEN. Hence, results obtained from the Keju's research were considered in this study to find a correlation for water loss as well as power consumption, using Equation 11 above.

Further, the influence on overall power generation from both the turbines was meticulously studied by performing the sensitivity analysis of multiple parameters like condensate pump pressure, water flow rate in the cycle, and the condensate pressure on outlet of turbine. As the energy recovery systems are interconnected and potentially affect each other during the calcination hours, the effect of similar parameters from both heat recovery systems were analyzed. With gradual rise of water flow rate in steam cycle has led to decreased steam temperature after collecting the waste heat, which further resulted in the decreased power generation in the cycle. Besides, the increment in the turbine outlet pressure has resulted into non-linear decrease in the power generation. The results obtained were found to be in line with the thermodynamic efficiency estimation method. The results of the rest of sensitivity analysis has been added in the section 9.6.

As the renewable energy is quite intermittent in nature, the influence of the climatic conditions at different locations and the capacity of CSP has been studied. For the same, 16 scenarios were considered in total having 4 CSP capacities and 4 potential locations. In the Figure 14 shown below, the carbon capture capacity obtained from the techno-economically most optimized process at different locations has been plotted.

Annual carbon capture capacity
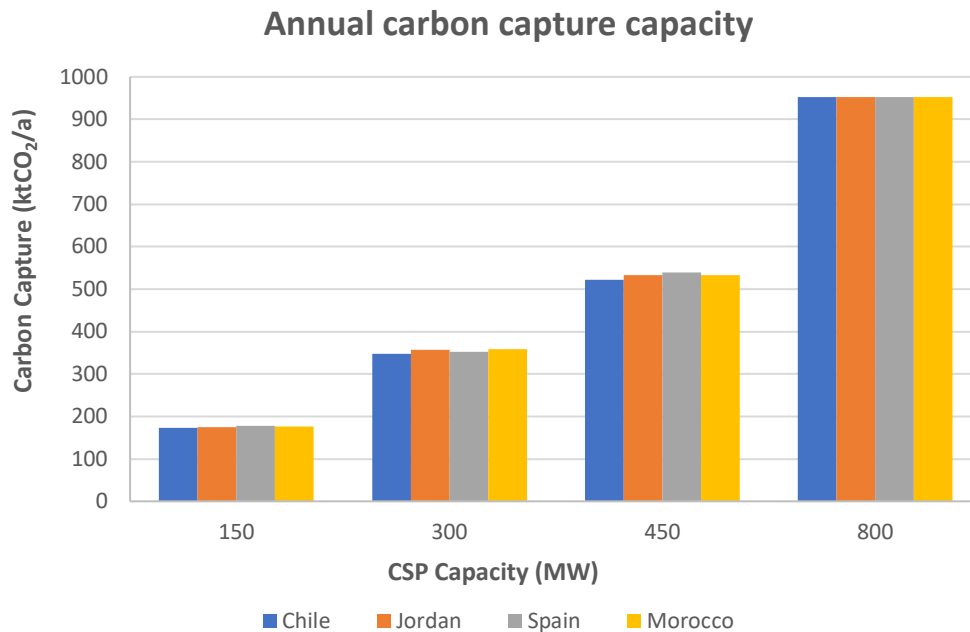
Figure 14: Annual carbon capture capacity for 16 scenarios.

By variating only calciner design capacity, the change in capture cost has been studied for all 16 scenarios. Figure 15 is the graphical representation of the same sensitivity analysis for scenario Jordan-800MW. Initially, the slant curve of decreasing capture cost with rising calciner design capacity has been noticed in a plot illustrated in Figure 15. For 500 MW design calciner capacity, the general cost of capture has been calculated to around 150 €/tCO$_2$. The cost continues to further reduce non-linearly to reach the local minimum of the graph, which indicates the optimal capacity of calciner. The local minimum has been indicated with the red bar in the plot.

Beyond the optimum capacity, very slight increment in the cost of capture has been observed because of the increased capital investment for the higher solar calciner capacity. This study of the influence of design calciner capacity on the cost of capture result into techno-economically optimized version of process, which indirectly result into attaining the lowest cost of carbon capture.

Because of this techno-economic optimization of process of every scenario, uneven trend in carbon capture capacity for any specific location at different CSP capacities has been observed. This uncommon trend in carbon capture capacity is illustrated in Figure 14. For example: compared to Jordan, Spain has higher carbon capture capacity

at 150 MW by around 300 tCO$_2$/a. Whereas, Spain shows lower capture capacity than Jordan at 800 MW with a net difference of 120 tCO$_2$/a. This plot indicates that every location favors different CSP capacities for the competitive DAC capacity.

Figure 15 represents the variation of carbon capture cost with the changing design capacity of solar calciner. For every scenario considered in this research, similar trend has been observed.

Calciner design capacity variation
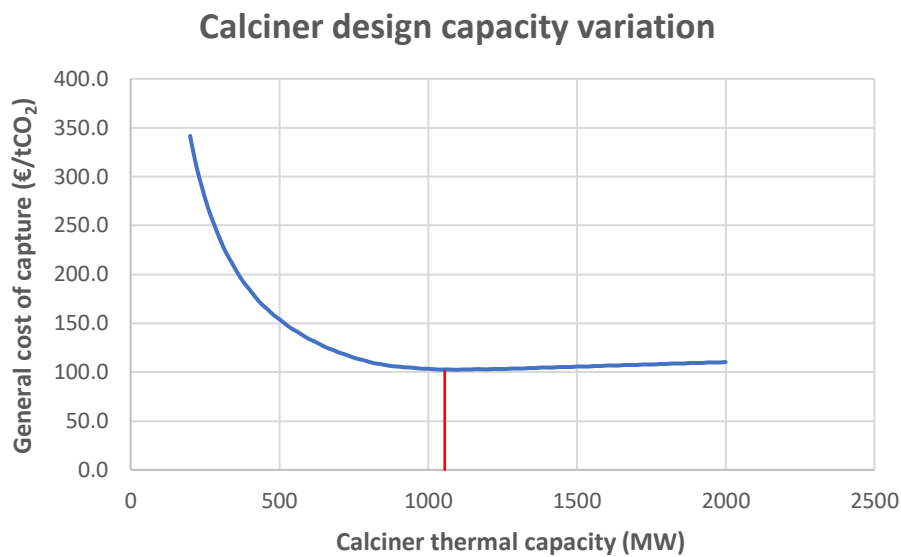
Figure 15: Influence of the calciner design capacity on capture cost for Jordan-800MW.

6.2 Utility consumption analysis

To meet the process demands, the CSP and PV system installations are already considered at locations having high DNI. However, most of these locations are situated in the water scarce regions. Hence, it is quite important to understand the influence of climatic conditions at different locations on water and power consumption.

In ASPEN simulation, the water and energy consumption has been initially optimized by performing a closed loop heat integration of process and by recovering energy from waste heat though turbines. This resulted in more than 50% of energy savings. Using these values in the energy analysis, the following plots for water and power consumption are obtained for techno-economically optimized 16 scenarios.
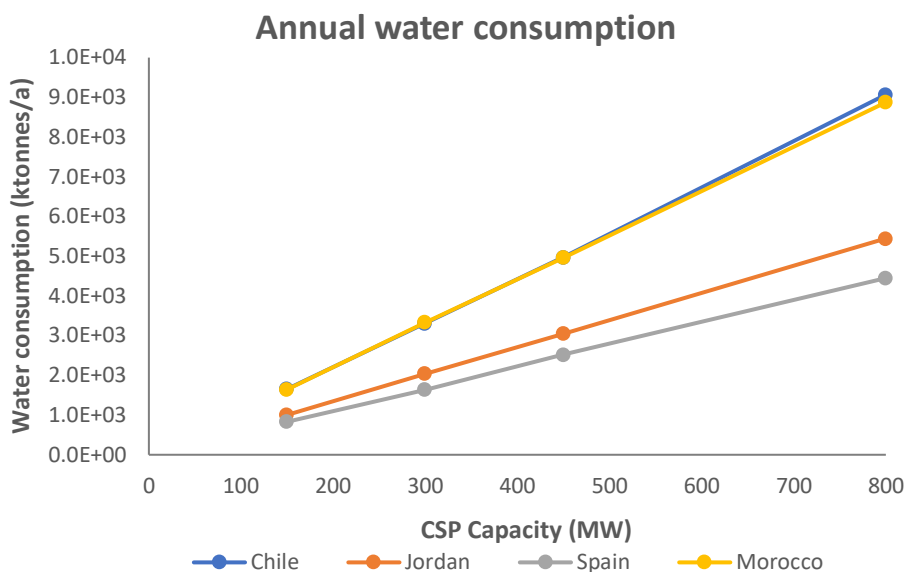
Figure 16: Water consumption results for 16 scenarios.

In Figure 16, water consumption has been observed to vary linearly with the CSP capacity. For the case of Morocco and Chile, water losses are found to be broadly overlapping with each other. When compared to the Keith's model having water losses of 4.7 tH_2O/tCO_2, Morocco-800MW and Chile-800MW scenario showcase the total water loss of around 9.3 and 9.5 tH_2O/tCO_2 respectively. Whereas, the analysis of Spain-800MW and Jordan-800MW scenario result into comparatively lower water losses values of around 4.7 and 5.7 tH_2O/tCO_2 respectively. From this analysis, it resembles that Spain could be a most favorable location for the solarized HT-DAC process from the water conservation point of view.

In addition to water consumption, the effect of climatic conditions on the overall consumption of power is also analyzed. For in-depth study of the power consumption, the simulation-based results are used with the estimated power consumption in various equipment, as per the method discussed in the power estimation method.

From Figure 17**,** the consumption of power varies linearly with CSP capacity. The total power consumed in Jordan and Chile based installations are found to be equivalent and maximum values are observed in the case of Morocco. Based on the variation in relative humidity and dry bulb temperature observed every hour of the year, hourly power consumption in AC has been calculated. Then, the annual sum of energy

required in AC is determined and compared with the Keith's results of 82 kWh/tCO$_2$. As shown in Figure 18, all locations are found to have relatively less power demand ranging from 58-76 kWh/tCO2

with Spain being the lowest. The red line marked on the graph indicates the result from Keith's research.
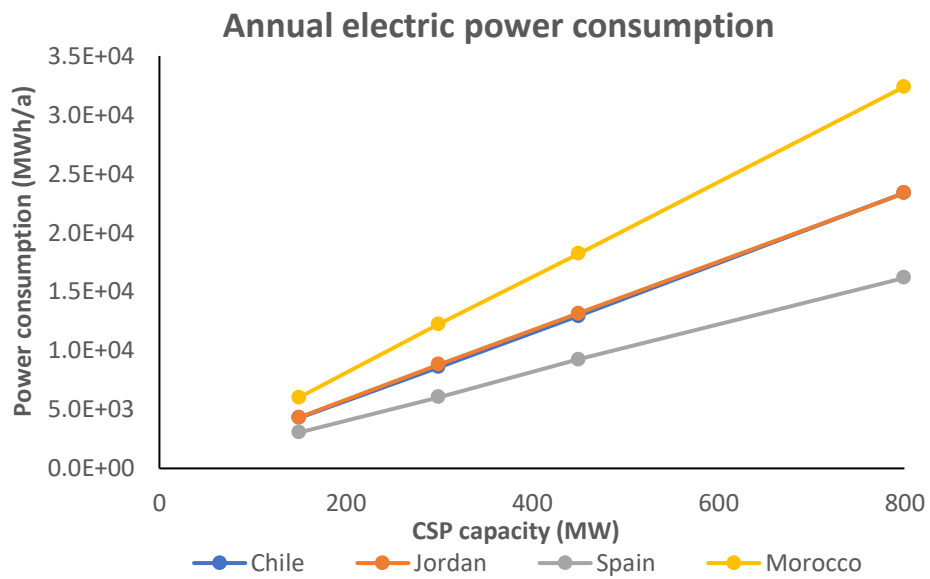
Figure 17: Power consumption results for 16 scenarios.
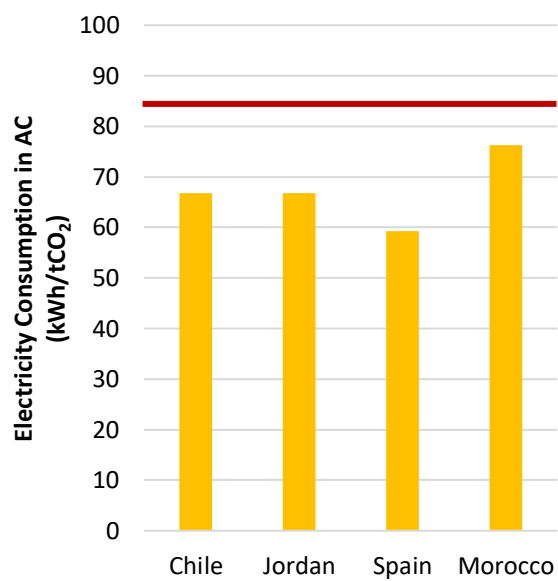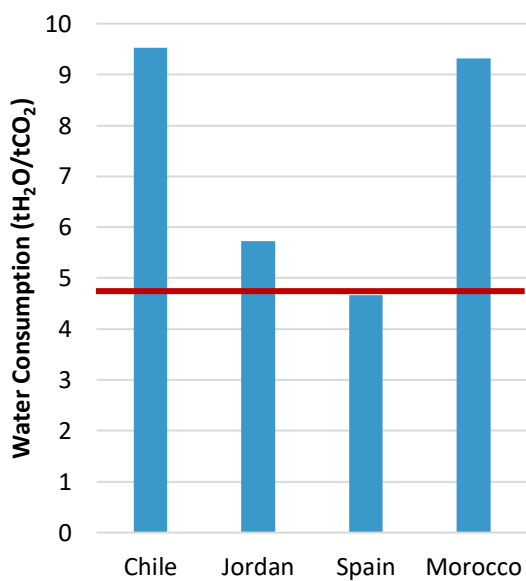
Figure 18: Utility consumption for 4 locations at 800 MW.

In order to understand the dynamics of power demand of the process, the novel method has been employed, which is explicitly explained in the section 4.5. From this calculation, the daily trend in the operational power demand has been observed throughout the year and it is shown in Figure 19. From this plot, generation of excess power from the entire process during non-solar hours of the day has been observed. Also, an additional power demand during solar hours of a day has been noticed.

Hourly power demand profile
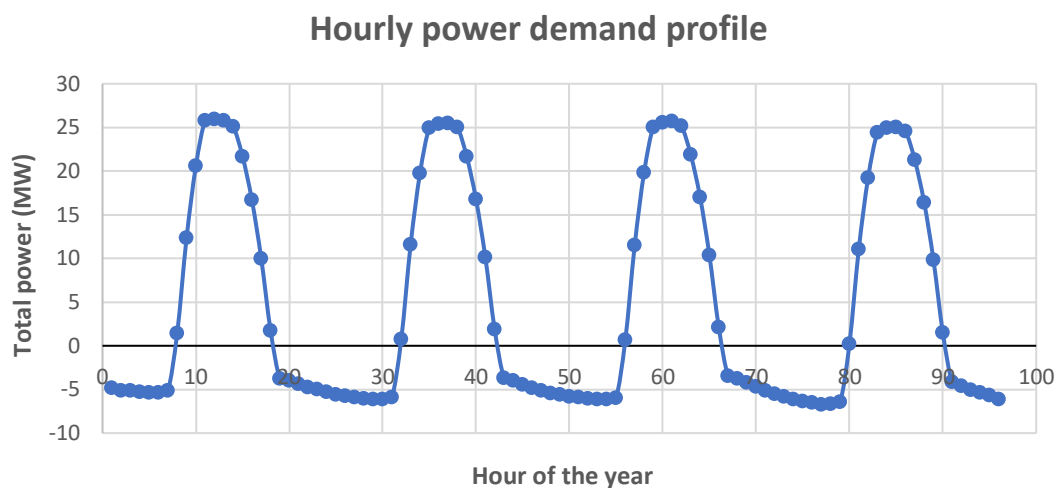
Figure 19: Hourly distribution of power demand.

With the curiosity to learn about the main contributors in this power demand profile, a detailed distribution of the energy flow during both solar and non-solar hours has been calculated and plotted in Figure 21 and Figure 21 respectively. In the waterfall chart shown in Figure 20, the energy demand and energy supply during solar hours are visualized. For the case of most cost-effective scenario Jordan-800MW, the net energy demand is estimated at around 3627 kWh/tCO$_2$.

The red colored bar indicating thermal energy demand of calciner shares around 88% of the total energy demand. On the power side, compressor, AC and miscellaneous applications share around 8%, 2% and 2% respectively. To fulfil the power demand, Turbine-1 and Turbine-2 generate around 195 and 97 kWh/tCO$_2$ respectively. These

sources of energy require an additional support from the PV plant contributing just 1% of total energy supplied. Moreover, grid power is also used, which shares around 17% of the total power supplied. Miscellaneous section considers the utilization of the power in equipment like pumps, air cooled heat exchanger, mixers, filters, etc.
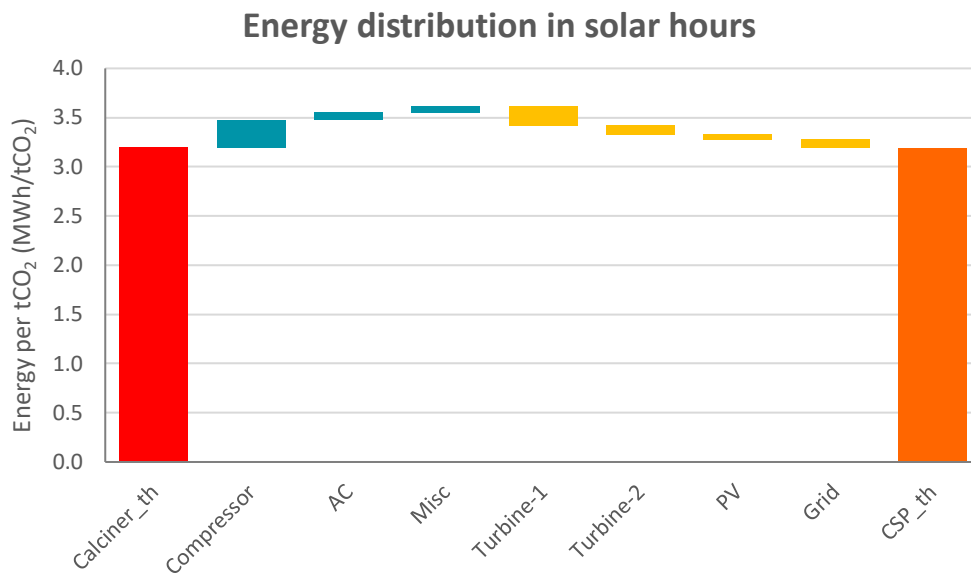
Figure 20: Energy distribution during the solar hours for Jordan-800MW.

In the case of non-solar hours, the intermittent part of process is not operating during this period. Therefore, thermal energy demand in the calciner, power demand in the CO_2 compressor and the power generation from Turbine-2 are not considered. Along with this, the PV plant will not be generating any power. Hence, only AC, miscellaneous equipment and Turbine-1 will be involved for energy flow during these hours. Both the AC and miscellaneous application of power equivalently share the total energy demand of around 115 kWh/tCO_2. In heat recovery system, turbine not only offsets the total power demand but also produces excess of energy of around 80 kWh/tCO_2 during the non-solar hours operation, shown as pale green section of the Turbine-1 bar in Figure 21. The same amount of energy is supplied back to the grid, displayed as an olive-colored bar.

Energy distribution in non-solar hours
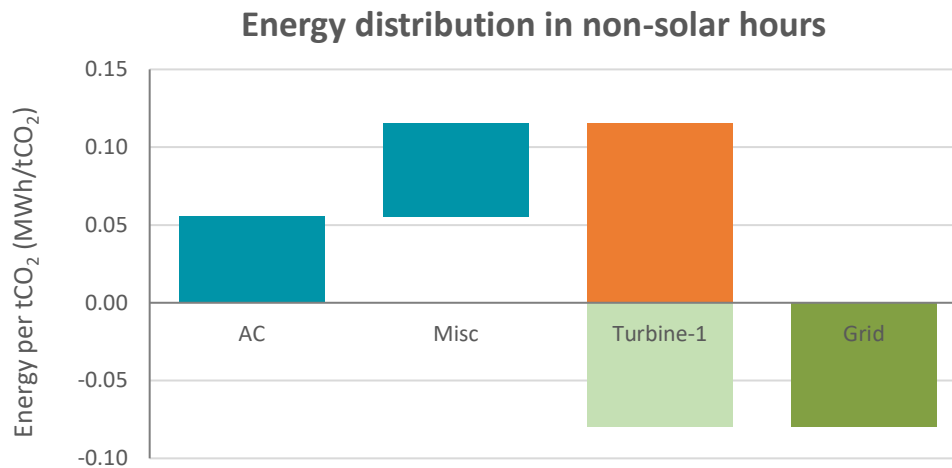
Figure 21: Energy distribution during non-solar hours for Jordan-800MW.

Based on this energy distribution analysis, the annual additional electric energy demand of process is estimated to be 23.35 GWh/a. Based on the specific yield efficiency of 5.32 kWh/kW$_p$, the accurate peak power load of 12 MW for the scenario of Jordan-800MW has been calculated. Similar, the calculation has been repeated for the other scenarios and the energy demand is found to lie in between 3000 and 32,500 MWh/a. In addition to this, the energy distribution broadly helped in quantitively understanding the major energy consumers and the producers. Using this peak power load value and the meteorological dataset of Jordan in the Greenius software, the equipment and installation cost of the PV plant has been further estimated for Jordan-800MW case to around 6.75 M€ and 8.02 M€ respectively.

6.3 Economic analysis

In order to perform the detailed economic analysis, the capital investment and the operating cost involved in every scenario has been evaluated as per the method explained in the cost analysis section. Capital investment in the 16 scenarios ranges from 535 to 1765 M€ and the operational cost for 25 years have also been found to lie in between 260 and 850 M€.

Before estimating various of the aforementioned economic parameters, the levelized cost of the captured carbon (LCOC$_{WACC}$) is determined. According to the method stated in section 5.5, the levelized cost of 16 scenarios has been determined, assuming the life time of equipment (n) of around 25 years and discount rate (r) of 7.5%.

After calculating the levelized cost of carbon capture, it is further compared with the results obtained from the Keith's analysis. Keith has considered multiple energy scenarios and therefore, has a set of values for the current year ranging from 108 to 181 €$_{2021}$/tCO$_2$ approximately. In comparison to these, the values for the 800 MW installations having mega tons capacity are found to be quite comparable. The cost of capture for 4 locations are estimated to lie between 178 and 201 €$_{2021}$/tCO$_2$. Out of all the locations, Jordan has the lowest LCOC$_{WACC}$ value.
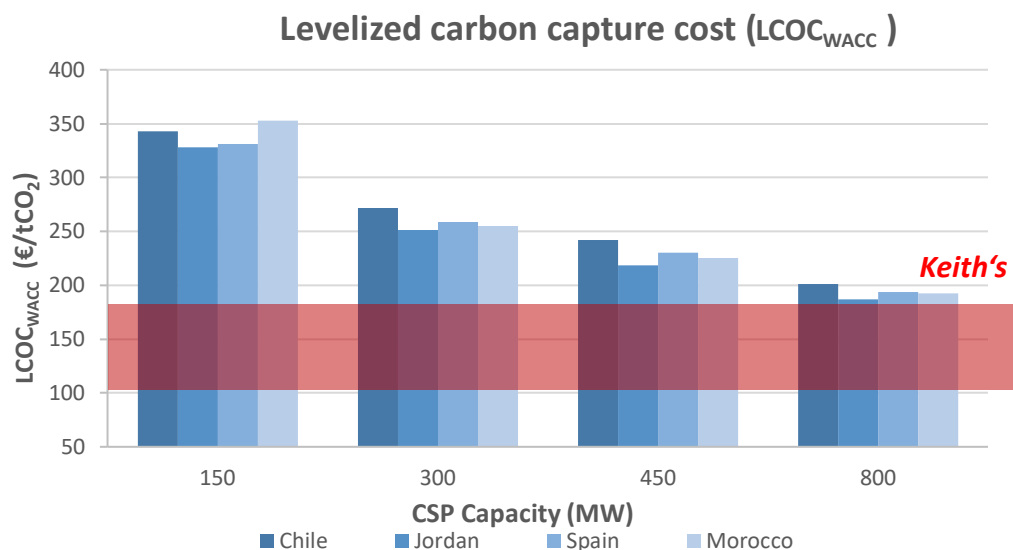
Figure 22: Levelized cost of carbon capture (LCOC$_{WACC}$) for 16 scenarios.

From the above analysis, the LCOC$_{WACC}$ values were majorly estimated to compare the carbon capture cost with the CNG based Keith's process, which is shown as red bar in Figure 22. It can be inferred from the previous analysis that Jordan seems to be a suitable location from an economic point of view to install the solarized version of Keith's process. Along with this, the CSP favored locations also found to have a competitive LCOC$_{WACC}$ in Figure 22 above. For example, the LCOC$_{WACC}$ for Morocco is

lower than the LCOC$_{WACC}$ for Spain in most of the cases. This indicates that the solarization of HT-DAC process is not restricted with only CSP favored locations.

Even though the previous mentioned method of LCOC$_{WACC}$ calculation considers the discount rate and the life time of equipment, the real-life carbon capture plant scenario is quite different. In order to understand the carbon capture business case, a financial model is developed. It consists of a balance sheet, an annual income statement and a cash flow statement. All these economic documents contain the revenue generated in business, the annual manufacturing cost, taxes over profit, EAI, cash flows, net annual profit, etc.

To apprehend the carbon capture business case in a more realistic way, the balance sheet for the total of 25 years of lifetime was developed. Table 12 in 9.3.2 indicates the balance sheet for 27 years for the case of Jordan-800MW, including the procurement period of two years. The revenue found to be constant for every 5 years and then slightly increased due to 5 €/tCO$_2$ rise in carbon tax has been considered. Plus, the labor cost is also considered to rise every year by 8%, leading to the total labor cost from 5.4 to 34.2 M€/a. In addition to this, the decreasing trend of interest paid ever year and increasing trend of principal paid as a part of annual installment has been noticed. Because of which, the 30% taxation levied on the profit EBIT is found to increase every year. Still, the PAT and annual cash flows have been noticed to rise every year.

Table 9: Balance sheet for first six years of operation.

Year	-1	0	1	2	3	4	5	6
Interest			_23.99_	_23.19_	_22.37_	_21.54_	_20.70_	_19.85_
Principle			56.3	57.1	57.9	58.8	59.6	60.4
Balance			_1621.4_	_1564.3_	_1506.4_	_1447.6_	_1388.1_	_1327.6_
Carbon tax			55	55	55	55	55	60
Annual Balance Sheet ($M)	**Procurement and installation period**		**Operation period**					
Total Earnings	_0.00_	_0.00_	_244.94_	_244.94_	_244.94_	_244.94_	_244.94_	_249.70_
Maufacturing Cost	-838.86	-838.86	-27.16	-27.16	-27.16	-27.16	-27.16	-27.16
Electricity			0.0	0.0	0.0	0.0	0.0	0.0
Gross Profit	_-838.86_	_-838.86_	_217.78_	_217.78_	_217.78_	_217.78_	_217.78_	_222.54_
Labor cost	0	0	-5.4	-5.8	-6.3	-6.8	-7.3	-7.9
EBITDA	_-838.86_	_-838.86_	_212.38_	_211.95_	_211.48_	_210.98_	_210.43_	_214.61_
Depreciation	0.0	0.0	-65.1	-65.1	-65.1	-65.1	-65.1	-65.1
EBIT	_-838.86_	_-838.86_	_147.27_	_146.84_	_146.37_	_145.87_	_145.33_	_149.50_
Interest	0.00	0.00	-23.99	-23.19	-22.37	-21.54	-20.70	-19.85
PBT	_-838.86_	_-838.86_	_123.28_	_123.65_	_124.00_	_124.33_	_124.62_	_129.65_
Taxes @30%	0.00	0.00	-36.98	-37.10	-37.20	-37.30	-37.39	-38.89
PAT	_-838.86_	_-838.86_	_86.30_	_86.56_	_86.80_	_87.03_	_87.24_	_90.75_
Cash flows	**-838.86**	**-838.86**	**151.41**	**151.67**	**151.91**	**152.14**	**152.35**	**155.86**
Principle			-56.30	-57.11	-57.92	-58.75	-59.59	-60.44
Net profit			_95.11_	_94.56_	_93.99_	_93.39_	_92.76_	_95.42_

After developing balance sheet-based model like Table 9 for every scenario, the NPV was nullified by variating the selling price of CO_2. This selling price indicates the realistic levelized cost of the carbon capture ($LCOC_{BS}$). In Figure 23 below, the variation of $LCOC_{BS}$ has been visualized for 16 scenarios. When compared to previously calculated $LCOC_{WACC}$ values, $LCOC_{BS}$ has always found to be greater, and the difference in these values has been observed to decrease gradually with rise CSP capacities.
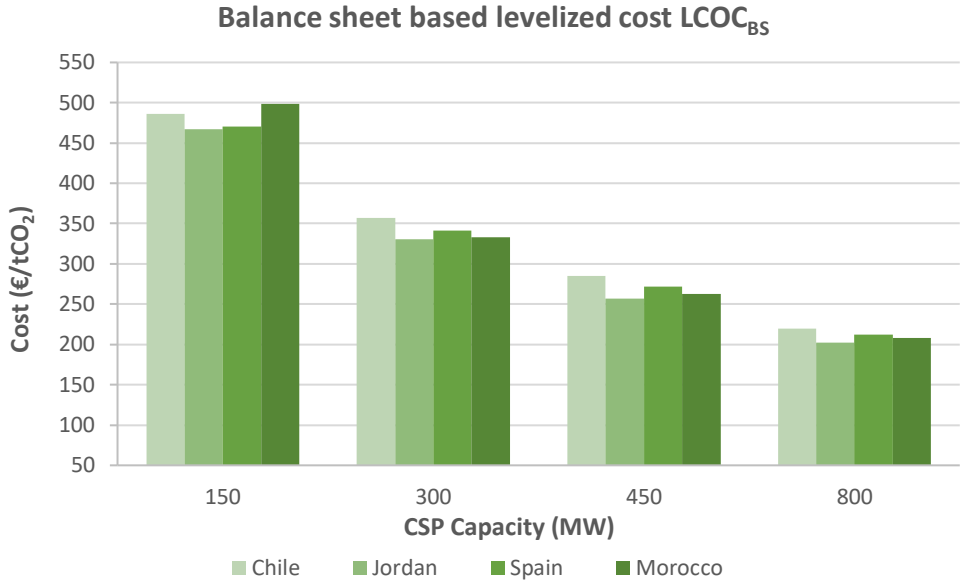
Figure 23: Levelized cost of carbon capture ($LCOC_{BS}$) for 16 scenarios.

This analysis was helpful in getting the realistic view of carbon capture business. In order to find a general CSP capacity, which will meet the Keith's maximum cost of 181 €/tCO_2. This capacity of CSP is called the break-even capacity. As shown in the Figure 24 below, the break-even capacity of CSP is estimated to be around 624 MW. Beyond this capacity value, the cost of the capture ($LCOC_{WACC}$) is expected to decrease further.

Break even CSP capacity for 181 €/tCO$_2$
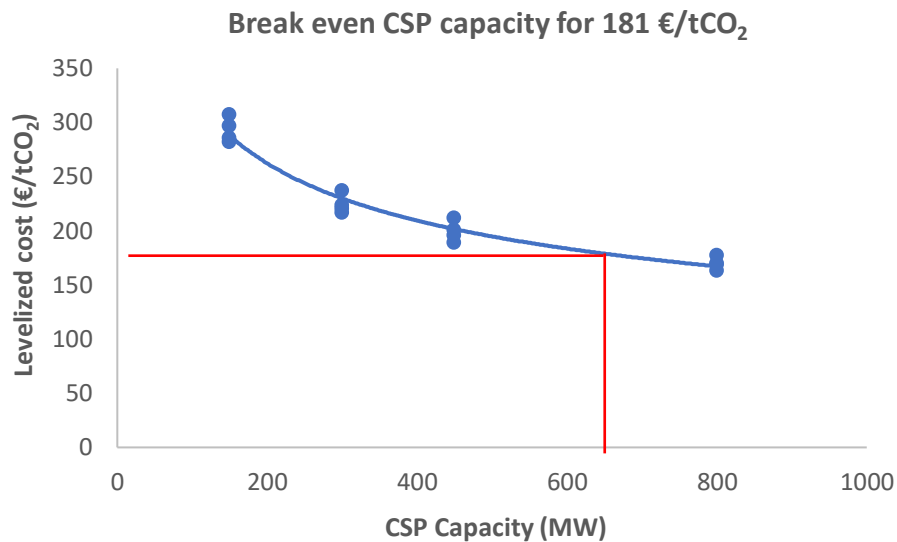
Figure 24: Break-even capacity for CSP technology.

Post rigorous estimation of LCOC$_{WACC}$ and LCOC$_{BS}$, the cost has been further diligently analyzed to investigate the reason for higher capture cost. From the investment distribution shown below in Figure 25, more than 50% of investment is found in the process equipment, making it the major cost share holder. When this analysis performed for other CSP capacities, the sharing of process equipment cost was found to grow further with lower capacities. After investigating further in the process cost, more than 60% of the investment is involved in three main reactors, i.e. Solar calciner, Pellet reactor, and Air contactor, as shown in Figure 26. Each of these pieces of equipment is sharing more than 20% of the investment for process equipment. This indicates that the cost of carbon capture is majorly dominated by the continuous process than the intermittent process.

Distribution of capital investment
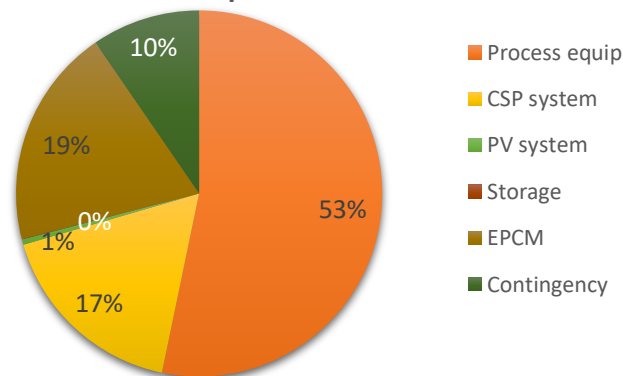
Figure 25: Distribution of capital investment required for Jordan-800MW.

Figure 25 and distributions of capital investment in other scenarios have indicated that the investment for the CSP energy system is comparatively lower than for the other equipment. Plus, sharing of the investment for the PV plant is just 1% of the total investment, as a very small capacity of PV installations is required to fulfil the annual power demand of process. If the total investment is segregated on the basis of intermittent and continuous process, the continuous process has found to dominate over the intermittent process with a minimum 65% sharing. Hence, it can be inferred that the continuous part is the main influencer in carbon capture cost.

In addition to this, the storage section has found to have negligible contribution in the overall investment as shown in Figure 25. Therefore, any further advancement in the equipment employed on the continuous side could significantly help in reducing the solarized HT-DAC.

Distribution of investment in process equipment
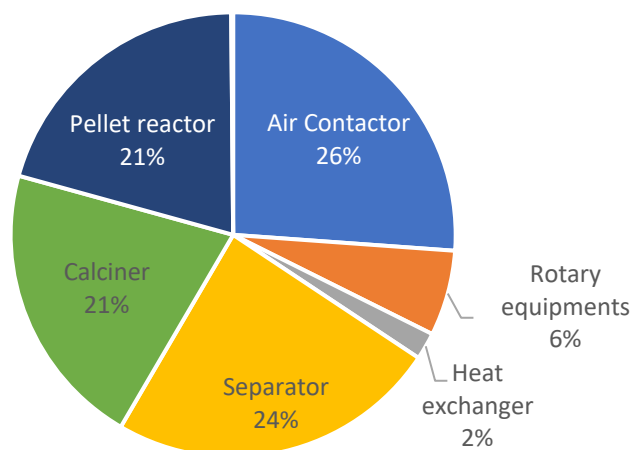
Figure 26: Distribution of investment required in process equipment for Jordan-800MW.

Additionally, the influence of the economic parameters on the $LCOC_{BS}$ values has been studied by performing an extensive sensitivity analysis. Equity of the company can be shared in exchange of the funding at zero percent. Therefore, the impact of funding in exchange of equity ranging from 0 to 100% on the $LCOC_{BS}$ value is described in the Figure 27. From this analysis, the funding received at zero interest rate is absolutely helpful in reducing the $LCOC_{BS}$. However, the impact is not laudable because only the interest well be saved over a required small loan

amount. Similarly, the variation in discount rate has been studied from 2.5% to 12.5% in Figure 27. The trend line for discount rate has comparatively higher slope, resulting into substantially low $LCOC_{BS}$ values at lower discount rates. For example, at discount rate of 2.5%, the $LCOC_{BS}$ value tends to reach 100 €/tCO$_2$.
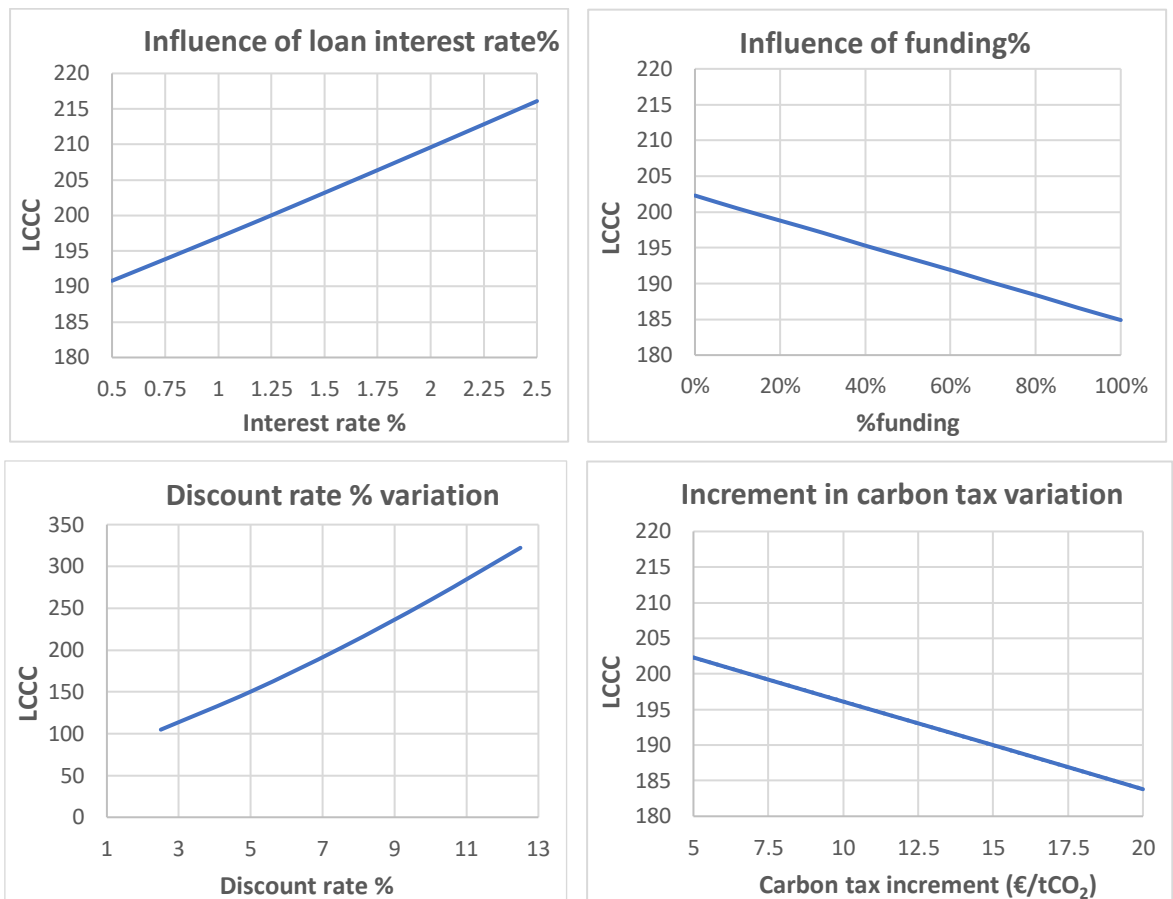
Figure 27: Sensitivity analysis of economic parameters on LCOC$_{BS}$.

Following the same procedure, the impact of variation in increment of carbon tax has been studied, which is considered to be 5 €/tCO$_2$ rise every half decade. For the results visualized in Figure 27, it can be inferred that this factor has miniscule impact on the $LCOC_{BS}$. Although the $LCOC_{BS}$ is found to decrease from 203 to 184 €/tCO$_2$ when the increment in carbon tax is happening at four times higher rate than normal rate, the change in $LCOC_{BS}$ is quite insignificant. Moreover, the loan interest rate is varied in the range of 0.5% to 2.5%. Since European countries already have lower interest rate, the $LCOC_{BS}$ values of this process installed in

countries having higher interest rates was a topic of interest. It actually causes rise in the LCOC$_{BS}$ values linearly.

Moreover, this study has also considered the influence of the differential power cost. The carbon capture process produces excess of green energy during non-solar hours and borrows required energy for operation during the solar hours. As this research is not majorly focused on timely energy production and effect of it on the final LCOC$_{BS}$ cost, no difference in the electric energy cost has been assumed. However, from the calculation of the Jordan-800 scenario, the possibility of significant amount of additional revenue generation is expected. This motivates to perform the sensitivity analysis of the difference between the cost of purchased and sold grid electricity to understand its effect on the LCOC$_{BS}$. Figure 28 shows the linear variation with a very minute slope in the trendline. It signifies that the constant difference in power value (ΔC) has a shallow effect on LCOC$_{BS}$.
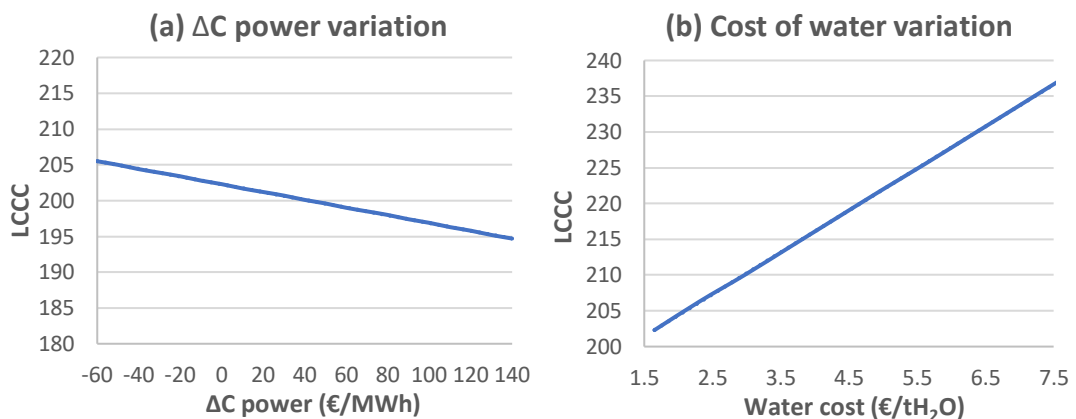
Figure 28: Sensitivity analysis of (a) Difference in power cost and (b) water cost.

At the end, the effect of the higher water cost has been studied on LCOC$_{BS}$. Since HT-DAC is a very water intensive process, the effect of cost of water on the final LCOC$_{BS}$ values is crucial point to speculate. In this study, desalinated water is considered as the main source of water. Therefore, the cost of water of around 1.65 €/tCO$_2$ is already the highest cost nowadays. However, this research is

focused on understanding the impact of higher water costs on LCOC$_{BS}$. From Figure 28, it can be inferred that LCOC$_{BS}$ varies slightly with the rise in the water cost.

Finally, economic parameters are determined for techno-economically optimized scenarios. To assess the carbon capture business case of Jordan-800MW scenario having a mega scale capture capacity, the following economic parameters were determined, as shown in Table 10 below. All values are obtained for zero NPV value, which is indicated by the equivalent IRR value to the discount rate.

Table 10: Economic indicators for Jordan-800MW.

Economic indicators (Jordan-800MW)	Value
Turnover ratio	0.15
Return over investment (ROI%)	111%
Pay back period (Y)	11
Internal rate of Return (IRR)	7.5%
Net present value (NPV)	0.00

7 Conclusion

In the rising awareness about the severe climate change effects, many institutions, governments, corporates and industries are looking for the sustainable, efficient as well as economical solution to reverse these phenomena. Even though large investments are pumped in the development of circular economy, fostering the complete independence of fossil-based resources, hefty amount of carbon from fossil sources will inevitably be released in atmosphere throughout this process. This addition of carbon will boost the rise in atmospheric temperature beyond the set limit of 1.5 °C. To solve this conundrum, today's world is in drastic need of negative emission technologies (NET). Recent scientific and strategic developments in the field of NETs have pointed the benefits of DAC over BECCS method. Hence, this project was focused on using solar based energy technology to minimize the carbon footprint of DAC process.

In comparison to the CE's continuous CNG based conventional HT-DAC process, the novel process has to be modified into intermittent and continuous process. Also, an adequate storage facility needs to be considered to optimize the overall energy consumption of the process and smoothen the operation. In case of million tons capacity, the energy consumption in entire process has been further optimized by nearly 30% using energy analysis tool in ASPEN. For the constant carbon capture capacity, significant difference in the design capacity of plant equipment has been observed for 4 potential locations. In order to capture carbon through solarized HT-DAC at the same cost, the break-even CSP capacity calculation was performed. It resulted with minimum 624 MW of CSP required to solarize the conventional process and capture carbon at 181 €/tCO$_2$.

The optimized version of the solarized HT-DAC has resulted in comparatively less power consumption in AC at all 4 potential locations. However, the water consumption of solarized model is highly location centric. For the CSP favored locations like Morocco and Chile, nearly two folds water consumption has been observed when compared to water consumption in Keith's model. Whereas, water consumption in the case of other two locations are observed to have almost similar water consumption per tCO$_2$ values of Keith's model. Even though the simulation results indicate the contribution of water

in the overall project investment of around 7.5% in 25 years of operation, it is highly impactful factor from the sustainability perspective.

For a mega ton scale, solarized version of HT-DAC demands for a large investment ranging from 1650-1774 M€, leading to the lowest range of levelized cost ($LCOC_{BS}$) of 200-220 €/tCO_2 for different locations. When the CSP thermal capacity varied from 150 to 800 MW at Jordan, non-linear variation of overall project cost has been noticed.

To understand the economics of the novel HT-DAC project, economic indicators for the 16 scenarios were determined. Further, the detailed sensitivity analysis of various influential parameters against the $LCOC_{BS}$ has been performed. The results obtained from this analysis suggests that the funding received at 0% interest rate and higher increment in carbon taxes vastly reduces the $LCOC_{BS}$. Referring to the Figure 27, higher impact of increment in taxes has been observed when compared to the equity shared in exchange to funding. In addition to this, the sensitivity analysis of the difference in cost of grid power and price of green power supports in generating additional revenue annually. This directly boosts the economics in the direction to reduce the $LCOC_{BS}$.

Moreover, the sensitivity analysis of discount rate and the loan interest rate has also been conducted. From the results of this analysis, the lower discount rate and the interest are found to be more favorable for the commercialization of this process by lowering the $LCOC_{BS}$ values. Out of all economic parameters, discount rate is found to have a most profound effect on lowering the $LCOC_{BS}$ up to 100 €/tCO_2, referring to Figure 27. Hence, the investor expecting lower returns and slower rate of returns on the investment in this project could perfectly match the needs. The result obtained from sensitivity analysis of loan interest rate symbolizes that the government subsidy on reducing the interest rate could actually help in making this process economically more viable.

After performing the root cause analysis for the higher $LCOC_{BS}$ values, the major capital investment sharing of more than 50% has been noticed on continuous side. This indicates that the HT-DAC is driven economically by the continuous side of the process. When capital investment is distributed as shown in Figure 25, the maximum share has been observed for process equipment. In addition to this, Figure 26 indicates that

investment for solar calciner share 10% of total project cost. Large number of low capacity solar calciners and the special arrangements required for the calciners around solar tower has increased the investment required for it. Plus, all non-conventional equipment like the pellet reactor, air contactor and solar calciners are each sharing nearly 10% of the total project cost. Therefore, more research on novel designs of equipment and technically advanced process intensified plant might be helpful in achieving lower LCOC$_{BS}$. Along with this, development of novel processes based on new salts or chemicals as an alternative for high temperature and high energy demand of CaCO$_3$ calcination process could be valuable research for this technology.

Overall, the employment of solar energy technology in fueling the HT-DAC has resulted into similar capture cost estimation. However, carbon captured in this process is completely concentrated CO$_2$ from the atmosphere. Hence, it can be directly utilized in further applications like aviation fuel production process, synthetic chemical production processes, etc. If we add up the cost of sequestration of one third portion of the capture carbon, then solarized version of HT-DAC is a more economical choice. Plus, the low carbon footprint of the operation of entire novel process, due to the green power harvested from PV plants, is an additional benefit of solarizing the conventional HT-DAC process. Since there is a lot of room for improvement from the process side as discussed above, the LCOC$_{BS}$ value of solarized HT-DAC is expected to fall further in the upcoming years.

8 References

1. Fasihi, M.; Efimova, O.; Breyer, C. Techno-economic assessment of CO2 direct air capture plants. *Journal of Cleaner Production* **2019,** *224*, 957–980. DOI: 10.1016/j.jclepro.2019.03.086.

2. United Nations Environment Programme. *Emissions Gap Report 2021: The Heat Is On – A World of Climate Promises Not Yet Delivered*.

3. Leeson, D.; Mac Dowell, N.; Shah, N.; Petit, C.; Fennell, P. S. A Techno-economic analysis and systematic review of carbon capture and storage (CCS) applied to the iron and steel, cement, oil refining and pulp and paper industries, as well as other high purity sources. *International Journal of Greenhouse Gas Control* **2017,** *61*, 71–84. DOI: 10.1016/j.ijggc.2017.03.020.

4. Committee on Developing a Research Agenda for Carbon Dioxide Removal and Reliable Sequestration; Board on Atmospheric Sciences and Climate; Board on Energy and Environmental Systems; Board on Agriculture and Natural Resources; Board on Earth Sciences and Resources; Board on Chemical Sciences and Technology; Ocean Studies Board; Division on Earth and Life Studies; National Academies of Sciences; Engineering; and Medicine. *Negative Emissions Technologies and Reliable Sequestration: A Research Agenda*, 2018. DOI: 10.17226/25259.

5. Lackner, K. S.; Wendt, C. H.; Butt, D. P.; Joyce, E. L.; Sharp, D. H. Carbon dioxide disposal in carbonate minerals. *Energy* **1995,** *20* (11), 1153–1170. DOI: 10.1016/0360-5442(95)00071-N.

6. Keith, D. W.; Holmes, G.; St. Angelo, D.; Heidel, K. A Process for Capturing CO2 from the Atmosphere. *Joule* **2018,** *2* (8), 1573–1594. DOI: 10.1016/j.joule.2018.05.006.

7. Lackner, K. S., Ziock, H.-J., Grimes, P., Eds. *Carbon Dioxide Extraction From Air: Is It An Option?*, 1999.

8. Zeman, F. Energy and material balance of CO2 capture from ambient air. *Environmental science & technology* **2007,** *41* (21), 7558–7563. DOI: 10.1021/es070874m.

9. Baciocchi, R.; Storti, G.; Mazzotti, M. Process design and energy requirements for the capture of carbon dioxide from air. *Chemical Engineering and Processing: Process Intensification* **2006,** *45* (12), 1047–1058. DOI: 10.1016/j.cep.2006.03.015.

10. Keith, D. W.; Ha-Duong, M.; Stolaroff, J. K. Climate Strategy with Co2 Capture from the Air. *Climatic Change* **2006,** *74* (1-3), 17–45. DOI: 10.1007/s10584-005-9026-x.

11. Stolaroff, J. K.; Keith, D. W.; Lowry, G. V. Carbon dioxide capture from atmospheric air using sodium hydroxide spray. *Environmental science & technology* **2008,** *42* (8), 2728–2735. DOI: 10.1021/es702607w.

12. Robert Socolow; Michael Desmond; Roger Aines; Jason Blackstock; Olav Bolland; Tina Kaarsberg; Nathan Lewis; Marco Mazzotti; Allen Pfeffer; Karma Sawyer; Jeffrey Siirola; Berend Smit; Jennifer Wilcox. *Direct Air Capture of CO2 with Chemicals*: *A Technology Assessment for the APS Panel on Public Affairs*.

13. Kulkarni, A. R.; Sholl, D. S. Analysis of Equilibrium-Based TSA Processes for Direct Capture of CO 2 from Air. *Ind. Eng. Chem. Res.* **2012,** *51* (25), 8631–8645. DOI: 10.1021/ie300691c.

14. Holmes, G.; Keith, D. W. An air-liquid contactor for large-scale capture of CO2 from air. *Philosophical transactions. Series A, Mathematical, physical, and engineering sciences* **2012,** *370* (1974), 4380–4403. DOI: 10.1098/rsta.2012.0137.

15. Mazzotti, M.; Baciocchi, R.; Desmond, M. J.; Socolow, R. H. Direct air capture of CO2 with chemicals: optimization of a two-loop hydroxide carbonate system using a countercurrent air-liquid contactor. *Climatic Change* **2013,** *118* (1), 119–135. DOI: 10.1007/s10584-012-0679-y.

16. An, K.; Farooqui, A.; McCoy, S. T. The impact of climate on solvent-based direct air capture systems. *Applied Energy* **2022,** *325*, 119895. DOI: 10.1016/j.apenergy.2022.119895.

17. Casaban, D.; Tsalaporta, E. Direct air capture of CO2 in the Republic of Ireland. Is it necessary? *Energy Reports* **2022,** *8*, 10449–10463. DOI: 10.1016/j.egyr.2022.08.194.

18. Schlömer, S.; Bruckner, T.; Fulton, L.; Hertwich, E.; McKinnon, A.; Perczyk, D.; Roy, J.; Schaeffer, R.; Sims, R.; Smith, P.; Wiser, R. *Annex III: Technology-specific Cost and Performance Parameters*.

19. World Bank. *Concentrating Solar Power: Clean Power on Demand 24/7*.

20. International Energy Agency. *Technology Roadmap: Solar Thermal Electricity*.

21. Lilliestam. *Concentrating Solar Power Projects*. https://solarpaces.nrel.gov/.

22. Lilliestam. *NOOR III CSP project*. https://solarpaces.nrel.gov/project/noor-iii.

23. Branker, K.; Pathak, M.; Pearce, J. M. A review of solar photovoltaic levelized cost of electricity. *Renewable and Sustainable Energy Reviews* **2011,** *15* (9), 4470–4482. DOI: 10.1016/j.rser.2011.07.104.

24. Konrad Mertens. *Photovoltaics: Fundamentals, technology and practice;* John Wiley & Sons Ltd., 2014.

25. IEA - International Energy Agency. Renewable Energy Market Update 2022.

26. Olivier, J. G. J.; Peters, J. A.; Janssens-Maenhout, G. Trends in global CO2 emissions. 2012 report **2012**.

27. Meier, A.; Bonaldi, E.; Cella, G. M.; Lipinski, W.; Wuillemin, D. Solar chemical reactor technology for industrial production of lime. *Solar Energy* **2006,** *80* (10), 1355–1362. DOI: 10.1016/j.solener.2005.05.017.

28. Wu, W. RHIM solar calcination final report 20211223.

29. Moumin, G.; Ryssel, M.; Zhao, L.; Markewitz, P.; Sattler, C.; Robinius, M.; Stolten, D. CO2 emission reduction in the cement industry by using a solar calciner. *Renewable Energy* **2020,** *145*, 1578–1596. DOI: 10.1016/j.renene.2019.07.045.

30. Meier, A.; Gremaud, N.; Steinfeld, A. Economic evaluation of the industrial solar production of lime. *Energy Conversion and Management* **2005,** *46* (6), 905–926. DOI: 10.1016/j.enconman.2004.06.005.

31. Kai Wang; Ting Yan; R.K. Li; W.G. Pan. A review for Ca(OH)2/CaO thermochemical energy storage systems. *Journal of Energy Storage* **2022,** *50*, 104612. DOI: 10.1016/j.est.2022.104612.

32. Falter, C.; Pitz-Paal, R. Water Footprint and Land Requirement of Solar Thermochemical Jet-Fuel Production. *Environmental science & technology* **2017,** *51* (21), 12938–12947. DOI: 10.1021/acs.est.7b02633.

33. Al-Malah, K. I. M. *Aspen plus*: *Chemical engineering applications;* Wiley, 2017.

34. Mostafa, M.; Antonicelli, C.; Varela, C.; Barletta, D.; Zondervan, E. Capturing CO2 from the atmosphere: Design and analysis of a large-scale DAC facility. *Carbon Capture Science & Technology* **2022,** *4*, 100060. DOI: 10.1016/j.ccst.2022.100060.

35. Schwarzbözl, P., Pitz-Paal, R., Schmitz, M., Eds. *Visual HFLCAL-A software tool for layout and optimisation of heliostat fields*, 2009.

36. Schwarzbözl, P. THE USER'S GUIDE TO HFLCAL A Software Program for Heliostat Field Layout Calculation. *Software Release Visual hflcal VH12, Cologne, Germany* **2009**.

37. Jan Remund. *Meteonorm 8;* Meteotest AG. https://meteonorm.com/ (accessed 07/26/2022).

38. UN Water. *Water scarcity*. https://unwater.org/water-facts/water-scarcity (accessed 2022-09-30).

39. Pranav Maheshwari. *CUF vs PLF*. https://medium.com/@pvdiagnostics/cuf-vs-plf-c2478cc82163 (accessed 2022-10-28).

40. Teresa Zhang. *What's a good value for kWh/kWp? An overview of specific yield*. https://www.solarpowerworldonline.com/2017/08/specific-yield-overview/ (accessed 2022-10-28).

41. World Bank Group. *Global Photovoltaic Power Potential by Country;* World Bank, Washington, DC, 2020. DOI: 10.1596/34102.

42. Leonics. *How to Design Solar PV System*: *Size the PV modules;* LEONICS Co., Ltd.

43. Solargis. *Global Solar Atlas*. https://globalsolaratlas.info/global-pv-potential-study (accessed 2022-09-11).

44. Jürgen Dersch; Simon Dieckmann. Greenius Help & Manual **2022,** *1* (accessed 10/28/2022).

45. Peters, M. S.; Timmerhaus, K. D.; West, R. E. *Plant design and economics for chemical engineers*, 5th ed. / Max S. Peters, Klaus D. Timmerhaus, Ronald West; McGraw-Hill chemical engineering series; McGraw-Hill, 2003.

46. Ulrich, G. D.; Vasudevan, P. T. *Chemical engineering process design and economics*: *A practical guide*, 2nd ed.; Process Pub, 2004.

47. Schwede, F. Techno-economic assessment of solar driven high temperature electrolysis. Bachelor's Thesis, University of Applied Science Hamm-Lippstadt, 2016.

48. Maggie Stehn, Ed. *Credit for Carbon Oxide Sequestration*: *Internal Revenue Services (IRS)*. TD 9944; Deartment of treasury, 2020.

49. Deeksha Anand. *Understanding 45Q: The Carbon Capture Tax Credit;* Energy Venture Analysis, 2020.

50. Nina Chestney. *Europe carbon prices expected to rise to 2030-industry survey*. Sustainable Business; REUTERS, 06/14/2021.

51. European Central Bank. *Euro area bank interest rate statistics: January 2022*, 2022.

52. Brealey, R. A.; Myers, S. C.; Allen, F. *Principles of corporate finance*, 10th ed.; The McGraw-Hill/Irwin series in finance, insurance, and real estate; McGraw-Hill/Irwin, 2011.

9 Appendix

9.1 Correlation of power consumption

In this section, the development of Equation 7 for the estimation of power consumption (P) in AC has been illustrated. Using the pressure drop across AC (ΔP), the volumetric flow rate ($\dot{Q}$) and the fan efficiency (η_{eff}), power can be determined as per the following equation.

$$P = \frac{\Delta P \cdot \dot{Q}}{\eta_{eff}}$$

Therefore,
$$P \propto \dot{Q}$$

$$P \propto \frac{\dot{n}_{CO_2} \cdot R \cdot T}{Pressure_{CO_2}}$$

$$P \propto \frac{\dot{n}_{air} \cdot R \cdot T}{X_{CO_2} \cdot Pressure_{atmosphere}}$$

Considering the atmospheric pressure and CO_2 concentration (X_{CO_2}) as constant, power is found to be directly proportional to molar flow rate of CO_2 ($\dot{n}_{air}$) and temperature.

$$P \propto \dot{n}_{CO_{2in}} \cdot T$$

As per the definition of capture rate (CR%),

$$CR\% = \frac{\dot{n}_{CO_{2absorbed}}}{\dot{n}_{CO_{2in}}}$$

Capture rate (CR%) of AC is highly dependent on the temperature and relative humidity values. It also varies with the designed structure of AC. From the above two equations, the power consumption in AC can be estimated using the following correlation.

$$P \propto T \cdot \frac{\dot{n}_{CO_{2absorbed}}}{CR\%}$$

In this study, the constant flow rate of CO_2 absorption has been assumed. Therefore, the power consumption is directly proportional to the temperature and inversely proportional to the capture rate.

$$P \propto \frac{T}{CR\%}$$

Using this correlation, the power consumption has been estimated as per the methodology shown shown in the following section.

9.2 Calculation for utility consumption

The power and water consumption of the process has been calculated using the Equation 7, Equation 8, Equation 9, Equation 10 and Equation 11 as well as hourly based meteorological data. Temperature and relative humidity (RH%) are the main parameters required for the following estimation process.

Considering a case of 8 AM of 1st of January with following parameters:

Temperature at the 8 AM on 01/01 (T) – 20.9 °C

Relative humidity at 8 AM on 01/01 (RH%) – 32%

Reference temperature – 21 °C

Reference power consumption (P_{ref}) from Keith's report = 8.66 MW

Reference capture rate – 72.13%

Using the Equation 7, the capture rate (CR%) can be calculated as follows.

$$CR\% = 47.66 + 0.89 \cdot 21 + 0.137 \cdot 32$$

$$\mathbf{CR}\% = 71.32\%$$

Further, this calculated CR% is used in the Equation 7, which is reframed for the constant concentration of CO_2 in atmospheric. This calculation result into the power demand for a specific hour of the year.

$$\frac{P}{P_{ref}} = \frac{T}{CR\%} \times \frac{CR\%_{ref}}{T_{ref}}$$

$$\frac{P}{8.66} = \frac{20.9}{71.32} \times \frac{72.13}{21}$$

$$\mathbf{P} = 8.767 \text{ MW}$$

Using the same calculation method, the power demand of AC throughout the year for 8760 hours of year has been determined. These values are later added to the power demand of other consumers to get an hourly total power demand of the process.

For the estimation of water consumption in AC, Equation 11 has been used. For the aforementioned case, the calculation for water consumption is as follows –

$$m = -0.006 \cdot T - 0.07$$

$$c = 0.159 \cdot T + 11.299$$

Here, the 'm' and 'c' represents the slope and y-axis intercept of the linear correlation between ratio (Y) and relative humidity (RH%). Using these values in the equation below, the ratio Y can be estimated. For this case, the Y is estimated to be around 8.77 MW.

$$Y = m \cdot RH\% + c$$

$$\mathbf{Y} = 8.767 \text{ MW}$$

This calculation steps are repeated for every hour of the year to get the hourly water consumption in AC. In addition to this, the annual water consumption for cleaning of CSP heliostats are also estimated using the annual constant of 58 l/m².

9.3 Economic analysis

9.3.1 Economic Indicators

Following are the formulae for the calculation of economic indicators-

i. **Turnover ratio:**

$$\text{Turnover ratio} = \frac{\text{Annual earnings}}{\text{Capex}}$$

ii.   Return over investment:

$$\text{ROI} = \frac{\text{Total net profit}}{\text{Capex}}$$

iii.   Net present value:

$$\text{NPV} = \frac{C_t}{(1 + i)^t}$$

Where,

C_t = Net cash flow in year t

i = discount rate

t = year of cash flow

9.3.2 Balance Sheet

In order to perform the economic analysis and find the levelized cost of capture, following model of balance sheet represented in Table 12 has been developed for each scenario. This model was used to estimate the required parameters like cashflows, annual net profit, pay-back period. Table 11 represents the modes of revenue generation in the carbon capture business for the scenario Jordan-800 MW. As the price of green electricity sold and cost of electricity bought from grid was assumed to be equivalent, no revenue collection from it has been considered.

Table 11: Sources of revenue generation for Jordan-800MW.

Revenue stream	Value	Units
Carbon tax	55.0	€ / tonne CO2
Levelised cost	202.3	€ /tonne CO2
Net selling price	257.3	€ / tonne CO2

For the case of Jordan-800MW, the raw material and utility cost sums to be around 13.74 M€. In addition to this, annual maintenance cost of the system has been determined to be around 13.42 M€. In total, the annual manufacturing cost is calculated to be 27.16 M€, as shown in Table 12**.** Moreover, the cost of labor was allowed to rise every year by 8%, starting from 5.4 M€. All these expenditures were

deducted from the total annual revenue generated. This results into gross profit, which has same values for every 5 years of duration.

Along with this, depreciation value was further subtracted from the gross profit, which was calculated using the straight line method. For the capex of 1677 M€ and amortization value of 50 M€, the annual depreciation value of equipment is estimated to be around 65.1 M€ for 25 years of operation. Additionally, the interest over the loan amount has been further deducted. As shown in the third row of Table 12, the interest is calculated separately for each year based on the remaining capital amount also referred as balance amount.

For the initial two years of procurement and installation, total capex of 1677 M€ has been evenly distributed as manufacturing cost and no revenue generation has been considered. Hence, the net cash flows for the initial two years is nothing but the capital invested in the project. Using the 27 cashflows obtained from the balance sheet of 25 years of operation and 2 years of installation period, the NPV has been determined at 7.5% of discount rate. For the levelized cost of 202.3 €/tCO$_2$, the IRR has been found to match with the discount rate.

Lastly, the pay-back period is calculated by subtracting the capital investment from the annual cash flows. For the initial few years, the result of this calculation will be negative. This step is repeated further for every year until the positive value is obtained. In the 11th year, the value in the pay back calculation row is found to be positive for the first positive. This indicates that the pay-back period of this project is around 11 years.

Balance Sheet

Table 12: Balance sheet for Jordan-800MW for zero NPV.

Year	-1	0	1	2	3	4	5	6	7	8	9	10	11	12	13	14	15	16	17	18	19	20	21	22	23	24	25
Interest			23.99	23.19	22.37	21.54	20.70	19.85	18.98	18.11	17.22	16.32	15.40	14.47	13.53	12.58	11.61	10.63	9.63	8.62	7.60	6.56	5.50	4.43	3.35	2.25	1.13
Principle			56.3	57.1	57.9	58.8	59.6	60.4	61.3	62.2	63.1	64.0	64.9	65.8	66.8	67.7	68.7	69.7	70.7	71.7	72.7	73.7	74.8	75.9	76.9	78.0	79.2
Balance			1621.4	1564.3	1506.4	1447.6	1388.1	1327.6	1266.3	1204.1	1141.1	1077.1	1012.2	946.4	879.6	811.9	743.2	673.6	602.9	531.2	458.5	384.8	310.0	234.1	157.2	79.2	**0.0**
Carbon tax			55	55	55	55	55	60	60	60	60	60	65	65	65	65	65	70	70	70	70	70	70	70	70	70	70
	Installation and procurement period		**Operation period**																								
Total Earnings	*0.00*	*0.00*	*244.94*	*244.94*	*244.94*	*244.94*	*244.94*	*249.70*	*249.70*	*249.70*	*249.70*	*249.70*	*254.46*	*254.46*	*254.46*	*254.46*	*254.46*	*259.22*	*259.22*	*259.22*	*259.22*	*259.22*	*259.22*	*259.22*	*259.22*	*259.22*	*259.22*
Manufacturing cost	838.86	838.86	27.16	27.16	27.16	27.16	27.16	27.16	27.16	27.16	27.16	27.16	27.16	27.16	27.16	27.16	27.16	27.16	27.16	27.16	27.16	27.16	27.16	27.16	27.16	27.16	27.16
Electricity	0.0	0.0	0.0	0.0	0.0	0.0	0.0	0.0	0.0	0.0	0.0	0.0	0.0	0.0	0.0	0.0	0.0	0.0	0.0	0.0	0.0	0.0	0.0	0.0	0.0	0.0	0.0
Gross Profit	*-838.86*	*-838.9*	*217.78*	*217.78*	*217.78*	*217.78*	*217.78*	*222.54*	*222.54*	*222.54*	*222.54*	*222.54*	*227.30*	*227.30*	*227.30*	*227.30*	*227.30*	*232.06*	*232.06*	*232.06*	*232.06*	*232.06*	*232.06*	*232.06*	*232.06*	*232.06*	*232.06*
Labor cost	0	0	-5.4	-5.8	-6.3	-6.8	-7.3	-7.9	-8.6	-9.3	-10.0	-10.8	-11.7	-12.6	-13.6	-14.7	-15.9	-17.1	-18.5	-20.0	-21.6	-23.3	-25.2	-27.2	-29.4	-31.7	-34.2
EBITDA	*-838.86*	*-838.9*	*212.38*	*211.95*	*211.48*	*210.98*	*210.43*	*214.61*	*213.97*	*213.29*	*212.55*	*211.75*	*215.64*	*214.71*	*213.70*	*212.62*	*211.44*	*214.93*	*213.56*	*212.08*	*210.48*	*208.76*	*206.89*	*204.88*	*202.70*	*200.36*	*197.82*
Depreciation	0.0	0.0	-65.1	-65.1	-65.1	-65.1	-65.1	-65.1	-65.1	-65.1	-65.1	-65.1	-65.1	-65.1	-65.1	-65.1	-65.1	-65.1	-65.1	-65.1	-65.1	-65.1	-65.1	-65.1	-65.1	-65.1	-65.1
EBIT	*-838.86*	*-838.9*	*147.27*	*146.84*	*146.37*	*145.87*	*145.33*	*149.50*	*148.86*	*148.18*	*147.44*	*146.64*	*150.53*	*149.60*	*148.59*	*147.51*	*146.33*	*149.82*	*148.45*	*146.97*	*145.37*	*143.65*	*141.78*	*139.77*	*137.60*	*135.25*	*132.71*
Interest	0.00	0.00	-23.99	-23.19	-22.37	-21.54	-20.70	-19.85	-18.98	-18.11	-17.22	-16.32	-15.40	-14.47	-13.53	-12.58	-11.61	-10.63	-9.63	-8.62	-7.60	-6.56	-5.50	-4.43	-3.35	-2.25	-1.13
PBT	*-838.86*	*-838.9*	*123.28*	*123.65*	*124.00*	*124.33*	*124.62*	*129.65*	*129.88*	*130.07*	*130.22*	*130.32*	*135.13*	*135.13*	*135.06*	*134.93*	*134.72*	*139.20*	*138.82*	*138.35*	*137.78*	*137.09*	*136.28*	*135.34*	*134.25*	*133.00*	*131.58*
Taxes @30%	0.00	0.00	-36.98	-37.10	-37.20	-37.30	-37.39	-38.89	-38.96	-39.02	-39.07	-39.10	-40.54	-40.54	-40.52	-40.48	-40.42	-41.76	-41.65	-41.51	-41.33	-41.13	-40.88	-40.60	-40.27	-39.90	-39.47
PAT	*-838.86*	*-838.9*	*86.30*	*86.56*	*86.80*	*87.03*	*87.24*	*90.75*	*90.92*	*91.05*	*91.15*	*91.22*	*94.59*	*94.59*	*94.54*	*94.45*	*94.31*	*97.44*	*97.17*	*96.85*	*96.44*	*95.96*	*95.40*	*94.74*	*93.97*	*93.10*	*92.11*
Cash flows	**-838.86**	**-838.9**	**151.41**	**151.67**	**151.91**	**152.14**	**152.35**	**155.86**	**156.02**	**156.16**	**156.26**	**156.33**	**159.70**	**159.70**	**159.65**	**159.56**	**159.41**	**162.55**	**162.28**	**161.96**	**161.55**	**161.07**	**160.51**	**159.85**	**159.08**	**158.21**	**157.21**
Principle deduction			-56.30	-57.11	-57.92	-58.75	-59.59	-60.44	-61.31	-62.18	-63.07	-63.97	-64.89	-65.82	-66.76	-67.71	-68.68	-69.66	-70.66	-71.67	-72.70	-73.73	-74.79	-75.86	-76.94	-78.04	-79.16
Net profit			*95.11*	*94.56*	*93.99*	*93.39*	*92.76*	*95.42*	*94.72*	*93.97*	*93.19*	*92.36*	*94.81*	*93.88*	*92.89*	*91.85*	*90.73*	*92.88*	*91.62*	*90.28*	*88.86*	*87.34*	*85.72*	*83.99*	*82.14*	*80.16*	*78.05*
Cumulative			95.11	189.67	283.66	377.05	469.80	565.22	659.94	753.91	847.10	939.46	1034.28	1128.16	1221.05	1312.90	1403.63	1496.51	1588.13	1678.42	1767.28	1854.62	1940.33	2024.32	2106.46	2186.62	2264.68
Pay back period			-1526.3	-1374.7	-1222.7	-1070.6	-918.26	-762.39	-606.4	-450.2	-294	-137.6	22.09	181.78	341.44	501.00	660.41	822.96	985.24	1147.19	1308.75	1469.82	1630.33	1790.17	1949.25	2107.46	2264.68

Yr	-1	0	1	2	3	4	5	6	7	8	9	10	11	12	13	14	15	16	17	18	19	20	21	22	23	24	25
Interest			23.99	23.19	22.37	21.54	20.70	19.85	18.98	18.11	17.22	16.32	15.40	14.47	13.53	12.58	11.61	10.63	9.63	8.62	7.60	6.56	5.50	4.43	3.35	2.25	1.13
Principle			56.3	57.1	57.9	58.8	59.6	60.4	61.3	62.2	63.1	64.0	64.9	65.8	66.8	67.7	68.7	69.7	70.7	71.7	72.7	73.7	74.8	75.9	76.9	78.0	79.2
Balance			1621.4	1564.3	1506.4	1447.6	1388.1	1327.6	1266.3	1204.1	1141.1	1077.1	1012.2	946.4	879.6	811.9	743.2	673.6	602.9	531.2	458.5	384.8	310.0	234.1	157.2	79.2	0.0
Carbon tax			55	55	55	55	55	60	60	60	60	60	65	65	65	65	65	70	70	70	70	70	70	70	70	70	70
Annual Balance Sheet ($M)																											
Total Earnings	0.00	0.00	244.94	244.94	244.94	244.94	244.94	249.70	249.70	249.70	249.70	249.70	254.46	254.46	254.46	254.46	254.46	259.22	259.22	259.22	259.22	259.22	259.22	259.22	259.22	259.22	259.22
Maufacturing Cost	838.86	838.86	27.16	27.16	27.16	27.16	27.16	27.16	27.16	27.16	27.16	27.16	27.16	27.16	27.16	27.16	27.16	27.16	27.16	27.16	27.16	27.16	27.16	27.16	27.16	27.16	27.16
Electricity			0.0	0.0	0.0	0.0	0.0	0.0	0.0	0.0	0.0	0.0	0.0	0.0	0.0	0.0	0.0	0.0	0.0	0.0	0.0	0.0	0.0	0.0	0.0	0.0	0.0
Gross Profit	-838.86	-838.86	217.78	217.78	217.78	217.78	217.78	222.54	222.54	222.54	222.54	222.54	227.30	227.30	227.30	227.30	227.30	232.06	232.06	232.06	232.06	232.06	232.06	232.06	232.06	232.06	232.06
Labor cost	0	0	-5.4	-5.8	-6.3	-6.8	-7.3	-7.9	-8.6	-9.3	-10.0	-10.8	-11.7	-12.6	-13.6	-14.7	-15.9	-17.1	-18.5	-20.0	-21.6	-23.3	-25.2	-27.2	-29.4	-31.7	-34.2
EBITDA	-838.86	-838.86	212.38	211.95	211.48	210.98	210.43	214.61	213.97	213.29	212.55	211.75	215.64	214.71	213.70	212.62	211.44	214.93	213.56	212.08	210.48	208.76	206.89	204.88	202.70	200.36	197.82
Depreciation	0.0	0.0	-65.1	-65.1	-65.1	-65.1	-65.1	-65.1	-65.1	-65.1	-65.1	-65.1	-65.1	-65.1	-65.1	-65.1	-65.1	-65.1	-65.1	-65.1	-65.1	-65.1	-65.1	-65.1	-65.1	-65.1	-65.1
EBIT	-838.86	-838.86	147.27	146.84	146.37	145.87	145.33	149.50	148.86	148.18	147.44	146.64	150.53	149.60	148.59	147.51	146.33	149.82	148.45	146.97	145.37	143.65	141.78	139.77	137.60	135.25	132.71
Interest	0.00	0.00	-23.99	-23.19	-22.37	-21.54	-20.70	-19.85	-18.98	-18.11	-17.22	-16.32	-15.40	-14.47	-13.53	-12.58	-11.61	-10.63	-9.63	-8.62	-7.60	-6.56	-5.50	-4.43	-3.35	-2.25	-1.13
PBT	-838.86	-838.86	123.28	123.65	124.00	124.33	124.62	129.65	129.88	130.07	130.22	130.32	135.13	135.13	135.06	134.93	134.72	139.20	138.82	138.35	137.78	137.09	136.28	135.34	134.25	133.00	131.58
Taxes @30%	0.00	0.00	-36.98	-37.10	-37.20	-37.30	-37.39	-38.89	-38.96	-39.02	-39.07	-39.10	-40.54	-40.54	-40.52	-40.48	-40.42	-41.76	-41.65	-41.51	-41.33	-41.13	-40.88	-40.60	-40.27	-39.90	-39.47
PAT	-838.86	-838.86	86.30	86.56	86.80	87.03	87.24	90.75	90.92	91.05	91.15	91.22	94.59	94.59	94.54	94.45	94.31	97.44	97.17	96.85	96.44	95.96	95.40	94.74	93.97	93.10	92.11
Cash flows	-838.86	-838.86	151.41	151.67	151.91	152.14	152.35	155.86	156.02	156.16	156.26	156.33	159.70	159.70	159.65	159.56	159.41	162.55	162.28	161.96	161.55	161.07	160.51	159.85	159.08	158.21	157.21
Principle			-56.30	-57.11	-57.92	-58.75	-59.59	-60.44	-61.31	-62.18	-63.07	-63.97	-64.89	-65.82	-66.76	-67.71	-68.68	-69.66	-70.66	-71.67	-72.70	-73.73	-74.79	-75.86	-76.94	-78.04	-79.16
Net profit			95.11	94.56	93.99	93.39	92.76	95.42	94.72	93.97	93.19	92.36	94.81	93.88	92.89	91.85	90.73	92.88	91.62	90.28	88.86	87.34	85.72	83.99	82.14	80.16	78.05
Cumulative			95.11	189.67	283.66	377.05	469.80	565.22	659.94	753.91	847.10	939.46	1034.28	1128.16	1221.05	1312.90	1403.63	1496.51	1588.13	1678.42	1767.28	1854.62	1940.33	2024.32	2106.46	2186.62	2264.68
Pay back period			-1526.32	-1374.65	-1222.74	-1070.60	-918.26	-762.39	-606.37	-450.21	-293.95	-137.62	22.09	181.78	341.44	501.00	660.41	822.96	985.24	1147.19	1308.75	1469.82	1630.33	1790.17	1949.25	2107.46	2264.68

9.3.3 Equipment cost estimation method

Table 13: Overview of cost estimation of various equipment.

Conventional equipment	Basis	Estimation method	Source of cost
Pellet reactor	Annual CO_2 output	Six-tenths rule	APEA
Heat exchanger	Annual CO_2 output	Six-tenths rule	APEA
Compressor	Annual CO_2 output	Six-tenths rule	APEA
Pump	Annual CO_2 output	Six-tenths rule	APEA
Separators	Annual CO_2 output	Six-tenths rule	APEA
Quick lime mixer	Annual CO_2 output	Six-tenths rule	APEA
Slaker	Annual CO_2 output	Six-tenths rule	APEA
Turbine	Annual CO_2 output	Six-tenths rule	Keith's research
Storage	Annual CO_2 output	Correlation	Timmerhaus
Filter	Annual CO_2 output	Six-tenths rule	Keith's research

Non-conventional equipment	Basis	Estimation method	Source of cost
Solar calciner	Thermal capacity	Linear	Moumin2020
Air contactor	Annual CO_2 output	Six-tenths rule	Keith's research
Solid-solid heat exchanger	Annual CO_2 output	Six-tenths rule	Solex
Solar tower	Tower height	Correlation	Meier2005
Heliostat field	Field mirror area	Correlation	Meier2005

9.4 ASPEN process flow sheet

The entire process flow sheet of ASPEN has been designed for the application of the solar based HT-DAC process. Figure 29 resembles the first loop of process responsible for the carbon absorption in the alkaline solution and transformation into $CaCO_3$. Air enters the AC through stream '3-AIRIN' and exits through stream '4-AIROU'. Whereas, circulating alkaline solution enter AC through stream '1-LIQIN' and exits at 'S2-LIQOU'. CO_2 rich stream 5 reacts with $Ca(OH)_2$ solution coming from stream '68' in the pellet reactor (CAUSTZR). The product stream '7' from pellet reactor undergoes separation of $CaCO_3$ and CaO coarse particles. These particles further are combined with new

CaCO₃ particles from stream '19'. The combined particles stream is washed in 'WASH' and flows on to slaker, shown in Figure 29 below.
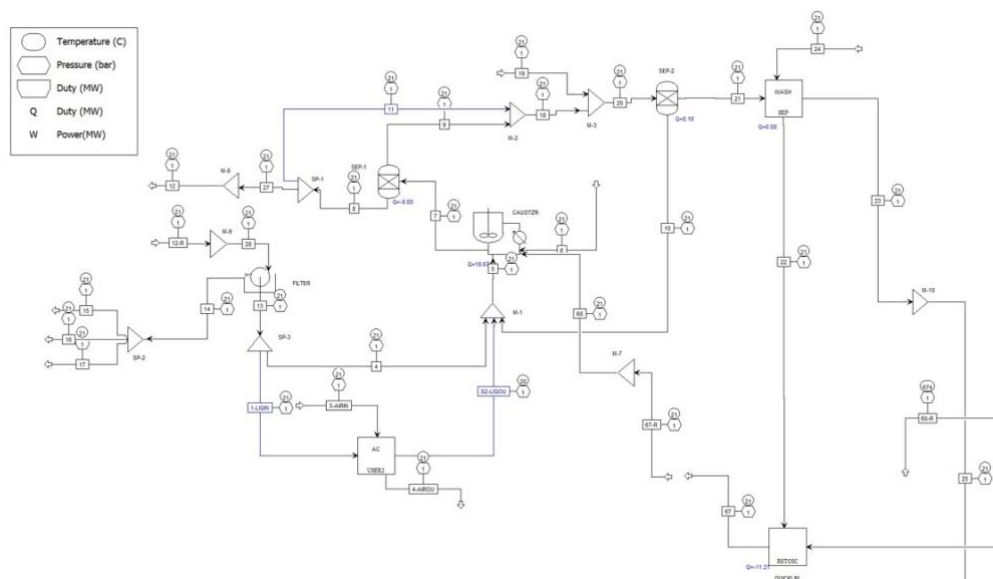
Figure 29: Capture and separation part of ASPEN process flowsheet.

In quick lime mixer (QUICKLIM), the alkaline solution with the CaO particles from slaker and the alkaline solution from 'WASH' are mixed to form $Ca(OH)_2$ solution. This solution is introduced to 'CAUSTZR' through stream '67'. It can be observed that some streams are split into parts to avoid the convergence problem.

The involvement of solar technology in the process is not directly shown in the flow diagram. However, the results of the duty required for the operation of calcination process has been obtained from ASPEN, referring to calciner duty of 385 MW in Figure 30. This heat demand is met externally by the CSP.

In Figure 30, 'SLAKER' is the slacker reactor. The green stream '40' circulating across it is nothing but the flow of steam. The pressurized steam causes the fluidization of mixture of particles and the slaking reaction simultaneously. Stream '48' and '48-R' represents the flow of pure $CaCO_3$ particles. However, they have different mass flow rate. Stream '48' is the product stream from slacker to $CaCO_3$ storage section. Whereas, stream '48-R' represents the flow of $CaCO_3$ particles to calciner during the solar hours. As solar hours last nearly 10 hours per day on average, the flow rate of

stream '48-R' is adjusted to be approximately 2.4 times flow rate of stream '48'. Similarly, the flow rate of stream '60-R' has been adjusted.

Figure 30: Regeneration part of ASPEN process flowsheet.

In order to recover the waste heat from the slaker and product streams of calciner, two different steam cycles have been designed. The pink cycle indicates the energy recovery loop for continuous part of process. The excess heat generated from the exothermic slaking process is collected by steam and later converted into electrical energy in Turbine-1. The condensate generated in Turbine-1 is cooled down in heat exchangers 'HX-9'. Finally, air cooled heat exchanger 'HX-1' are used to cool down further.

Similarly, the excess heat available in the product streams of calciner has been recovered. The heat available in CO_2 product stream 'VAP' enhances the temperature of the incoming $CaCO_3$ particles. Here, more than 60% of available energy is recovered. Whereas, the rest is transferred to the green steam loop at heat exchanger 'HX-5'. The

steam generated collects heat from the CaO product stream of calciner, which is further converted into electrical energy at Turbine-2. Lastly, the condensate generated in Turbine-2 is further cooled by the air-cooled heat exchanger 'HX-8'. The duty displayed in both the figures are obtained when the process has been simulated for the million tons carbon capture capacity.

Finally, the CO_2 gas produced in calciner is cooled and passed through the water scrubber to separate out impurities associated with gas. Then, it is compressed by the multi-stage compressor up to 151 bar for storage.

9.5 Stream results of ASPEN model

Variable	Units	1-LIQIN	3-AIRIN	4	4-AIROU	5	6	7	8	9	10	11	12	12-R	13	14	15	16	16-R	17	18	19	20	21	22	23	24	25	27
Temperature	°C	21.0	21.0	21.0	21.0	20.9	21.0	21.0	21.0	21.0	21.0	21.0	21.0	21.0	21.0	21.0	21.0	21.0	21.0	21.0	21.0	21.0	21.0	21.0	21.0	21.0	21.0	21.0	21.0
Pressure	bar	1.0	1.0	1.0	1.0	1.0	1.0	1.0	1.0	1.0	1.0	1.0	1.0	1.0	1.0	1.0	1.0	1.0	1.0	1.0	1.0	1.0	1.0	1.0	1.0	1.0	1.0	1.0	1.0
Molar Vapor Fraction		0.000	1.000	0.000	1.000	0.000	0.000	0.000	0.000	0.000	0.000	0.000	0.000	0.000	0.000	0.000	0.000	0.000	0.000	0.000	0.000	0.000	0.000	0.000	0.000	0.000	0.000	0.000	0.000
Molar Liquid Fraction		1.000	0.000	1.000	0.000	1.000	0.000	1.000	1.000	0.000	1.000	1.000	1.000	1.000	1.000	0.000	0.000	0.000	0.000	0.000	0.952	0.000	0.950	0.556	1.000	0.477	1.000	0.477	1.000
Molar Solid Fraction		0.000	0.000	0.000	0.000	0.000	1.000	0.000	0.000	1.000	0.000	0.000	0.000	0.000	0.000	1.000	1.000	1.000	1.000	1.000	0.048	1.000	0.050	0.444	0.000	0.523	0.000	0.523	0.000
Enthalpy Flow	MW	-132893	-9861	-1.49E+06	-12298	-1.63E+06	-32	-1.63E+06	-1.63E+06	-761	-3321	-3554	-1.63E+06	-1.63E+06	-1.63E+06	-99	-11	-72	-72	-15	-4315	-11	-4326	-1005	-3265	-940	-3201	-940	-1.63E+06
Mole Flows	kmol/s	463.4	2431.5	5207.4	2442.0	5671.1	0.0	5683.8	5683.2	0.6	11.3	12.1	5670.8	5670.8	5670.7	0.1	0.0	0.1	0.1	0.0	13.0	0.0	12.7	1.4	11.4	1.2	11.2	1.2	5518.3
Mole Fractions																													
CO2		0.000	0.000	0.000	0.000	0.000	0.000	0.000	0.000	0.000	0.009	0.008	0.000	0.000	0.000	0.000	0.000	0.000	0.000	0.000	0.000	0.000	0.008	0.000	0.000	0.000	0.000	0.000	0.008
H2O		0.938	0.016	0.938	0.020	0.938	0.000	0.938	0.938	0.000	0.954	0.956	0.938	0.938	0.938	0.000	0.000	0.000	0.000	0.000	0.893	0.000	0.908	0.548	0.999	0.477	1.000	0.477	0.956
KOH		0.000	0.000	0.000	0.000	0.000	0.000	0.000	0.000	0.000	0.037	0.036	0.000	0.000	0.000	0.000	0.000	0.000	0.000	0.000	0.000	0.000	0.034	0.008	0.001	0.000	0.000	0.000	0.036
CACO3		0.000	0.000	0.000	0.000	0.000	0.000	0.000	0.000	0.000	0.000	0.000	0.000	0.000	0.000	0.000	0.000	0.000	0.000	0.000	0.000	0.000	0.000	0.000	0.000	0.000	0.000	0.000	0.000
K2CO3		0.000	0.000	0.000	0.000	0.000	0.000	0.000	0.000	0.000	0.000	0.000	0.000	0.000	0.000	0.000	0.000	0.000	0.000	0.000	0.000	0.000	0.000	0.000	0.000	0.000	0.000	0.000	0.000
CA(OH)2		0.000	0.000	0.000	0.000	0.000	0.000	0.000	0.000	0.000	0.000	0.000	0.000	0.000	0.000	0.000	0.000	0.000	0.000	0.000	0.000	0.000	0.000	0.000	0.000	0.000	0.000	0.000	0.000
N2		0.000	0.778	0.000	0.775	0.000	0.000	0.000	0.000	0.000	0.000	0.000	0.000	0.000	0.000	0.000	0.000	0.000	0.000	0.000	0.000	0.000	0.000	0.000	0.000	0.000	0.000	0.000	0.000
O2		0.000	0.206	0.000	0.205	0.000	0.000	0.000	0.000	0.000	0.000	0.000	0.000	0.000	0.000	0.000	0.000	0.000	0.000	0.000	0.000	0.000	0.000	0.000	0.000	0.000	0.000	0.000	0.000
CA++		0.000	0.000	0.000	0.000	0.000	0.000	0.000	0.000	0.000	0.000	0.000	0.000	0.000	0.000	0.000	0.000	0.000	0.000	0.000	0.000	0.000	0.000	0.000	0.000	0.000	0.000	0.000	0.000
H3O+		0.000	0.000	0.000	0.000	0.000	0.000	0.000	0.000	0.000	0.000	0.000	0.000	0.000	0.000	0.000	0.000	0.000	0.000	0.000	0.000	0.000	0.000	0.000	0.000	0.000	0.000	0.000	0.000
CAOH+		0.000	0.000	0.000	0.000	0.000	0.000	0.000	0.000	0.000	0.000	0.000	0.000	0.000	0.000	0.000	0.000	0.000	0.000	0.000	0.000	0.000	0.000	0.000	0.000	0.000	0.000	0.000	0.000
K+		0.035	0.000	0.035	0.000	0.035	0.000	0.035	0.035	0.000	0.000	0.000	0.035	0.035	0.035	0.000	0.000	0.000	0.000	0.000	0.033	0.000	0.000	0.000	0.000	0.000	0.000	0.000	0.000
CACO3(S)		0.000	0.000	0.000	0.000	0.000	1.000	0.000	0.000	1.000	0.000	0.000	0.000	0.000	0.000	1.000	1.000	1.000	1.000	1.000	0.048	1.000	0.050	0.444	0.000	0.523	0.000	0.523	0.000
K2CO3(S)		0.000	0.000	0.000	0.000	0.000	0.000	0.000	0.000	0.000	0.000	0.000	0.000	0.000	0.000	0.000	0.000	0.000	0.000	0.000	0.000	0.000	0.000	0.000	0.000	0.000	0.000	0.000	0.000
CA(OH)2S		0.000	0.000	0.000	0.000	0.000	0.000	0.000	0.000	0.000	0.000	0.000	0.000	0.000	0.000	0.000	0.000	0.000	0.000	0.000	0.000	0.000	0.000	0.000	0.000	0.000	0.000	0.000	0.000
HCO3-		0.000	0.000	0.000	0.000	0.000	0.000	0.000	0.000	0.000	0.000	0.000	0.000	0.000	0.000	0.000	0.000	0.000	0.000	0.000	0.000	0.000	0.000	0.000	0.000	0.000	0.000	0.000	0.000
OH-		0.019	0.000	0.019	0.000	0.019	0.000	0.019	0.019	0.000	0.000	0.000	0.019	0.019	0.019	0.000	0.000	0.000	0.000	0.000	0.018	0.000	0.000	0.000	0.000	0.000	0.000	0.000	0.000
CO3--		0.008	0.000	0.008	0.000	0.008	0.000	0.008	0.008	0.000	0.000	0.000	0.008	0.008	0.008	0.000	0.000	0.000	0.000	0.000	0.007	0.000	0.000	0.000	0.000	0.000	0.000	0.000	0.000
CAO		0.000	0.000	0.000	0.000	0.000	0.000	0.000	0.000	0.000	0.000	0.000	0.000	0.000	0.000	0.000	0.000	0.000	0.000	0.000	0.000	0.000	0.000	0.000	0.000	0.000	0.000	0.000	0.000

28	34	35	36	37	39	40	40-R	42	43	46	47	48	48-R	49	50	51	52	54	58	59	60	60-R	61	67	67-R	68	COMPRCO2	COOLAIR	COOLAR-2	HOTAIR
21.0	96.7	96.7	154.4	300.0	300.0	300.0	300.0	96.7	96.7	99.1	297.2	90.6	90.6	348.1	25.6	250.4	250.4	388.1	900.0	674.0	674.0	674.0	674.0	21.0	21.0	21.0	40.0	21.0	21.0	42.8
1.0	0.9	0.9	0.9	1.0	1.0	1.0	1.0	0.9	0.9	1.0	33.0	0.9	0.9	0.9	40.0	40.0	40.0	0.9	0.9	0.9	0.9	0.9	0.9	1.0	1.0	1.0	151.0	1.0	1.0	1.0
0.000	1.000	0.000	0.630	0.000	0.000	1.000	1.000	0.166	0.000	0.000	1.000	0.000	0.000	0.000	0.000	0.315	0.368	1.000	0.495	0.000	0.000	0.000	0.000	0.000	0.000	0.000	1.000	1.000	1.000	1.000
1.000	0.000	0.093	0.000	0.000	0.000	0.000	0.000	0.000	0.000	0.000	0.000	0.000	0.000	0.000	1.000	0.685	0.632	0.000	0.000	0.000	0.000	0.000	0.000	0.951	1.000	1.000	0.000	0.000	0.000	0.000
0.000	0.000	0.907	0.370	1.000	1.000	0.000	0.000	0.834	1.000	1.000	0.000	1.000	1.000	1.000	0.000	0.000	0.000	0.000	0.505	1.000	1.000	1.000	1.000	0.049	0.000	0.000	0.000	0.000	0.000	0.000
-1.63E+06	-107	-1240	-709	-784	-623	-136	-136	-466	-768	-636	-411	-841	-2012	-1967	-264	-239	-237	-620	-1582	-1027	-989	-413	-38	-3912	-3912	-3912	-659	-12	-7	50
5670.8	0.4	1.5	1.9	1.3	0.7	0.6	0.6	0.8	0.6	0.7	1.8	0.7	1.7	1.7	0.9	0.9	0.9	1.6	3.3	1.7	1.6	0.7	0.0	12.0	12.0	12.0	1.6	96.6	57.9	96.6
0.000	0.000	0.000	0.000	0.000	0.000	0.000	0.000	0.000	0.000	0.000	0.000	0.000	0.000	0.000	0.000	0.000	0.000	1.000	0.495	0.000	0.000	0.000	0.000	0.000	0.000	0.000	1.000	0.000	0.000	0.000
0.938	1.000	0.093	0.630	0.460	0.000	1.000	1.000	0.166	0.000	0.000	1.000	0.000	0.000	0.000	1.000	1.000	1.000	0.000	0.000	0.000	0.000	0.000	0.000	0.942	0.942	0.942	0.000	0.000	0.000	0.000
0.000	0.000	0.000	0.000	0.000	0.000	0.000	0.000	0.000	0.000	0.000	0.000	0.000	0.000	0.000	0.000	0.000	0.000	0.000	0.000	0.000	0.000	0.000	0.000	0.001	0.001	0.001	0.000	0.000	0.000	0.000
0.000	0.000	0.000	0.000	0.000	0.000	0.000	0.000	0.000	0.000	0.000	0.000	0.000	0.000	0.000	0.000	0.000	0.000	0.000	0.000	0.000	0.000	0.000	0.000	0.000	0.000	0.000	0.000	0.000	0.000	0.000
0.000	0.000	0.000	0.000	0.000	0.000	0.000	0.000	0.000	0.000	0.000	0.000	0.000	0.000	0.000	0.000	0.000	0.000	0.000	0.000	0.000	0.000	0.000	0.000	0.000	0.000	0.000	0.000	0.000	0.000	0.000
0.000	0.000	0.000	0.000	0.000	0.000	0.000	0.000	0.000	0.000	0.000	0.000	0.000	0.000	0.000	0.000	0.000	0.000	0.000	0.000	0.000	0.000	0.000	0.000	0.009	0.057	0.057	0.000	0.000	0.000	0.000
0.000	0.000	0.000	0.000	0.000	0.000	0.000	0.000	0.000	0.000	0.000	0.000	0.000	0.000	0.000	0.000	0.000	0.000	0.000	0.000	0.000	0.000	0.000	0.000	0.000	0.000	0.000	0.000	0.811	0.811	0.811
0.000	0.000	0.000	0.000	0.000	0.000	0.000	0.000	0.000	0.000	0.000	0.000	0.000	0.000	0.000	0.000	0.000	0.000	0.000	0.000	0.000	0.000	0.000	0.000	0.000	0.000	0.000	0.000	0.189	0.189	0.189
0.000	0.000	0.000	0.000	0.000	0.000	0.000	0.000	0.000	0.000	0.000	0.000	0.000	0.000	0.000	0.000	0.000	0.000	0.000	0.000	0.000	0.000	0.000	0.000	0.000	0.000	0.000	0.000	0.000	0.000	0.000
0.000	0.000	0.000	0.000	0.000	0.000	0.000	0.000	0.000	0.000	0.000	0.000	0.000	0.000	0.000	0.000	0.000	0.000	0.000	0.000	0.000	0.000	0.000	0.000	0.000	0.000	0.000	0.000	0.000	0.000	0.000
0.035	0.000	0.000	0.000	0.000	0.000	0.000	0.000	0.000	0.000	0.000	0.000	0.000	0.000	0.000	0.000	0.000	0.000	0.000	0.000	0.000	0.000	0.000	0.000	0.000	0.000	0.000	0.000	0.000	0.000	0.000
0.000	0.000	0.438	0.000	0.000	0.000	0.000	0.000	0.000	1.000	0.000	0.000	1.000	1.000	1.000	0.000	0.000	0.000	0.000	0.010	0.020	0.000	0.000	1.000	0.000	0.000	0.000	0.000	0.000	0.000	0.000
0.000	0.000	0.000	0.000	0.000	0.000	0.000	0.000	0.000	0.000	0.000	0.000	0.000	0.000	0.000	0.000	0.000	0.000	0.000	0.000	0.000	0.000	0.000	0.000	0.000	0.000	0.000	0.000	0.000	0.000	0.000
0.000	0.000	0.000	0.000	0.459	0.850	0.000	0.000	0.000	0.000	0.850	0.000	0.000	0.000	0.000	0.000	0.000	0.000	0.000	0.000	0.000	0.000	0.000	0.000	0.049	0.000	0.000	0.000	0.000	0.000	0.000
0.019	0.000	0.000	0.000	0.000	0.000	0.000	0.000	0.000	0.000	0.000	0.000	0.000	0.000	0.000	0.000	0.000	0.000	0.000	0.000	0.000	0.000	0.000	0.000	0.000	0.000	0.000	0.000	0.000	0.000	0.000
0.008	0.000	0.000	0.000	0.000	0.000	0.000	0.000	0.000	0.000	0.000	0.000	0.000	0.000	0.000	0.000	0.000	0.000	0.000	0.000	0.000	0.000	0.000	0.000	0.000	0.000	0.000	0.000	0.000	0.000	0.000
0.000	0.000	0.469	0.370	0.081	0.150	0.000	0.000	0.834	0.000	0.150	0.000	0.000	0.000	0.000	0.000	0.000	0.000	0.000	0.495	0.980	1.000	1.000	0.000	0.000	0.000	0.000	0.000	0.000	0.000	0.000

HOTAIR-2	S1	S2	S2-LIQOU	S3	S4	S5	S6	S7	S8	S9	S10	S11	S13	S16	S17	S19	SOLIDS	VAP
42.7	147.8	50.4	20.0	25.0	260.4	30.0	30.0	30.0	25.0	81.3	50.0	81.3	302.5	81.3	80.0	50.0	900.0	900.0
1.0	33.0	33.0	1.0	0.5	0.9	0.9	0.8	0.8	0.5	0.5	1.0	0.5	40.0	0.5	1.0	0.5	0.9	0.9
1.000	0.000	0.000	0.000	0.000	0.000	1.000	1.000	0.000	0.000	0.855	0.000	0.786	1.000	0.867	0.000	0.000	0.000	1.000
0.000	1.000	1.000	1.000	1.000	0.000	0.000	0.000	1.000	1.000	0.145	1.000	0.214	0.000	0.133	0.477	1.000	0.000	0.000
0.000	0.000	0.000	0.000	0.000	1.000	0.000	0.000	0.000	0.000	0.000	0.000	0.000	0.000	0.000	0.523	0.000	1.000	0.000
30	-486	-499	-130047	-265	-40	-646	-646	345	-265	-228	-499	-438	-216	-432	-934	-499	-1006	-576
57.9	1.8	1.8	452.2	0.9	0.0	1.6	1.6	0.0	0.9	0.9	1.8	1.8	0.9	1.8	1.2	1.8	1.7	1.6
0.000	0.000	0.000	0.000	0.000	0.000	1.000	1.000	0.000	0.000	0.000	0.000	0.000	0.000	0.000	0.000	0.000	0.000	1.000
0.000	1.000	1.000	0.938	1.000	0.000	0.000	0.000	1.000	1.000	1.000	1.000	1.000	1.000	1.000	0.477	1.000	0.000	0.000
0.000	0.000	0.000	0.000	0.000	0.000	0.000	0.000	0.000	0.000	0.000	0.000	0.000	0.000	0.000	0.000	0.000	0.000	0.000
0.000	0.000	0.000	0.000	0.000	0.000	0.000	0.000	0.000	0.000	0.000	0.000	0.000	0.000	0.000	0.000	0.000	0.000	0.000
0.000	0.000	0.000	0.000	0.000	0.000	0.000	0.000	0.000	0.000	0.000	0.000	0.000	0.000	0.000	0.000	0.000	0.000	0.000
0.000	0.000	0.000	0.000	0.000	0.000	0.000	0.000	0.000	0.000	0.000	0.000	0.000	0.000	0.000	0.000	0.000	0.000	0.000
0.811	0.000	0.000	0.000	0.000	0.000	0.000	0.000	0.000	0.000	0.000	0.000	0.000	0.000	0.000	0.000	0.000	0.000	0.000
0.189	0.000	0.000	0.000	0.000	0.000	0.000	0.000	0.000	0.000	0.000	0.000	0.000	0.000	0.000	0.000	0.000	0.000	0.000
0.000	0.000	0.000	0.000	0.000	0.000	0.000	0.000	0.000	0.000	0.000	0.000	0.000	0.000	0.000	0.000	0.000	0.000	0.000
0.000	0.000	0.000	0.000	0.000	0.000	0.000	0.000	0.000	0.000	0.000	0.000	0.000	0.000	0.000	0.000	0.000	0.000	0.000
0.000	0.000	0.000	0.036	0.000	0.000	0.000	0.000	0.000	0.000	0.000	0.000	0.000	0.000	0.000	0.000	0.000	0.000	0.000
0.000	0.000	0.000	0.000	0.000	1.000	0.000	0.000	0.000	0.000	0.000	0.000	0.000	0.000	0.000	0.523	0.000	0.020	0.000
0.000	0.000	0.000	0.000	0.000	0.000	0.000	0.000	0.000	0.000	0.000	0.000	0.000	0.000	0.000	0.000	0.000	0.000	0.000
0.000	0.000	0.000	0.000	0.000	0.000	0.000	0.000	0.000	0.000	0.000	0.000	0.000	0.000	0.000	0.000	0.000	0.000	0.000
0.000	0.000	0.000	0.017	0.000	0.000	0.000	0.000	0.000	0.000	0.000	0.000	0.000	0.000	0.000	0.000	0.000	0.000	0.000
0.000	0.000	0.000	0.010	0.000	0.000	0.000	0.000	0.000	0.000	0.000	0.000	0.000	0.000	0.000	0.000	0.000	0.000	0.000
0.000	0.000	0.000	0.000	0.000	0.000	0.000	0.000	0.000	0.000	0.000	0.000	0.000	0.000	0.000	0.000	0.000	0.980	0.000

9.6   Results of sensitivity analysis

Variation of temperature on causticisation reaction
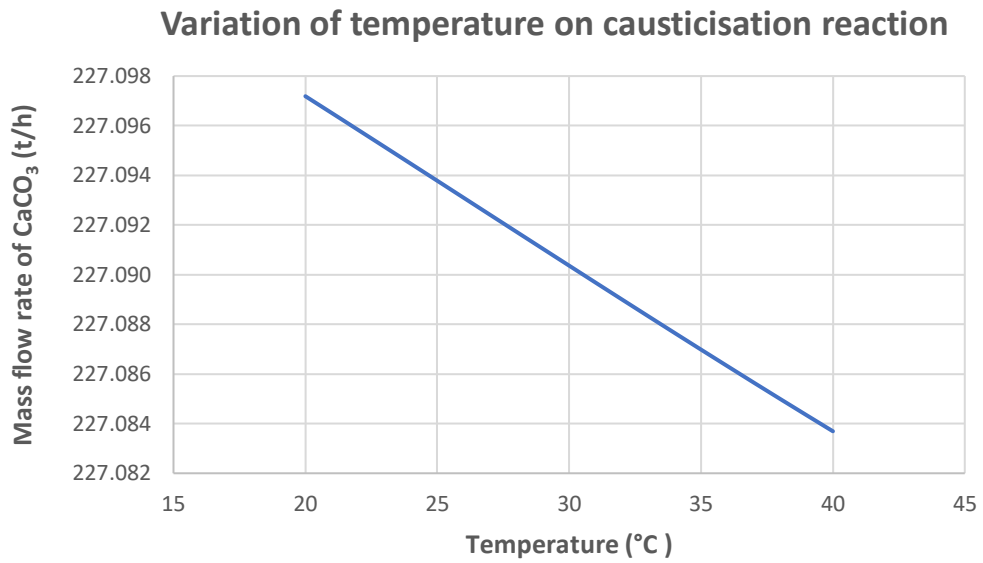
Figure 31: Sensitivity analysis of pellet reactor temperature against product mass flow rate of CaCO₃.
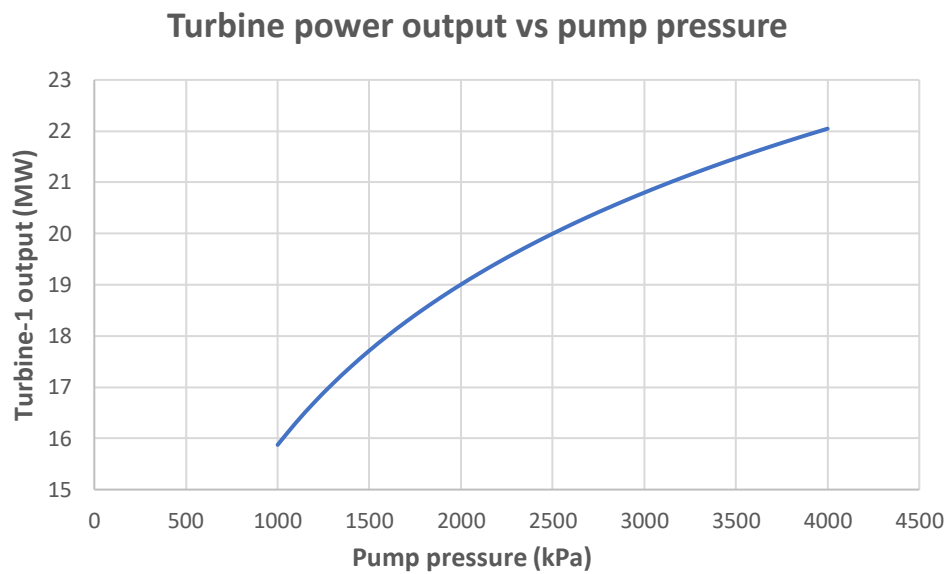
Turbine power output vs pump pressure

Figure 32: Sensitivity analysis of pump outlet pressure against Turbine-1 power output.